RADIOLOGY AND ONCOLOGY

March 2005
Vol. 39 No. 1
Ljubljana

ISSN 1318-2099

GEMZAR je indiciran za zdravljenje:

- lokalno napredovalega ali metastatskega nedrobnoceličnega karcinoma pljuč v kombinaciji z drugimi citostatičnimi zdravili,
- lokalno napredovalega ali metastatskega adenokarcinoma trebušne slinavke pri bolnikih v dobrem splošnem stanju, z zadostnimi rezervami kostnega mozga,
- lokalno napredovalega ali metastatskega karcinoma sečnega mehurja v kombinaciji z drugimi citostatičnimi zdravili.

Podrobnejše informacije o zdravilu so vam na voljo pri lokalnem predstavništvu:
Eli Lilly (Suisse) S.A., Podružnica v Ljubljani, Dunajska 156, 1000 Ljubljana,
telefon: 01/5688 280, telefaks: 01/5691 705, spletna stran: www.lilly.com

GEMZAR®
{ gemcitabin }

Lilly

RADIOLOGY AND ONCOLOGY

Editorial office
Radiology and Oncology
Institute of Oncology
Zaloška 2
SI-1000 Ljubljana
Slovenia
Phone: +386 1 5879 369
Phone/Fax: +386 1 5879 434
E-mail: gsersa@onko-i.si

March 2005
Vol. 39 No. 1
Pages 1-89
ISSN 1318-2099
UDC 616-006
CODEN: RONCEM

Aims and scope

Radiology and Oncology is a journal devoted to publication of original contributions in diagnostic and interventional radiology, computerized tomography, ultrasound, magnetic resonance, nuclear medicine, radiotherapy, clinical and experimental oncology, radiobiology, radiophysics and radiation protection.

Publisher
Association of Radiology and Oncology

Affiliated with
Slovenian Medical Association – Slovenian Association of Radiology, Nuclear Medicine Society, Slovenian Society for Radiotherapy and Oncology, and Slovenian Cancer Society
Croatian Medical Association – Croatian Society of Radiology
Societas Radiologorum Hungarorum
Friuli-Venezia Giulia regional groups of S.I.R.M. (Italian Society of Medical Radiology)

Reader for English
Mojca Čakš

Key words
Eva Klemenčič

Secretaries
Milica Harisch
Mira Klemenčič

Design
Monika Fink-Serša

Printed by
Imprint d.o.o., Ljubljana, Slovenia

Published quarterly in 700 copies

Beneficiary name: DRUŠTVO RADIOLOGIJE IN ONKOLOGIJE
Zaloška cesta 2,
1000 Ljubljana
Slovenia
Beneficiary bank account number: SI56 02010-0090006751
IBAN: SI560201000900067 51
Our bank name: Nova Ljubljanska banka, d.d.,
Ljubljana, Trg republike 2,
1520 Ljubljana; Slovenia
SWIFT: LJBASI2X

Subscription fee for institutions EUR 100 (16000 SIT), individuals EUR 50 (5000 SIT)

The publication of this journal is subsidized by the Ministry of Education, Science and Sport of the Republic of Slovenia.

Indexed and abstracted by:
BIOMEDICINA SLOVENICA
CHEMICAL ABSTRACTS
EMBASE / Excerpta Medica
Sci Base

This journal is printed on acid- free paper

Radiology and Oncology is available on the internet at: http://www.onko-i.si/radiolog/rno.html

ISSN 1581-3207

RADIOLOGY AND ONCOLOGY

Ljubljana, Slovenia
March 2005
Vol. 39 No. 1

ISSN 1318-2099
UDC 616-006
CODEN: RONCEM

CONTENTS

ONCOLOGY

RADIATION PHYSICS

Radiology and Oncology is covered in *Biomedicina Slovenica, Chemical Abstracts, EMBASE / Excerpta Medica, and Sci Base*

Radiol Oncol 2005; 39(1): 1-4.

case report

Symptomatic imperforate Cowper's syringocele in a 5-year-old boy

Goran Roić[1], Igor Borić[1], Vesna Posarić[1], Mislav Bastić[2], Božidar Župančić[2]

[1]*Department of Pediatric Radiology,*
[2]*Department of Pediatric Surgery, Children's Hospital Zagreb, Zagreb, Croatia*

Background. *Cowper's syringocele is a rare anomaly in childhood. It is caused by the obstruction of the duct of Cowper's gland. Depending of the type and size of the syringocele, and the age of the patient, the treatment for symptomatic lesions could be endoscopic deroofing or open perineal surgery.*

Case report. *We report a case of symptomatic imperforate syringocele in a 5-year-old boy. Although the syringocele are usually best shown on voiding cysto-urethrography, there was not any detectable extrinsic impression or filling defect in the bulbar urethra. Ultrasonography guided perineal puncture with contrast filling of the cystic lesion was used to detect the connection of the Cowper's duct to the ventral surface of bulbar urethra.*

Conclusions. *In imperforate syringocele, ultrasonography could be useful imaging technique especially in young patients, to evaluate urethra and perineal lesions and for percutaneous guided procedures.*

Key words: bulbourethral glands-abnormalities; child; preschool

Introduction

Cowper gland is an accessory sexual organ that contributes to semen coagulation and urethral lubrication.[1] The two main Cowper's glands are situated within the urogenital diaphragm, with a second pair of accessory glands situated in the bulbous spongiosal tissue. The main Cowper's ducts enter the ventral surface of the bulbar urethra near the midline by piercing the spongiosum.

The accessory ducts can enter the urethra directly or drain into the main duct.

A retention cyst of a Cowper gland duct (syringocele) is caused by the obstruction of the duct of the gland; it causes a smooth rounded filling defect in the bulbous urethra just proximal to the expected site of the Cowper duct insertion. The true aetiology of Cowper's duct cysts remains uncertain; most Cowper's gland duct lesions are congenital; they are present in boys with reports of cystograms and have an incidence of 1.5%.[2,3] Although usually asymptomatic, large reten-

Received 30 June 2004
Accepted 20 July 2004

Correspondence to: Goran Roić, MD, Department of Pediatric Radiology, Children's Hospital Zagreb, Klaićeva 16, 10 000 Zagreb, Croatia; Phone: +385 1 46 00 231; Fax: +385 1 46 00 228; E-mail: goran.roic@zg.htnet.hr

tion cysts may cause urethral obstruction, urinary infection and hematuria.[4,5] The differential diagnosis of a Cowper's duct retention cyst includes urethral diverticulum, urethral duplication, fistula and Mullerian duct remnant.[6] Depending of the type and size of the syringocele, and the age of the patient, the treatment for symptomatic lesions could be endoscopic deroofing or open perineal surgery.[3,4]

Case report

A 5-year old boy presented with a one-month history of scrotal and perineal pain and discomfort, without dysuria or haematuria. On physical examination, fullness and medially protruding mass in the perineum were observed. The patient's urinary flow rate, blood and urinary profiles were normal. Scrotal and perineal ultrasonography revealed a well delineated thin-walled cystic lesion located in the lower scrotum and perineum; no clear communication with urethra could be detected (Figures 1a, 1b).

There was not any detectable extrinsic impression or filling defect in the bulbar urethra during the voiding cysto-uretrography (Figure 2). Because of these findings, we decided to perform ultrasonography guided perineal puncture with contrast filling of the cystic lesion instead of cystourethroscopy; there was a small duct emerging from the proximal end of the cyst towards the bulbous urethra (Figure 3).

Due to the age of the patient and type of the syringocele, an open perineal surgery was carried out with complete resection of the syringocele. During the dissection of the cyst, there was a small duct emerging from the proximal end of the cyst towards the pelvic diaphragm, which was mostly resected after cannulation. During the follow-up period there was complete relief of perineal pain with normal urine profile and flow rate.

Discussion

According to urethrographic and endoscopic findings, the lesions of the Cowper's gland have been classified by Maizels *et al*[7] into four groups: (1) simple syringocele - minimally dilated duct; (2) perforate syringocele - a

Figure 1a. Syringocele. Ultrasonography demonstrated well defined cystic lesion proximal to the urethra; longitudinal view.

Figure 1b. Syringocele. Ultrasonography demonstrated well defined cystic lesion proximal to the urethra; transversal view.

Figure 2. Voiding cysto-uretrography. The normal urethra without filling defects or impression in the floor of the bulbous urethra.

Figure 3. US-guided puncture of the cystic lesion; contrast material injected into the cystic dilatation of the Cowper's gland with small duct emerging from the proximal end of the cyst towards the bulbous urethra.

bulbous duct that drain into the urethra via the patulous ostium and appears as a diverticulum; (3) imperforate syringocele - a bulbous duct that resembles a submucosal cyst and appears as a radiolucent mass; and (4) ruptured syringocele - the fragile membrane that remains in the urethra after dilated duct ruptures. Furthermore, syringoceles can be either within the corpus spongiosum (bulbar) or outside, lying posteriorly to it (perineal).[8]

The diagnosis of Cowper's syringocele is based on the voiding cysto-urethrography, cystourethroscopy and ultrasonography. Schultheiss *et al*[8] reported MRI appearance of imperforate syringocele. Although the syringocele are usually best shown on voiding cysto-urethrography, if imperforate, there shouldn't be any filling defect in the bulbous urethra or reflux into the Cowper's gland ducts. In such cases, ultrasonography could be a useful imaging technique especially in young patients, to evaluate urethra and perineal lesions and for percutaneous guided procedures.[9]

References

1. Moskowitz PS, Newton NA, Lewotiz RL. Retention cyst of Cowper's duct. *Radiology* 1976; **120:** 377-80.

2. Brock WA, Kaplan GW. Lesion of Cowper's glands in children. *J Ural* 1979; **122:** 121-3.

3. Bevers RFM, Abbekerk EM, Boon TM. Cowper's syringocele: Symptoms, classification and treatment of unappreciated problem. *J Urol* 2000; **163:** 782-4.

4. Salinas Sanchez AS, Segura Martin M, Lorenzo Romero J, Hernandez Millan I, Ruiz Mondejar R, Virseda Rodriguez JA. [Ruptured syringocele of the Cowper's gland. Report of a case]. [Spanish]. *Actas Urol Esp* 1998; **22:** 712-5.

5. Pastor NJ, Liegro GJ, Garcia GF, Ros TM, Galiano RJL, Gutierrez SA, et al. Syringocele of the Cowper's gland. Report of 2 cases diagnosed in adulthood. *Arch Esp Urol* 2002; **55:** 322-4.

6. Barnewolt CE, Harriet JP, Lebowitz RL, Kirks DR. Genitourinary Tract. In: Kirks RD, editor. *Practical pediatric imaging*. Philadelphia: Lippincot-Raven Publishers; 1998. p. 1086-7.

7. Maizels M, Stephens FD, King Lr, Firlit CF. Cowper's syringocele: Classification of dilatations of Cowper's gland duct based on clinical characteristics of 8 boys. *J Urol* 1983; **129:** 111-4.

8. Schultheiss D, Loty J, Hofner K, Jonas U. Symptomatic imperforate Cowper's syringocele in an adult. *BJU International* 2000; **86:** 4-6.

9. Pavlica P, Barozzi L, Stasi G, Viglietta G. Ultrasonography in syringocele of the male urethra (ultrasound-urethrography). *Radiol Med* 1989; **78:** 348-50.

Radiol Oncol 2005; 39(1): 5-8.

Sonography of pleural space in healthy pregnants - preliminary results

Igor Kocijančič

Department of Radiology, Institute of Oncology, Ljubljana, Slovenia

Background. *The purpose of our study was to determine the incidence of sonographically visible normal pleural fluid finding in healthy pregnants.*

Methods. *Chest sonography was performed in 47 pregnant volunteers, searching for pleural fluid, first leaning on the elbow and than in a sitting position. 9-12 MHz linear probe was used. If the result of the first examination was positive (at least 2 mm thick anechoic layer), we repeated the procedure with 3-6 MHz large radius convex probe.*

Results. *The fluid layer of typical wedge-shaped appearance was visible in the pleural space of 28/47 (59.5%) pregnant volunteers, on both sides in 18/47 (38.3%) and unilaterally in 10/47 (21.2%). The mean thickness of fluid layer (mean of positive results in both positions) was 2.86 mm (SD 1.09 mm, range from 1.8 mm to 6.4 mm). More than 3 mm thick fluid layer was easily detected with 3-6 MHz abdominal convex probe in 7/47 (15%).*

Conclusions. *Small amounts of pleural fluid can sometimes be detected by chest sonography, and hence also by abdominal sonography, in otherwise healthy pregnants. Such a positive result, if isolated, should not be taken as a sign of occult thoracic disease.*

Key words: pleura-ultrasonography; pregnancy

Introduction

A small amount of fluid (5-15 ml) is often present in the pleural space of healthy individuals.[1] No data could be found in the literature on imaging of normal pleural fluid in healthy individuals. Only an older textbook by Felson[2] reports that »in some normal individuals a small amount of free fluid, as little as 5 to 10 cc, can be demonstrated and even aspirated«, basing the claim on 50 to 70 year old references. He continues that »the incidence is higher during pregnancy« without providing a reference.

Data on the smallest amount of pleural fluid detectable by imaging methods vary considerably, but they are essentially within the same broad range whether computed tomography, sonography or X-ray examination are

Received 28 November 2004
Accepted 15 December 2004

Corespondence to: Igor Kocijančič, MD, PhD, Department of Radiology, Institute of Oncology, Zaloška 2, SI - 1000 Ljubljana, Slovenia; Phone: + 386 1 587 9 505; Fax. + 386 1 587 9 400; E-mail: ikocijancic@onko-i.si

used.[3-8] Cadaveric studies[9] have shown that volumes of pleural fluid as little as 5 ml may be detected with chest radiographs taken in lateral decubitus position. Recent reports have proved that minute pleural effusions can be easily detected using chest ultrasonography.[4,10] The latest study, comparing chest sonography with expiratory lateral decubitus radiography in the diagnosis of very small pleural effusions, showed that sonography appears to assess the fluid layer more accurately than radiography.[11]

We undertook this study to determine the possibility of sonographic detection of normal pleural fluid in healthy pregnants and to assess the frequency of this finding.

Patients and methods

Chest sonography was performed in 47 healthy pregnant volunteers, searching for pleural fluid. They had no signs of respiratory infects and normal results of laboratory tests. They were found healthy throughout regularly check-ups with their obstetrician. They all delivered healthy babies on term. The sonographic criterion for the presence of pleural fluid was detection of an anechoic zone between the parietal and visceral pleura, at least 2 mm thick (in the elbow position), changing appearance between inspiration and expiration and/or changing appearance with different positions during examination.[4,6,12]

The subject was placed in the lateral decubitus position for 5 minutes; sonography of the lower pleural space was performed with the subject leaning on her elbow[11] and then in a sitting position. An SSA-390 ultrasound scanner (Toshiba, Tokyo, Japan) was used, initially with a 9-12 MHz linear, 5.7 cm long transducer. If pleural fluid was observed, we repeated the examination of the pleural space with 3-6 MHz large convex transducer, commonly used during abdominal examinations. Maximal fluid layer thickness was measured, with the position of the probe perpendicular to the thoracic wall.[13]

Descriptive statistics were calculated for all the studied parameters. Mean differences were tested using t-test (for independent or paired samples, as appropriate), correlation was assessed using Pearson's correlation co-

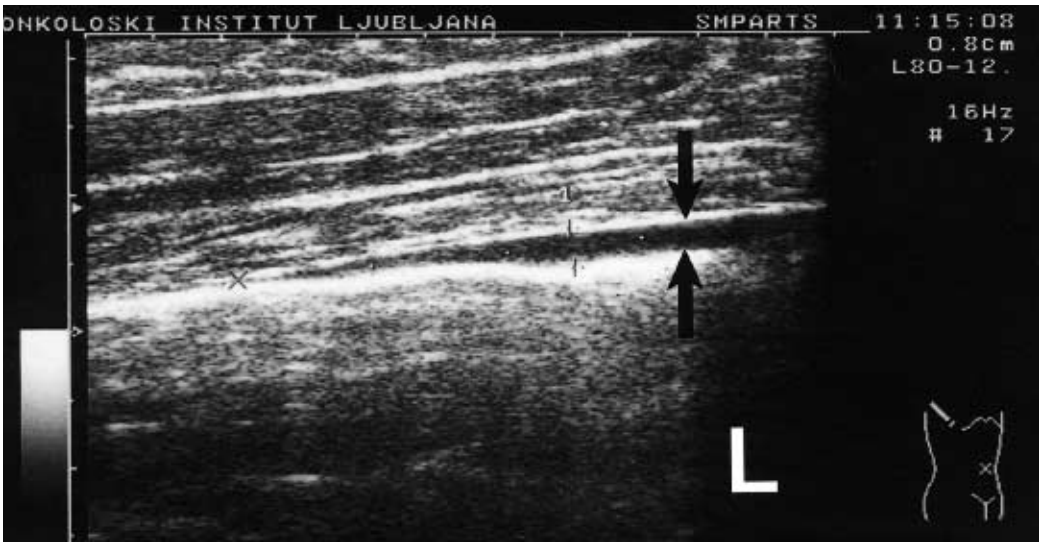

Figure 1. Wedge shaped echofree fluid layer measuring 3 mm (between arrows) represents normal pleural fluid accumulation; L=liver.

efficient and Fisher's exact test was used for analyzing contingency tables.

The study was approved by the Medical Ethics Committee of the Republic of Slovenia, and written informed consent was obtained from each subject prior to inclusion in the study.

Results

We examined 47 healthy pregnant volunteers with mean gestational age of 24.4 weeks (SD 4.6 weeks, range from 16 to 32 weeks) and we sonographically detected anechoic fluid layer in the pleural space in 28 subjects (59.5%). Fluid was observed bilaterally in 18 subjects (38.3%) and unilaterally in 10 subjects (21.2%), 9 of those on the left-hand side.

The mean fluid layer thickness was 2.95 mm (SD 0.99, range from 2.0 mm to 6.0 mm) in patients leaning on the elbow. In sitting position the mean thickness was 2.66 mm (SD 0.97, range from 1.8 mm to 6.4 mm). The difference between the two positions proved to be statistically significant (t-test: p=0.001). Fluid layer detected with the linear probe was clearly visible with the large radius convex probe if it measured 3 mm or more, which was the case in 7 subjects (15% of all subjects, 25% of subjects with visible fluid layer).

In the total sample, there were 24 male and 23 female fetuses. Among the pregnants with visible pleural fluid there was also an equal number (14) of male and female fetuses. Fluid layer thickness (mean of positive results in both positions) in pregnants carrying male fetuses was 3.18 mm (SD 1.12, range from 2.0 mm to 6.4 mm) while in pregnants carrying female fetuses the mean fluid layer was 2.44 mm (SD 0.58, range from 1.8 mm to 4.5 mm). The difference in mean fluid layer thickness proved to be statistically significant (t-test: p=0.041). Association between fetus gender and mean fluid layer thickness equal to or above 3 mm was marginally significant (Fisher exact test: p=0.077) in our sample, whereby 6 out of 7 mothers with visible fluid layer at least 3 mm thick carried male fetuses.

We found no correlation between age of pregnant woman and mean fluid layer thickness (r=0.044; p=0.823), no correlation between gestation age of the fetus and mean fluid layer thickness (r=-0.189; p=0.335), as well

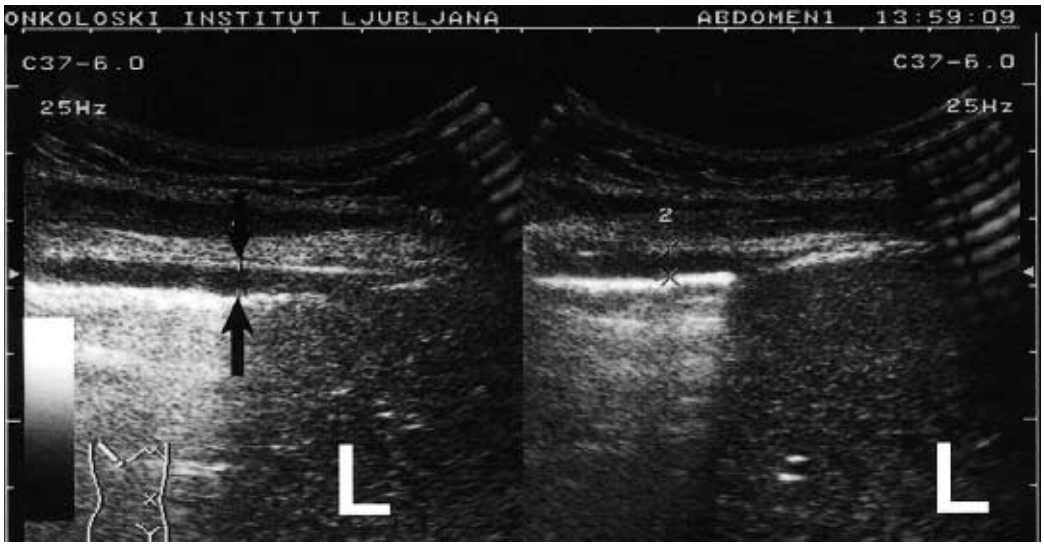

Figure 2. Detection of pleural fluid using 6 MHz abdominal large radius convex probe (between arrows); L=liver.

as no difference in mean fluid layer thickness between left and right pleural space (t-test: p=0.451).

Discussion

Parietal and visceral pleura and the space in-between usually measure only 0.3 to 0.4 mm.[10] On sonograms, normal pleural fluid accumulation typically appears as a wedge-shaped echofree layer with the base oriented towards frenicocostal sulcus (Figure 1). Since our examination revealed pleural fluid in both elbow and sitting position in almost 60% of subjects, we believe that there is a possibility to observe pleural fluid during routine sonographic examination of abdominal organs in perfectly healthy pregnant women. Fluid layer at least 3 mm thick was easily detectable with large convex 3-6 MHz probe (Figure 2) in 25% of the pregnants with visible pleural fluid. If one misinterprets this as a pathologic condition (sign of occult thoracic disease), it can lead to unnecessary diagnostic examinations, such as X-ray, potentially harmful to the fetus.

In our group of 16 - 32 weeks pregnancies results showed no association between gestation age of the fetus and mean fluid layer thickness. However the value of this finding is limited as the sample was relatively small and early/late pregnancies were not examined. As expected, we found a statistically significant difference in mean fluid layer thickness regarding the subject's position during examination (on the elbow vs. sitting). Unexpectedly, we found male fetuses corresponding to thicker fluid layer on average.

References

1. Black LF. The pleural space and pleural fluid. *Mayo Clin Proc* 1972; **47:** 493-506.

2. Felson B. Chest roentgenology. Philadelphia: W.B. Saunders; 1973. p. 352.

3. Hessen I. Roentgen examination of pleural fluid. A study of the localisation of free effusions, the potentialities of diagnosing minimal quantities of fluid and its existence under physiological conditions. *Acta Radiol* 1951; **86(Suppl):** 1-80.

4. Mathis G. Thoraxsonography-part I. Chest wall and pleura. *Ultrasound Med Biol* 1997; **23:** 1131-39.

5. Eibenberger KL, Dock WI, Ammann ME, Dorffner R, Hörmann MF, Grabenwörger F. Quantification of pleural effussions: sonography versus radiography. *Radiology* 1994; **191:** 681-84.

6. Mc Loud TC, Flower CDR. Imaging of the pleura: sonography, CT and MR imaging. *AJR Am J Roentgenol* 1991; **156:** 1145-53.

7. Leung AN, Muller NL, Miller RR. CT in the differential diagnosis of pleural disease. *AJR Am J Roentgenol* 1990; **154:** 487-92.

8. Maffesanti M, Tommasi M, Pellegrini P. Computed tomography of free pleural effusions. *Europ J Radiol* 1987; **7:** 87-90.

9. Moskowitz H, Platt RT, Schachar R, Mellins H. Roentgen visualization of minute pleural effusion. *Radiology* 1973; **109:** 33-5.

10. Reuß J. Sonographic imaging of the pleura: nearly 30 years experience. *Eur J Ultrasound* 1996; **3:** 125-39.

11. Kocijančič I, Vidmar K, Ivanovi-Herceg Z. Chest sonography versus lateral decubitus radiography in the diagnosis of small pleural effusions. *J Clin Ultrasound* 2003, **31:** 69-74.

12. Targhetta R, Bourgeois JM, Marty - Double C Chavagneux, Proust A, Coste E, Balmes P. Towards another diagnostic approach of peripheral lung masses. Ultrasonically guided needle aspiration. [French]. *J Radiol* 1992; **73:** 159-64.

13. Marks WM, Filly RA, Callen PW. Real - time evaluation of pleural lesions: New observations regarding the probability of obtaining free fluid. *Radiology* 1982; **142:** 163-4.

Radiol Oncol 2005; 39(1): 9-13.

case report

Injury of the axillary artery: duplex ultrasound detects postoperative occlusion of the artery with the establishment of the collateral network

Anton Krnić[1], Zvonimir Sučić[1], Niksa Vučić[2], Ante Bilić[2]

[1]Department of Radiology, [2]Internal Medicine Clinic, Sveti Duh General Hospital, Zagreb, Croatia

Background. *Injury of the axillary artery is a life-threatening condition. The injury requires immediate, on-place treatment (compression) and a number of patients require prompt explorative surgery. Whenever a vascular injury is suspected, radiological follow-up (angiography), intra-operative or post-operative, should be performed.*

Case report. *We report a case of axillary artery injury in 28-year- old woman. Though postoperative duplex ultrasound gave an accurate finding, i.e. pre-stenotic, high resistant Doppler wave spectrum proximal to and post-stenotic, monophasic distal to the injury, angiography was performed. It showed extensive collateral network in the axilla and the blocked perfusion in the axillary artery. The patient underwent re-operation. Thrombectomy in the axillary artery was performed, with a subsequent radical improvement of the arm perfusion.*

Conclusions. *In these particular circumstances, duplex ultrasound displayed a characteristic pattern and the angiography might even be avoided.*

Key words: axillary artery-injuries-ultrasonography-surgery; thrombosis; thrombectomy

Introduction

Injury of the axillary artery is a life threatening condition. Seventy-five percent of the patients die before being deported to the hospital.[1] Out of the rest, 82% are deported to the hospital within 24 hours, and others between 24 and 48 hours or more.[1] The injury requires immediate, on-place treatment (compression) and many patients (38%) require prompt explorative surgery.[1] In reports, some 85% of axillary artery traumas are caused by penetrating (stab) injuries and 15% by blunt injuries.[2]

Some 40-50% of the patients suffer from brachial plexus trauma: 2/3 from direct injury (partial or complete resection), 1/3 from compression due to enlarging haematoma.[2,3] Unlike in cases of compression due to

Received 19 May 2004
Accepted 20 June 2004

Correspondence to: Anton Krnic, M.D., Department of Radiology, Sveti Duh General Hospital, Andrije Hebranga 9, 10 000 Zagreb, Croatia; Phone: +385 1 48 56 209; Fax: +385 1 37 72 136; Fax: +385 1 37 72 136; E-mail: anton.krnic@zg.t-com.hr or luka.krnic@zg.htnet.hr

haematoma, in cases in which a direct injury of the brachial plexus occur, most patients do not have subsequent neurological improvement.[2,3]

Arterial repair is usually successful.[4] However, even if it fails, a severe ischemia is a rarity and the amputation rate is low.[4,5] In cases of ischemia of the upper extremity, the patients usually undergo saphenous vein interposition grafting that generally yields good results.[4]

The most frequently recurring symptoms are motor and sensitive deficiencies and distal ischemia, which, in some cases, may not occur, owing to an extensive collateral network.[3]

However, whenever vascular injury is suspected, radiological follow-up (angiography), intra-operative or post-operative, should be performed.[1,3,6] Our case reports a very synchronous cooperation between surgeons and radiologists, which led to a high-quality evaluation of the patient.

Case report

A 28-year-old woman fell through a glass door in a nightclub. An hour later, she was deported to the hospital in shock due to profuse bleeding in the left axillary fossa. Her peripheral pulses where not palpable, and her pupils where dilated. The breathing was very shallow, barely registered.

She underwent an immediate explorative surgery of the axilla. The axillary artery, vein and the brachial plexus were resected and the surgeons performed the reconstruction with an end-to-end anasthomoses of the vein and artery and tried to repair the brachial plexus.

However, after the operation, the pulsations of the arteries of the left arm were not palpable, although the arm was not pale, but warm and blushing.

The surgeons decided to refer the patient for radiological evaluation. First, she underwent duplex ultrasound scanning. The examiner found a pre-stenotic high resistant spec-

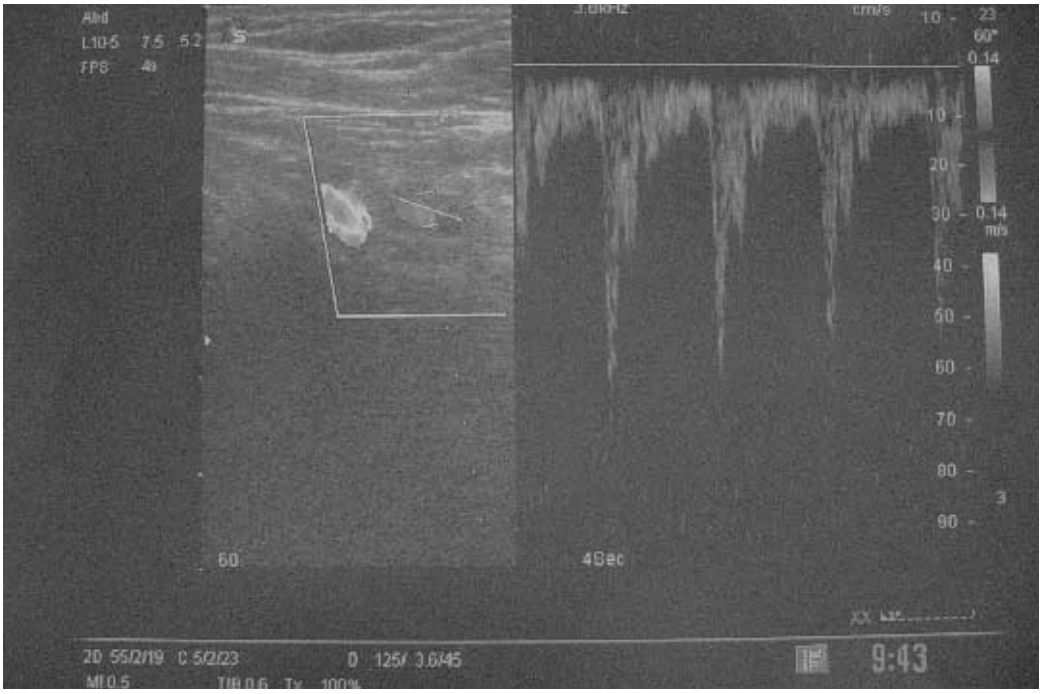

Figure 1a. Duplex ultrasound: high resistant, pre-stenotic attenuated spectra in the subclavian artery.

trum in the subclavian artery and a post-stenotic, monophasic spectra in all left arm arteries (brachial, ulnar, radial), (Figures 1a, 1b). The axillary artery was not examined because the patient complained of heavy pain and the arm could not be elevated. The venous circulation, however, was satisfactory. The next day, she underwent selective angiography. Using Seldinger technique, the sublcavian artery was reached with the catheter and the contrast was injected. The subclavian and the proximal portion of the axillary artery were opacified, but the other two portions of the axillary artery were not. The brachial artery was filled with a delay, through the network of collateral vessels. The distal arteries of the left arm were later also opacified (Figure 2). These findings confirmed the Doppler findings that there was an obstruction in the axillary artery.

The patient was planned to undergo saphenous vein grafting, but during the second operation, exploration with the Fogarty catheter through the incision in the brachial artery was performed and thrombi were found proximal to the incision, and so, she was successfully thrombectomised. Immediately afterwards, the reperfusion was established: the previously thin artery, very poorly filled with

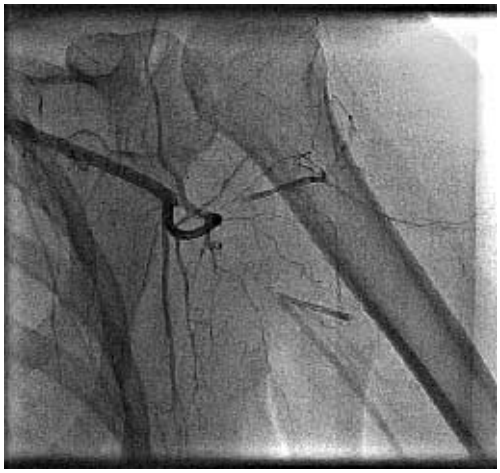

Figure 2. Angiography: occlusion of the axillary artery and the collateral network establishment.

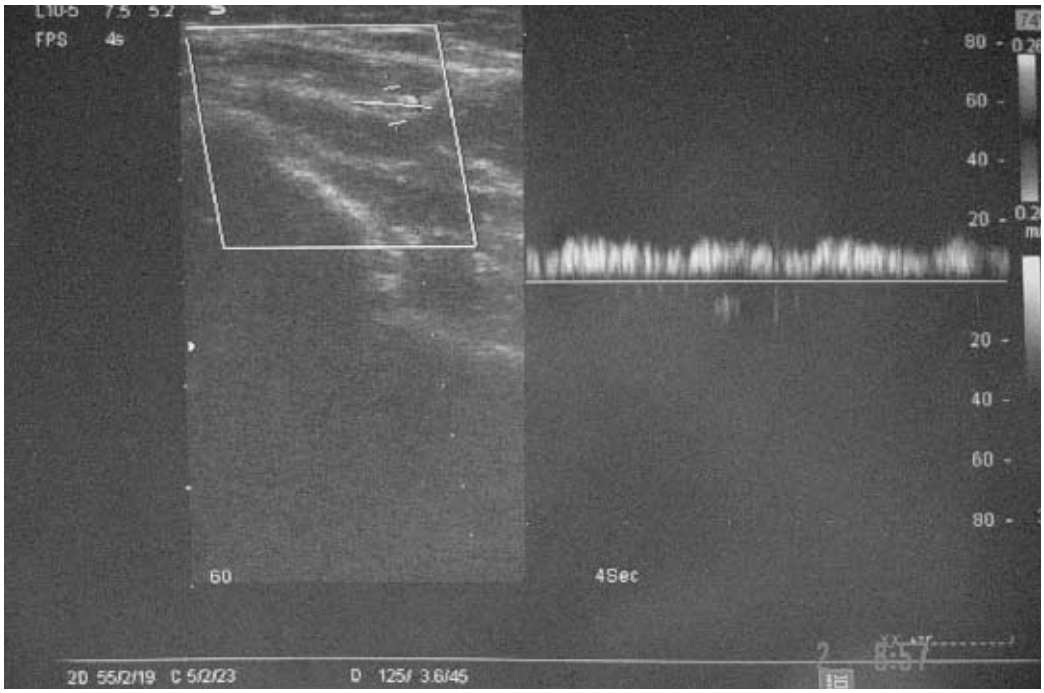

Figure 1b. Duplex ultrasound: low resistant, post-stenotic monophasic spectrum in the ulnar artery.

blood and initially very hard to find, started to inject blood through the hole of the incision and became obviously much better filled after the arterial wall was sewed. Congruently, its diameter was considerably increased afterwards.

The follow-up after this, second, operation proved almost normal (lightly attenuated) Doppler spectra in left arm arteries, almost symmetric to the contra-lateral one and the surgeons did not indicate the second angiography (they did not find it necessary any more).

Discussion

Due to the trauma of the axillary fossa and postoperative thromboembolism of the axillary artery in our patient, the blood perfusion through the axillary artery was blocked and collateral perfusion network was established. Duplex ultrasound showed a characteristic pattern, pre-stenotic, high resistant spectra in the subclavian artery, and post-stenotic, »parvus-tardus« spectra in the left arm arteries. These findings seemed to be almost pathognomonic. Despite the very convincing duplex ultrasound findings, angiography was performed to confirm the findings.

Angiography is highly invasive; some patients often refuse it. It has a 1-2-percent risk for complications and may be expensive.[1,7,8] However, in circumstances when angiography is not possible or not preferable for various reasons, the duplex scanning, as it seems, might be sufficient to set up the diagnosis.[9,10] Some data report the overall accuracy of 98% of Doppler ultrasonography in the detection of vascular trauma.[5] Besides, duplex scanning equipment is portable, the test is non-invasive and relatively easy to perform and no contrast is required.[8]

When the examinations are correctly performed, there should be, as in this case, high concordance between clinical presentation, radiological findings and surgical, intra operative findings.[6] With such concordance, the duplex ultrasound may be a gold standard for the evaluation of this kind of patients.

On the other hand, according to some reports, in case of axillary artery trauma the sensitivity of duplex ultrasound examination is usually low and therefore, the examiner has to be very cautious.[8] We thereby recommend the examiner to compare the findings of the subclavian and arm arteries of the injured body side to the contra-lateral to make sure the Doppler wave spectra differ highly in its morphology and resistance index.

When postoperative thromboembolism of the axillary artery develops, collateral axillary network might be established,[3,4] although it may provide, as is shown here, only attenuated, temporary sufficient arterial perfusion of the arm. In such cases, re-operation is required in order to establish normal, fully functional perfusion. As seen here, exploration with the Fogarty catheter and thrombectomy may be sufficient, and the saphenous vein interposition grafting may not be needed.

In this very case, though the surgeons tried to repair the resected brachial plexus, the left arm is still under palsy (»flail limb«).[1] Although reperfusion initially worsened the nerve function and aggravated the fibre degeneration, it allowed the fibre regeneration to occur in the longer time frame.[11] Though the necessary condition for a possible recovery of the nervous function, i.e. normal blood supply, was fulfilled, the patient still had to undergo a long-term rehabilitation with neurological follow-up (electromyography) and with uncertain and probably only partial improvement of the nervous function.[3] Further duplex ultrasound follow-up was also necessary.

Since the injuries of the subclavian-axillary arteries have taken many lives,[1] and, as shown here, can happen in relatively benign, peaceful circumstances, we highlight the im-

portance of prompt reaction on-place, as well as prompt hospital admittance and surgical exploration whenever the vascular and/or nervous injury is suspected.[1] This way, many lives could be saved and disabilities prevented.[1,5] We assume that the experience from the war in Croatia (1991-1995) of the surgeon on duty was probably beneficial in this situation, since these kinds of injuries are uncommon and most surgeons lack familiarity with their management and few are able to gain significant experience (operative mortality rate ranges between 5 and 30%).[1]

The importance of radiology in such cases is high.[1,3,6] It is applicable for possible intraoperative and is necessary for postoperative evaluation and follow-up.[1,3,6] Although the angiography is considered to be a »gold standard«,[3,6-8] a correctly performed duplex ultrasound should give sufficient information and can even exclude the need for angiography.[5,8-10] We offer our duplex ultrasound findings as an example of that.

In these, particular circumstances (postoperative thromboembolism in the axillary artery and establishment of the axillary collateral perfusion network), duplex ultrasound gave a highly typical and recognizable pattern (Figure 1). It is also the method we recommend for postoperative follow-up.

References

1. McKinley AG, Carrim AT, Robbs JV. Management of proximal axillary and subclavian artery injuries. *Br J Surg* 2000; **87:** 79-85.

2. McCready RA, Procter CD, Hyde GL. Subclavian-axillary vascular trauma. *J Vasc Surg* 1986; **3:** 24-31.

3. Adovasio R, Visintin E, Sgarbi G. Arterial injury of the axilla: an unusual case after blunt trauma of the shoulder. *J Trauma* 1996; **41:** 754-6.

4. Bastounis E, Pikoulis E, Leppaniemi AK, Michail P, Alexiou D. Revascularization of the limbs using vein grafts after vascular injuries. *Injury* 1998; **29:** 105-8.

5. Nanobashvili J, Kopadze T, Tvaladze M, Buachidze T, Nazvlishvili G. War injuries of major extremity arteries. *World J Surg* 2003; **27:** 134-9.

6. Julia J, Lozano P, Gomez F, Corominas C. Traumatic pseudoaneurysm of the axillary artery following anterior dislocation of the shoulder. Case report. *J Cardiovasc Surg (Torino)* 1998; **39:** 167-9.

7. Ofer A, Nitecki SS, Braun J, Daitzchman M, Goldsher D, et al. CT angiography of the carotid arteries in trauma to the neck. E*ur J Vasc Endovasc Surg* 2001; **21:** 401-7.

8. Bergstein JM, Blair JF, Edwards J, Towne JB, Wittmann DH, Aprahamian C, et al. Pitfalls in the use of color-flow duplex ultrasound for screening of suspected arterial injuries in penetrated extremities. *J Trauma* 1992; **33:** 395-402.

9. Bynoe RP, Miles WS, Bell RM, Greenwold DR, Sessions G, Haynes JL, et al. Noninvasive diagnosis of vascular trauma by duplex ultrasonography. *J Vasc Surg* 1991; **14:** 346-52.

10. Schwartz M, Weaver F, Yellin A, Ralls P. The utility of color flow Doppler examination in penetrating extremity arterial trauma. *Am Surg* 1993; **59:** 375-8.

11. Iida H, Schmelzer JD, Schmeichel AM, Wang Y, Low PA. Peripheral nerve ischemia: reperfusion injury and fiber regeneration. *Exp Neurol* 2003; **184:** 997-1002.

Radiol Oncol 2005; 39(1): 15-21.

Ultrasound signs of acute appendicitis in children - clinical application

Sandra Vegar-Zubović[1], Lidija Lincender[1], Salahudin Dizdarević[2], Irmina Sefić[1], Faruk Dalagija[1]

[1]Institute of Radiology, [2]Pediatric Surgery, Clinical Center of University in Sarajevo, Bosnia and Herzegovina

Background. *Acute appendicitis is a leading cause of the abdominal pain in children that need an urgent surgical treatment. Neither of individually clinical variables doesn't have a real discriminational nor predictive strength to be used as the only diagnostic test. A goal of this study is to define ultrasound criteria of the acute appendicitis by appointing of ultrasound parameters for this pathological condition, determine the relation between ultrasound signs and pathohistological finding, determine the connection of several ultrasound signs with a degree of the inflammation of the acute appendicitis.*

Methods. *In the prospective study with an ultrasound method we examine 50 patients with clinical signs of the acute abdomen. In these patients, the sonographic diagnosis is confirmed by the surgical finding, in fact with a pathohistological diagnosis. A basic, positive sonograph finding of the acute appendicitis was the identification of tubular, noncompresive, aperistaltic bowel which demonstrates a connection with coecum and blind terminal. In our work we analysed the lasting of the symptoms until the hospital intervention in patients stratified according to the pathohistological finding. We used ultrasound equipment- Toshiba Sonolayer with convex 3.75 MHz and linear 8 MHz probes.*

Results. *From 8 ultrasound signs of the acute appendicitis, only an anterior-posterior (AP) diameter of appendices, FAT (width of periappendicular fat tissue) and a peristaltic absence are positive ultrasound signs of the acute appendicitis. Appendicitis phlegmonosa is the most common pathohistological finding in our study (44%). Perforate gangrenous appendicitis and gangrenous appendicitis are represented in more than half of patients (30% + 22%), which suggests a long period of persisting symptoms until a hospital treatment. A statistic analysis shows a great possibility for using values of AP diameter, width of periapendicular fat tissue, just like the values of mural thickness in the evaluation of the appendix inflammation level.*

Conclusions*. Ultrasound is an absolute method of choice in the eventual doubt of the existing state of acute appendicitis, with 8 ultrasound signs that defined this pathological condition.*

AP appendix diameter, mural thickness and width of periapendicular fat tissue represents highly significant ultrasound criteria in the evaluation of the appendix inflammation level.

Key words: appendicitis-ultrasonography; child

Received 7 June 2004
Accepted 23 August 2004

Correspondence to: Sandra Vegar-Zubović, MD, Institute of Radiology, Clinical Center of University in Sarajevo, Bosnia and Herzegovina; E-mail: denin@bih.net.ba

Introduction

Acute abdomen is characterized by appearing of a sudden pain in the abdomen with a dysfunction; it appears suddenly and unexpectantly and it is caused with large number of changes on different abdomen organs. A clinical picture of the acute abdomen is one of the most divert and most complex conditions in the human body because of the beginning and course of the illness which is dependent o a large number of different organs in the abdomen. Acute appendicitis is a leading cause of an abdominal pain in children which demands an urgent surgical treatment. Clinical symptoms and signs depend, in the first place, on children's age, as well as on the pathological phase of appendicitis during the clinical examine. Beside the abdominal pain the acute inflammation of appendix is characterized with nausea, vomiting, anorexia, fever, diarrhoea, constipation, face blushing and tachycardia. Little patients preferred lying on the back in the supinatory position or on the right decubitus, quietly, because every motion causes pains. Cope made a list of 34 illnesses which lead to acute abdominal pains, and those conditions, according to signs and symptoms, which imitate the acute appendicitis. This list could be a longer, if we include immunodeficiency syndromes and another immunodeficiency states.[1]

The differential diagnosis of an abdominal pain is one of the fascinating, but mysterious questions for the clinical surgery. Reginald Fitz (1886) gave his own historical session describing a new pathological entity - appendicitis. And after 100 years, the exact diagnosis of this mysterious disease is still a huge problem.[1,2]

A diagnostic imaging of an acute abdominal pain in children is very hard, because little patients are not capable to give us relevant data. Besides, an acute, non-specific abdominal pain, which is very common in children, these little patients with an abdominal pain usually have symptoms that last longer than 24 hours (2/3 patients). If diagnosis and treatment are delayed, the morbidity and mortality of little patients increase. A diagnosis of typical clinical picture of the acute appendicitis is relatively easy, but in 30-45% of little patients it is presented with atypical clinical signs and symptoms which implicates the additional diagnostic imaging.[3,4]

Neither diagnostic variable individually (clinical and laboratory parameters) doesn't have significant discriminating nor predictive strength to be used as a relevant diagnostic test. There is a high risk of the incorrect diagnosis in some populations, especially in children without the existence of a relevant diagnostic test. The exact and prompt diagnosis is essential for minimizing of morbidity.

The goal of a modern surgical approach essentially is the same as in the 19th century, but today it is focused between percent of false negative appendectomy and percent of perforation in the time of the surgical observation. Introducing of ultrasound in the diagnosis of acute appendicitis, as this study shows, represents our aspect in leading of a modern medical protocol for young patients in this condition.

Methods

In the prospective study we analysed the possibilities of ultrasound in diagnosis of the acute appendicitis in children.

The research compassed 50 children in age from 0 to 16 years in whom ultrasound findings are confirmed with an operative, respectively, with a pathohistological finding (verification). These patients are observed and treated in the Clinic for Children's Surgery of Clinical Center Sarajevo initiated from Dom zdravlja Sarajevo. The study includes patients with both genders, with a clinical picture of the acute abdomen with its symptoms that occurred for the first time.

All patients are initially examined by the children's surgeon who, after clinical and laboratory findings, referred children to the ultrasound examination.

After the examination of the pelvis minor abdomen - the area of a maximum pain which a patient pointed with his/her finger (self-localisation) - the ileocoecal area was examined with a systematic ultrasound approach because of the possibility of the aberrant localisation of appendix.

A definition of the positive acute appendicitis sonograph finding was based on the identification of tubular, non-compressed, aperistaltic bowel which demonstrates a connection with caecum and clearly visible bowel blind terminal. By a careful approach, on the basis of eight ultrasound signs of acute appendicitis, we determined a connection between some US signs and a degree of the inflammation of the acute appendicitis. In the study we tried to analyse the lasting of symptoms until the hospital intervention in patients divided according to the pathohistological finding.

All examinations were done with the ultrasound unit Toshiba Sonolayer SAL 77 with convex (3.7 MHz) and linear (8 MHz) probes. Little patients were coming to be ultrasound examined as the urgent cases during the day or in the evening hours after they had been examined by their surgeon. A dosed compression in the ileocaecal area with a linear probe enabled the approach of ultrasound waves by gaping bowels with its content. Patients can suffer moderate compression as long as it is gentle, and according to the intensity it is identical to moderate deep palpation of the physical examination. For the identification of appendix it is necessary to find essential constraints: identify coecum and right colon in the transversal and longitudinal plane, identify musculus psoas and external iliac artery, and also identify terminal ileum.

Results

Table 1 shows basic demographic data of all patients. There is no significant statistical difference of the mean value (using age frequencies) between two groups of patients ($p>0.05$).

Table 2 shows eight ultrasound signs of acute appendicitis that are individually analysed in each patient.

Figure 1 shows pathohistological findings of the examined group of little patients. From these data we can see that appendicitis flegmonosa is the most common pathohistological finding (44%) (Figures 2a, 2b). In more than half of examined patients gangrenous appendicitis and perforate gangrenous appendicitis (30% + 22%) were found, which suggests a long existence of symptoms until the hospital treatment. Table 3 analysed the lasting of symptoms until the hospital inter-

Table 1. Basic demographic data in the examined group of patients

		Group I	Total
	Male	Female	
Age interval	3-16	4-16	3-16
N	26	24	50
X	9.864	11.083	10.440
S	3.518	3.900	3.721
Sx	0.690	0.796	0.526
Mediana	9.5	11.5	11
X2= 0.0801; p=0.777			

Table 2. Ultrasound signs in the examined group of patients

Anterior-posterior diameter (AP)	Mural wall thickness (MWT)	Air in lumen (AIR)	Inflame surrounding fat tissue (FAT)	Lack of peristaltic	Intra-luminal appendicolitis	Persistence of lymphonodes in appendix region	Local pericoecal fluid in abdomen
NegativeUS signs 0	0	0	0	0	15 (30%)	4 (8%)	29 (78%)
Uncertain signs 0	6 (12%)	10 (20%)	0	0	9 (18%)	11 (22%)	0
Positive US signs 50 (100%)	44 (88%)	40 (80%)	50 (100%)	50 (100%)	26 (52%)	35 (70%)	11 (22%)

Table 3. Existing of symptoms until hospital intervention

Appendicitis catharalis	Appendicitis flegmonosa	Appendicitis gangrenosa	Appendicitis gangrenosa perforata
N 2	22	11	15
Interval 4-8	4-48	10-48	14-72
X 6	20.091	24.909	34.067
S 2.828	12.641	12.661	19.073
Sx 2	2.695	3.817	4.925
Mediana 6	16	20	24
Mann-Whitney test		t = 5.00 , p= 0.042	

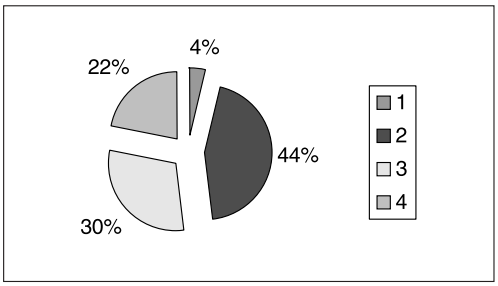

Figure 1. Patohistological findings in the examined group of patients. 1 apendicitis gangrenosa perforata; 2 apendicitis flegmonosa; 3 apendicitis catharalis; 4. apendicitis gangrenosa.

vention in all patients divided according to the pathohistological finding.

Using a suma range test we can see that 2/3 of patients with acute appendicitis have symptoms which last more than 24 h. There is a direct correlation between the percent of perforations and the period of lasting symptoms; and also time of delay of the hospital treatment and time of the observation before admitting to hospital have a significant influence.

In the following tables, using suma range test, we tested the possibility of using values

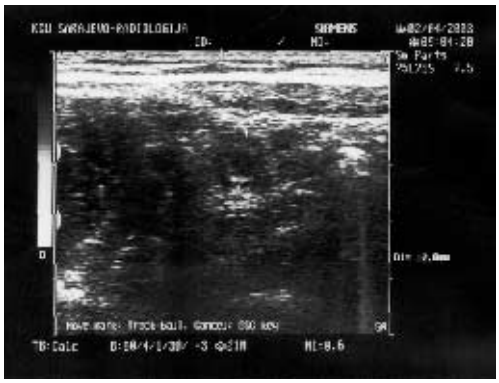

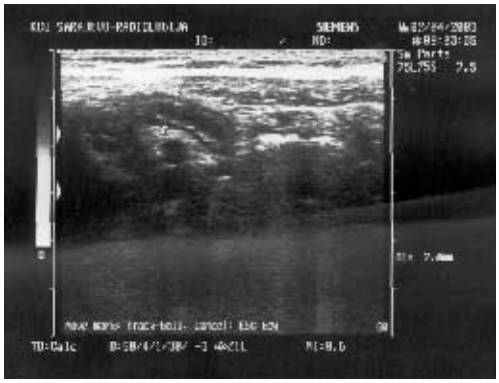

Figures 2a, 2b. Appendicitis phlegmonosa.

Table 4. Anterior-posterior (AP) diameter of appendix in the examined group of patients (n=48), except appendicitis catharalis (n=2)

	Appendicitis flegmonosa	Appendicitis gangrenosa	Appendicitis gangrenosa perforata
N	22	11	15
Interval AP diameter	7-12	10-18	9-14
X	9.318	13.455	11.067
S	1.427	2.659	1.534
Sx	0.304	0.802	0.396
Mediana	9	13	11
	T=-5,854; p<0,001	T=2.894; p=0,008	
Mann-Whitney test (app.flegmonosa vs app. perforata gangrenosa)		P=0,003	

Table 5. Mural wall thickness (MWT) of appendix in the examined group of patients (n=48), except appendicitis catharralis (n=2)

	Pathohistological finding		
	Appendicitis. flegmonosa	Appendicitis gangrenosa	App. gangrenosa perforata
N	22	11	15
MWT interval	2.5-4	3-5	2.8-5
X	3.145	3.664	4.056
S	0.436	0.612	0.816
Sx	0.093	0.185	0.204
Mediana	3	3.5	4
	p = 0.012*		
			p = 0.217*
Mann-Whitney test (app.flegmonosa vs. app. perforata gangrenosa)		p = 0.001*	

Table 6. Inflame surrounding fat tissue (FAT) around appendix in the examined group of patients (n=48) except appendicitis catharralis (n=2)

	Pathohistological finding		
	Appendicitis. flegmonosa	Appendicitis gangrenosa	App. gangrenosa perforata
n	22	11	15
MWT interval	7-13	9-15	11-20
X	10.045	12.182	14.200
S	1.430	2.272	2.426
Sx	0.305	0.685	0.626
mediana	10	12	14
	p = 0.013		
			p = 0.042
Mann-Whitney test (app.flegmonosa vs. app. perforata gangrenosa)		p < 0.001	

of: Anterior-posterior diameter (AP), Mural wall thickness (MWT), Inflame surrounding fat tissue (FAT) (Tables 4, 5, 6) in estimating of degree of appendix inflammation. Statistic analysis shows a great potential and possibilities of using AP and FAT in estimation of the inflammation degree in everyday practice. A statistical analysis shows the limited possibility of using mural wall thickness values in gangrenous appendicitis and perforate gangrenous appendicitis. In that case we use other ultrasound signs that can determinate these pathological conditions. Sensitivity of ultrasound method in our study is 85%.

Discussion

The incidence of appendicitis appearance is usually between 5-10 years of age. Homogeneity of the group is showed with mean value where it is proved that there is no significant difference in the examined age frequency ($p > 0.05$). Homogeneity of our group also showed that the appearance of acute appendicitis will be most common in age between 5 and 10 years, without gender predominance. Until puberty, the incidence of appendicitis is the same at boys and girls, and in the puberty prevalence is in male population with rate 2:1.[5] There is no significant connection between life style, taking some specific food or genetic predispose for arising of the acute inflammation of appendix.[6] Until 1986, the conventional radiography, including standard abdomen radiography and irigography, represents the only radiological methods, beside clinical and laboratory findings, that tried to limit the differential diagnosis of the acute appendicitis. Detailed classifying of the clinical examination can in certain percent reduced the differential diagnosis and constrains it to possible acute appendicitis: pain migration to lower right quadrant, pain deterioration because of motion, cough, anorexia and vomiting and indirect tenderness (Rovsing sign). Children with an »uncertain« diagnosis deserved further diagnostic imaging or observation depending to aspect and lasting of symptoms.

High percent of acute gangrenous appendicitis and perforate gangrenous appendicitis, which our study shows, suggests a long period of persisting symptoms until the hospital treatment. Unfortunately, only two patients had appendicitis catharalis. Percent of perforations and complications of the acute appendicitis in children's age is still very high. The reasons for that are because little patients don't recognise and don't show signs and symptoms of the disease, appearance of clinically atypical picture of the acute appendicitis, quick evaluation of disease in these patients, health ignorance of parents. Worell S *et al.* in its study on 200 patients offered only four criteria for the analysis of acute appendicitis: 1. visualisation of appendix, 2. anterior-posterior diameter AP > 6 mm, 3. mural thickness of appendix MWT > 3 mm, 4. appearance of complex mass in ileocaecal area. Because of limiting factors that characterized this study, its sensitivity was only 68%.[7]

Our study offered eight ultrasound signs of the acute appendicitis. Results showed that AP diameter, FAT and peristaltic absence are certain ultrasound signs of the acute appendicitis, and also FAT and AP have a great potential in defining the appendix inflammation degree, while MWT have a limited possibility in that case. According to the experience in our study, in patients without the possibility of visualisation of appendix, and with the appearance of good and clearly visible pericaecal fluid and changed pericaecal fat tissue, we can make a conclusion that it is perforate appendicitis.

Most common mistakes in US imaging of appendicitis compassed the commutation between appendix and terminal ileum, and also between normal and inflame appendix.[8]

Terminal ileum doesn't rise from caecum base, doesn't have blind terminal but shows

very accelerating peristaltic, and in transversal scanning it is oval describing to appendix which is clearly round as a »target«. False negative results in the ultrasound examination can appear in overweight patients and in atypical localisation of appendix.[9]

Conclusions

The initiation of ultrasound in diagnostic imaging of the acute abdomen allowed a high percent of diagnostic assurance in little patients. With the experience true continuous work with an ultrasound technique and by understanding of criteria of acute appendicitis, the improvement of diagnostic assurance can be achieved. The continuation of hospital observation and treatment increase the morbidity and mortality of patients with the acute abdomen. Concretely, the persistence of symptoms from beginning of the disease until the initial ultrasound examinations and surgical treatment is in a direct proportional relation with the degree of appendix inflammation. Anterior-posterior diameter (AP), mural thickness (MWT), periapendicular fat tissue width (FAT) represent highly reliable US signs in the evaluation of degree of the acute appendicitis inflammation. Ultrasound is a cheap method, without a harmful effect, quick and simple, and using a real-time interactive technique.

The aim of a modern surgical approach is essentially the same as in the 19th century, but today, it is focused between the percent of false negative appendectomies and the one of the perforation during the time of the surgical observation. The initiation of ultrasound in imaging of specific cases of the acute appendicitis, as this study shows, represents a modern (up to date) surgical approach and qualifies a modern medical protocol for little patients in this condition.

References

1. Tarjan Z, Jaray B. What are the sonographic sing of appendicitis? *European Congress of Radiology* 2000; **10(2 Suppl 1):** 115.
2. Wilson EB, Cole JC, Nipper ML, Cooney DR, Smith RW. Computed tomography and ultrasonography in the diagnosis of appendicitis: when are they indicated? *Arch Surg* 2001; **136:** 670-5.
3. Sivit CJ, Siegel MJ, Applegate KE, Newman KD. When appendicitis is suspected in children. *Radiographics* 2001; **21:** 247-62.
4. Pena BM, Taylor GA, Fisheman SJ, Mandl KD. Cost and effectiveness of ultra sonography and limited computed tomography for diagnosing appendicitis in children. *Pediatrics* 2000; **106:** 672-6.
5. Rettenbacher T, Hollerweger A, Macheiner P, Rettenbacher L, Tomaselli F, Schneider B, et al. Outer diametar of the verifirm appendix as a sign of acute appendicitis: evaluation at US. *Radiology* 2001; **218:** 757-62.
6. Hartamn GE. Acute Appendicitis. In: Jensen BK, editor. *Text book of pediatric*.16th edition. Philadelphia: W.B. Saunders Company; 2000. p. 1178-81.
7. Rettenbacher T, Hollerweger A, Macheiner P, Rottenbacher L, Frass R, Schneider B, et al. Presence or absence of gas in appendix: Additional criteria to rule out of confirm acute appendicitis - evaluation with US. *Radiology* 2000; **214:** 183-7.
8. Gutierrez CJ, Mariano MC, Faddis DM, Sullivan RR, Wong RS, Lourie DJ, et al Doppler ultrasound accurately screens patients with appendicitis. *Am Surg* 1999; **65:** 1015-7.
9. Velanovich V, Harkabus MA, Tapia FV, Gusz JR, Vallance SR. When its not appendicitis. *Am Surg* 1998; **64:** 7-11.

Radiol Oncol 2005; 39(1): 23-35.

review

The MR imaging as a one-way shopping tool for detecting and staging renal tumours

Galina Kirova

Department of Radiology, University Hospital Lozenetz, Sofia, Bulgaria

Background. *Magnetic resonance imaging is one of the most attractive approaches: the technology is widely available, it is not associated with the exposure to ionizing radiation, and does not require the injection of iodinated contrast agent. High-field strength clinical magnets, high-performance gradient hardware, and ultrafast pulse sequence technology are rapidly making the vision of a comprehensive »one-stop shop« urologic MR imaging examination a reality.*

Conclusions. *Difficulties that remain are related to the variable protocols of the examination and, therefore, it is mandatory to standardize as much as possible the techniques that are used in order to obtain reproducible information.*

Key words: kidney neoplasms - diagnosis; magnetic resonance imaging; neoplasms staging

Introduction

Since the only successful curative treatment of renal tumours is surgery, accurate radiological information is crucial during the initial tumour staging for an optimal operative planning. The preoperative assessment of renal carcinoma includes tumour size, tumour extent, in particular capsule invasion with tumour spread to perinephric fat with or without direct invasion of adjacent organs outside Gerota's fascia, regional lymph node metastasis, venous tumour thrombosis, and distant metastases.[1] Intravenous urography, angiography and ultrasound have been the main investigations for a long period of time. All these methods are complementary and each has advantages and disadvantages. None of these single methods are sufficient for the evaluation of all aspects involved in oncologic urologic pathology. Nowadays the pretherapeutic planning of renal carcinoma has dramatically improved in the use of cross-sectional imaging, in particular CT and MRI. Magnetic resonance imaging is one of the most attractive approaches: the technology is widely available, it is not associated with the exposure to ionizing radiation, and does not require the injection of iodinated contrast agent.[2]

Received 5 July 2004
Accepted 10 September 2004

Correspondence to: Galina Kirova, MD. PhD, Department of Radiology, University Hospital Lozenetz, 1 Koziak st, 1407 Sofia, Bulgaria; Phone: +359 888 401 678; E-mail: kirovag@yahoo.com

In recent years a number of reports on dynamic MRI have evaluated renal functioning and morphological changes. Dynamic MRI has proven able to integrate renal scintigraphy in documenting functional impairment and to supplement the information acquired by other imaging techniques on the morphology of the kidney.[3] Stimulated by the philosophy and results of the all-in-one examination for pancreatic neoplastic disease, Verswijvel *et al* invade a similar approach for the evaluation of urologic disease. Cross-sectional sequences, MR angiography in the arterial and venous phase, evaluation of the renal parenchymal and lesional perfusion, and contrast-enhanced MR urography were combined in one imaging session.[4] The method gained a widespread acceptance as a standard for patients in which several conventional complementary modalities must be performed and is fairly well illustrated for patients with neoplasms of the renal parenchyma or urothelium.

The aim of the paper is to describe an all-in-one approach protocol for MR examination of patients with suspected or proved renal tumours in order to achieve all necessary preoperative (pretreatment) information. Some explications of the possibilities and clinical usefulness of each one MR series will be done.

Paramagnetic contrast materials

Advances in the application of MRI in kidney's pathology depend predominantly on the use of magnetic resonance contrast

Table 1. Example of order of the sequences for an all-in-one approach protocol

1. AX T1 WI
2. AX T2 FSE WI
3. COR T2 FSE WI double echo half-Fourier acquisition single-shot turbo spin echo
   + FAT SAT
   + IN/OUT Phase T1
4. Furosemide+Gd (Gd-DTPA 0,2mmol/kg body weight, injection rate 2,5ml/s and Furosemide 0,1mg/kg body weight)
   Breath-hold 3D gradient echo MRA
   Breath-hold 3D gradient echo MRU
5. Postprocessing

Table 2. Parameters of the MR sequences (for GE 1.5T Signa). Phased-array torso coil. (TE-echo time, TR-repetition time, FA-flip angle, ST-slice thickness, FOV-field of view)

Pulse sequence	TR(ms)	TE(ms)	FA(')	ST(mm)	FOV(mm)	Matrix(mm)	orientation	Scan time
COR T2 SSFSF	2300	80	-	8	36	256/256	coronal	48s
COR T2 SSFSE	1300	200	-	3	36	256/160	obl	16s
AX T1 BH dual echo	160	2,2/4,4	80	8	36	256/128	axial	33s
AX T2 FRFSE	3000	85	-	8	36	256/256	axial	4,07min
AX 3D SPGR Dyn+CM	4,6	1,8	15	5	36	256/160	axial	20sec/phase
URO COR 3D SPGR	150	6	80	8	36	256/128	coronal	20s

agents to enhance both parenchyma and tumours. The most widely used contrast agents are chelates of gadolinium (Gd). Its chemical structure comprises a Gd-ion with a triple positive charge combined with a DTPA derivate, forming a very stable complex. The strongly paramagnetic gadolinium has several effects. It can change (relax) the magnetic state of hydrogen atoms in water molecules; this markedly changes the appearance of tissues, with a high contrast agent uptake in T1-weighted images, causing tissues to appear bright. High concentrations of gadolinium chelates can also induce local changes in the magnetic field (magnetic susceptibility). This is most apparent during the first pass of a bolus of contrast agent after the rapid intravenous injection. On gradient echo T2*-weighted images, this effect is apparent as a darkening of the image in well-perfused areas of tissue.

Gadolinium-DTPA is eliminated rapidly and completely by the renal excretion without tubular reabsorbtion. The half-time of Gd-DTPA in blood is ~90 minutes. More than 91% of the administrated dose is eliminated after 24 hours. The elimination depends only upon the glomerular filtration rate. The renal insufficiency is not a contraindication for the contrast material administration.

The recommended contrast dosage for magnetic resonance imaging of the kidneys is 0.1 mmol Gd-DTPA/kg BW. The administration of contrast material should be mechanical with the use of automatic injector after the correct timing of the bolus injection in order to synchronize the moment of the peak renal artery enhancement with the acquisition of central k-space data.[5]

The intravenous administration of an extracellular paramagnetic contrast material provides a means for imaging the circulation. Dynamic measurements, in which the uptake and washout of contrast in tissues is monitored with time, can assist in the diagnosis and can provide information on vascular permeability and perfusion, by quantifying and analyzing image intensity changes, and fitting these to analytical or model functions. Dynamic information shows the rate at which tissue enhances, and subsequently the rate at which contrast agent washes out. This depends on the delivery of the agent (perfusion), the ability of the agent to leak out of the vasculature (vascular permeability), and the extracellular volume. Usually, a region of interest (ROI) is selected within the tumour, and the software that is provided with the magnetic resonance scanner is used to evaluate the change in signal intensity with time in that ROI.

Technique of MR imaging of the kidneys

Patient positioning and coils

The patient is examined in supine position with both arms lying flat against the body, using a phased-array torso coil to optimize signal-to-noise ratio. Prior the examination patients would be informed about the necessity of breath-holding in some sequences.

Field strength

Presently recommended systems for the performance of MRI of the kidneys with contrast material have the field strength of 0.5 to 1.5T and most published studies using fast GE sequences have been performed on higher field strength systems. The advantage is that the paramagnetic contrast material has a greater effect on the signal due to the increased T1 relaxation time of enhancing tissues at higher field strengths. At the same time the high-field strength machines allow to perform fast techniques, required for the angiographic and dynamic studies.

Imaging protocol

The imaging protocol should be designed for the evaluation of the kidney and the entire upper urinary tract and should include unenhanced and enhanced phases.

Morphological assessment

The imaging protocol for renal tumour staging should include conventional or fast-spin echo sequences in axial and coronal projections for assessing the morphology of both kidney and tumour parenchyma.[6]

T2-weighted sequences

In T2-weighted sequences, hydrous or oedematous structures emit an intense signal. Spin-echo (SE) or fast-spin-echo (FSE) sequences are the T2-weighted sequences most commonly used in MR imaging of the abdomen. COR T2 weighted images using the half-Fourier acquisition single-shot turbo spin echo technique permits in a very short examination time to visualize kidneys, ureters and urinary bladder, giving the possibility for the rough orientation. Usually they are acquired before performing contrast enhanced dynamic measurements (Figures 1, 2a, 2b, 2c).

T2-weighted images are useful in recognizing small cysts only a few millimetres in diameter with high sensitivity.[7] This is an advantage of MR imaging compared with the CT, where the partial volume effect leads to confusion in such kind lesion characterization.

T1-weighted images

The axial T1WI focused at the kidney gives an excellent T1 contrast independent of patient breathing. If »bright« spots (hyperintense lesions in T1) are detected, breath-hold T1 *fat suppressed gradient echo pulse sequences* should be obtained to exclude or confirm the presence of fat lesion. This technique is especially useful in cases of the suspected intratumoural haemorrhage or fat-containing lesions.[8]

Chemical shift can be used as a tool for delineating structures that are surrounded by fat. Out-of phase images can aid in the demarcation of the renal contour, the margin of the adrenal glands, and the liver edge. Gradient-echo images that use out-of phase chemical shift demonstrate dark lines around organs embedded in fat. Those dark lines are created by the phase cancellation of the fat and water signals that exist within the voxels of the lipid-water interface. The width of the dark lines can be accentuated by increasing the field of view. The use of a narrower bandwidth will also increase the chemical sift banding seen on the images (Figures 3a, 3b, 3c).[9]

Chemical shift MR imaging has become a popular technique for diagnosing adrenal adenomas. Benign adrenal adenomas, which are typically composed of approximately 16% lipid based on *in vivo* studies,[10] can demon-

Figure 1. COR T2WI of a female patient with transitional cell renal cancer (arrow) of the left kidney. Note high-intensity bilobulated mass, obstructing the pelvicaliceal system of the kidney.

strate measurable differences in signal intensity when their appearance on in-phase gradient-echo images is compared with that on the

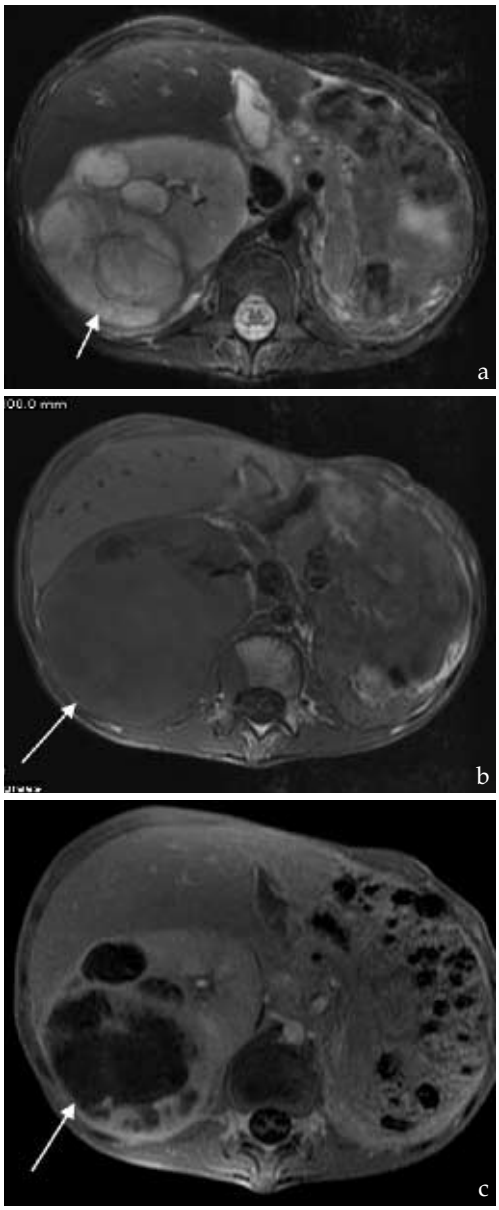

Figures 2a, 2b, 2c. 2WI (a), T1WI (b) and contrast enhanced T1WI (c) in a patient with relapsing Wilm's tumour demonstrating definite spread into the perirenal space (arrow). The structure of the tumour is nonhomogeniuos, highly vascularized with large areas of necrosis.

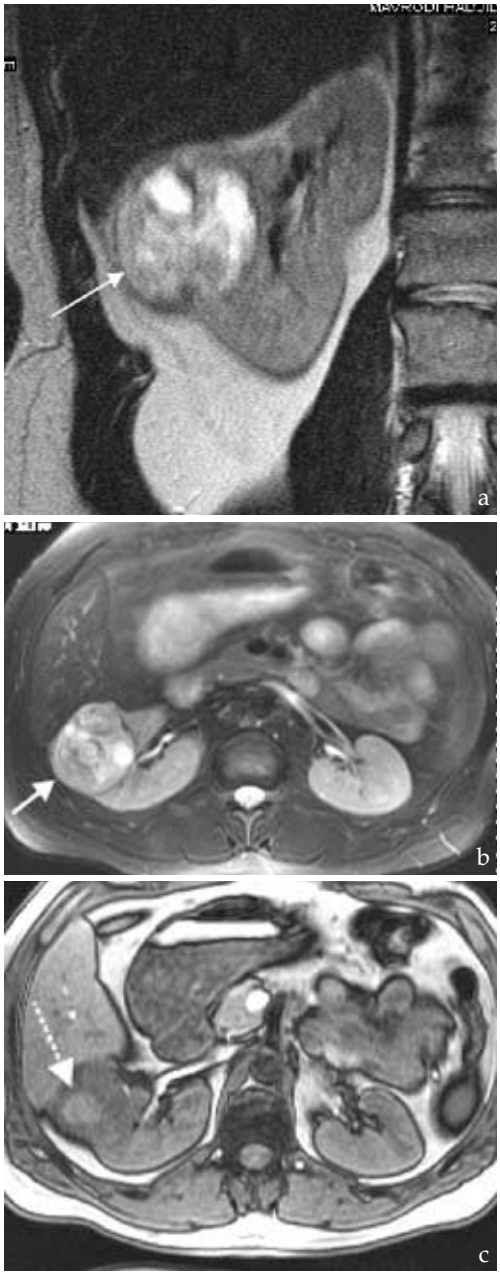

Figures 3a, 3b, 3c. COR and Ax T2WI of a 34 years old man with renal cancer demonstrate round high-intensity renal tumour, protruding the renal contours and invading the perirenal space (arrow in a and b). AX out-of phase T1 image of the same patient shows a mass invading into the inferior aspect of the liver, as evidenced by the interruption of the dark cortical line (arrow in c.) that demarcates the liver margin (c).

out-of-phase counterparts. A decrease in the signal intensity of greater than 20% within an adrenal mass on out-of-phase images helps to confirm the diagnosis of an adrenal adenoma.[11] Adrenal metastases, on the other hand, typically do not contain any significant lipid elements and will not demonstrate an appreciable change in the signal intensity with in-phase and out-of-phase chemical shift imaging (Figures 4a, 4b).

Combined morphological and functional assessment

Contrast-enhanced MRI

Multi-phase breath-hold 3D volume acquisition is the technique of choice for evaluating renal vessels and dynamic changes in renal parenchyma.[12,13]

Two technical developments are essential to the successful use of fast 3D MR sequence: the availability of high-performance gradient systems as well as dedicated surface coils. The implementation of high-performance gradient has enabled the acquisition of complex 3D sets with ultrashort repetition (TR) and echo (TE) times within a comfortable breath-hold period. The ultrashort TR in conjunction with a relatively high flip angle minimizes the signal of all abdominal tissues. Against this background, structures containing T1-shortening contrast agents can be made selectively visible.[14]

In the 3D technique, the entire part of the body is exited as a volume. This volume can be divided into the so-called partitions, or slices of variable thickness, in any desired plane. 3D imaging allows the depiction of thin slices without gaps in a defined slice profile. Generally a volume block of 150mm with, for example, 30 partitions is used for an examination with axial angulation. The resulting slice thickness is 5mm. The coronal angulation permits the use of a rectangular FOV. The resulting time gain allows the acquisition of a greater number of partitions, optimizing the spatial resolution.

For the purpose of tumor staging MRA is performed in the axial plane, with the top of the volume at the diaphragmatic level and the base below the level of lower renal poles. The volume should extend posteriorly to encompass both kidneys. This large field of view combined with an acquisition matrix of 512

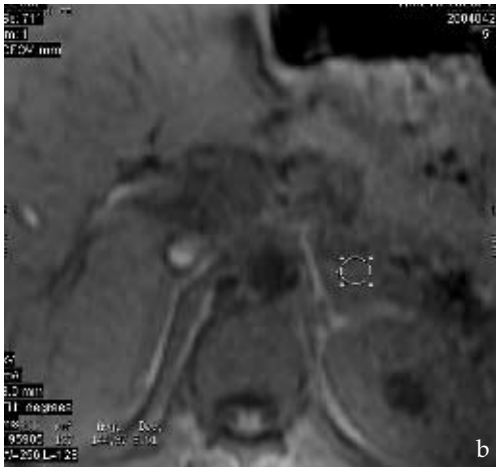

Figures 4a, 4b. AX in-phase (a) and out-of phase (b) T1 images of a 56-years-old man with metastatic clear cell renal carcinoma in the left adrenal glad. No differences in signal are seen on the two images. Metastases generally do not contain fat and do not exhibit the signal loss by chemical shift effects.

in frequency and 128-256 in phase-encoding direction is typically used. The use of multiphase sequence gives the possibility to repeat the series from three to ten times, depending on the suspected pathology.[5]

Angiography for preoperative arterial and venous mapping

The determination of the extent of intravenous tumour growth is of paramount importance, since it affects the operative approach in many cases. Venous involvement is one of the cornerstones of the surgical planning in renal tumours. A few studies have reported the usefulness of MR angiography in the preoperative assessment of venous involvement in patient with renal cell carcinoma, as well in tumour characterization. In the study of J.P. Laissay et al venous diameter enlargement was the hallmark of tumour thrombus, with a sensitivity of 84% and a specificity of 94%. At the same time the use of Gd-enhanced imaging improved the diagnostic yield of morphological data by additional information upon the thrombus enhancement (Figures 5, 6, 7a, 7b).[15]

Serial MR imaging for evaluation of renal parenchyma and tumour vascularity

Regarding the functional evaluation, the kinetics of gadolinium chelates during passage through the kidneys has been described in many reports. In the normal kidney four phases can be distinguished in the transit of the paramagnetic contrast agent through the parenchyma: the cortical, corticomedullary, medullary and excretory phases. For these reasons, the generally accepted guidelines require that dynamic measurements (at least five measurements after CM administration) have a temporal resolution of 20-25sec per sequence. This makes possible the discrimination between pathological processes and surrounding parenchyma, as well as the acquisition of a sufficiently accurate dynamic curve. Researches in this field have established the way in which changes in the kinetics of the

Figure 5. MR angiography in the arterial phase demonstrating gradual compression of the right external iliac artery from enlarged parailiac lymph nodes (arrow).

Figure 6. Parasagital T1 contrast-enhanced image of a retroperitoneal tumour in a 17 years-old male showing compression of the vena cava (arrow) and upper right renal pole (punctuate arrow) without invading or obstructing the vein.

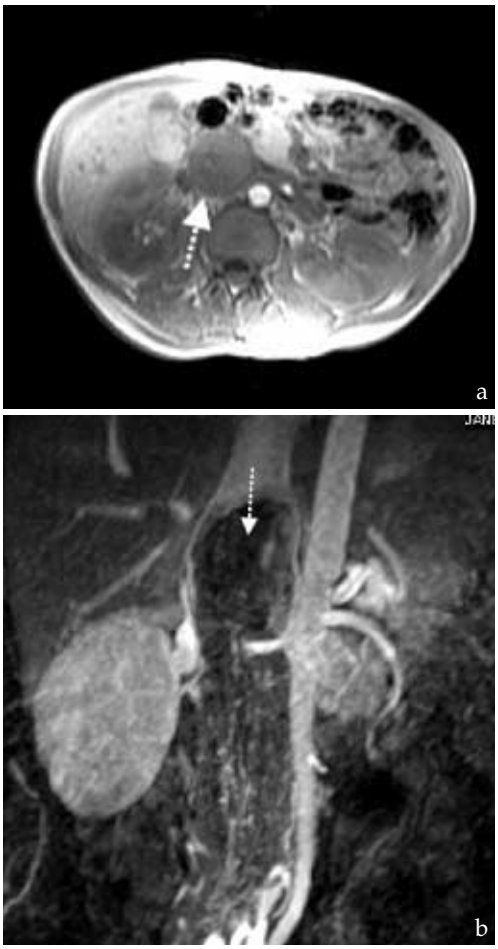

Figures 7a, 7b. Postcontrast MR imaging of a patient with large left renal cell carcinoma with thrombus within the left renal vein and IVC. Ax image shows thrombus within IVC (arrow in a.) resulting in a filling defect. Reconstructive image in coronal plane in the same patient shows the large thrombus extending into the vena cava up to the level of hepatic veins (punctuate arrow in b.).

contrast agents in the kidney reflect alterations in the renal function.[16-19] Administration of gadolinium compounds is not contraindicated in patients with the impaired renal function, and it is therefore possible to study renal perfusion and excretion in patients with a chronic renal failure by dynamic MRI.[20]

Assessing the corticomedullary phase alone may result in clinically significant errors, since small hypovascular tumours of the renal medulla may be missed since they are not sufficiently enhanced and hypervascular cortical renal cell carcinomas may enhance to the same degree as the normal cortex. During the early nephrographic phase inhomogeneous enhancement of the medulla may be also misinterpreted as a mass lesion. This artifact disappears later in the nephrographic phase.[21] Advantages of the corticomedullary phase include the differentiation of the normal variants of renal parenchyma from renal masses and the better depiction of tumour hypervascularity improving the characterization of solid renal mass lesions.[22]

The nephrographic phase is considered the optimal phase for the detection and characterization of renal masses, in particular of small renal masses, providing both homogeneous enhancement of cortex and medulla and lesion enhancement (Figures 8a, 8b).

In principle, it is possible to perform MRI examinations at any angulation. For dynamic MRU, the coronal slice orientation is generally preferred. The main advantage of the coronal slice orientation is that it permits the selection of a rectangular FOV, which makes to allow the reduction of the slice thickness and the optimization of the spatial resolution to ~2mm. The disadvantages are that the whole volume of the slab is reduced and it is not always possible to visualize the whole abdomen. This is very important in cases of abundant collateral vessels (after CVI thrombosis) or in cases of tumour staging, when the condition of the liver is crucial.

The axial slice orientation is that it makes a good assessment of the whole abdomen, which is of great importance in case of oncologic disease.

The sagittal and parasagittal orientation is not routinely recommended for use. They are, however, employed in the examination of pyelo-ureteral junction pathology and ob-

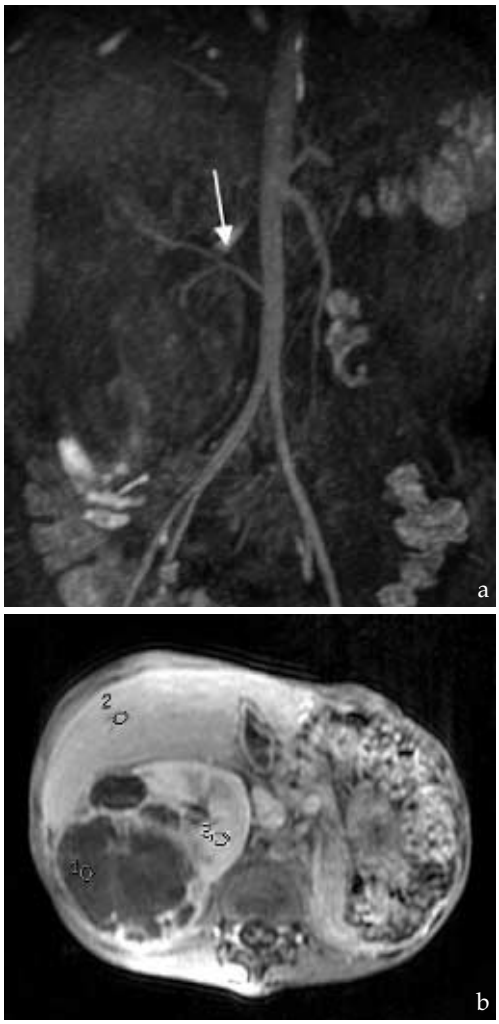

Figures 8a, 8b. Angiographic phase in a patient with relapsed Wilm's tumour (the same patient as in picture 2) showing a strengthed and displaced right renal artery (arrow in a.). Axial image of the same patient in the parenchymal phase, demonstrating the possibility of comparing the signal intensity levels in different tumor levels and the spared part of the kidney (b).

tained for each individual excretory system having the major advantage of data acquisition of nearly isovolumetric voxels. This is due to the fact that the effective slice thickness can significantly be reduced which increases the image resolution both in the native and MIP images.

MRU for evaluation of collecting system

The term MRU is used for a MR examination which combines different techniques for visualizing the urinary tract.[23] This can be performed with the so-called heavy T2 techniques receiving a signal from fluid-field structures or at the end of contrast-enhanced MR of the kidneys.[24,25] Later the collecting system and the ureters are visualized during the excretory phase as reformatted 3D images. MRU in the excretory phase provides the volume scanning of the kidney and the upper urinary tract within one breath hold. The visualization of the renal collecting system and ureter is significantly improved due to the avoidance of respiratory data misregistration improved resolution and data sets suitable for 2D and 3D reconstructions. The multiplanar reformation creates images similar in appearance to IVU. For this purpose the measurement volume should extend as far posteriorly as possible to encompass the pelvic segment of the ureters and anteriorly to encompass the anterior bladder wall. The top of the coronal volume should be set above the upper pole of the kidneys at the one end and just inferior of the bladder base at the other. In particular cases sagitally oriented images for each kidney could be performed using smaller field of view, reduced effective slice thickness and respective generating, more detailed images. The latter is obtained for each individual excretory system and has the major advantage of data acquisition of nearly isovolumetric voxels, which has a major benefit in the MIP images.

The lumen, the wall, the structures adjacent to the collecting system and ureter as well as the contrast enhancement are assessed on axial and MPR views. When pathology is depicted on axial images the reformatted images are of additional diagnostic value to the axial ones being not only a means to present an abnormality in an easily understandable manner. MRU has the potential to

become a primary investigation in the evaluation on the upper urinary tract; however, its sensitivity for the diagnosis of subtle urothelial lesions is unknown and needs to be evaluated by clinical validation studies (Figures 9, 10).

The evaluation of the images could be done on the original images (a), or on the edited MIP images (b) (Figures 11a, 11b, 11c).

Figure 9. Late pyelographic phase in the patient with relapsing Wilm's tumour showing the invasion of the collecting system and the level of displacement.

Figure 10. Picture in the late pyelographic phase in the patient with retroperitoneal tumour and the caudal displacement of the pelvi-caliceal system.

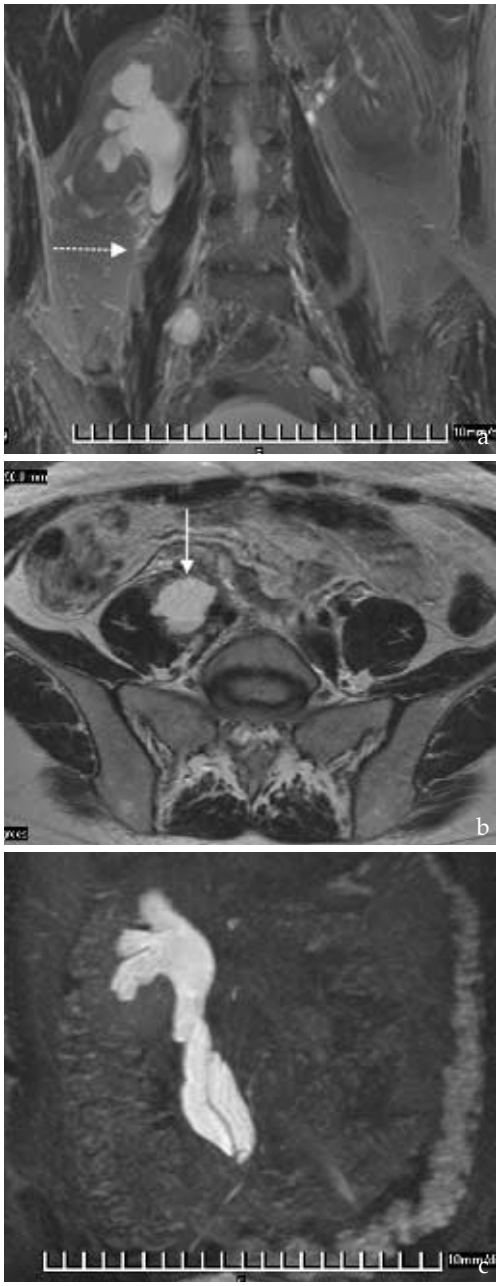

Figures 11a, 11b, 11c. Coronal and axial images in a patient with left renal cell carcinoma and retroperitoneal lymph nodes, leading to an obstruction of the right pyelo-ureteral system (arrow in a). Note the necrotic parailiac lymph node on the right side (arrow in b). Edited maximum intensity projection (MIP) of the MR urogram of the same patient (c).

Post processing

Postprocedure processing of the MRA and MRU data could be supplementary obtained by means of a maximum intensity projection algorithm. MIP technique yields a three-dimensional comprehensive view of both kidneys and their vessels. Based on post processed subtraction images in which only image pixels having at least a certain signal intensity are taken into account (threshold value algorithm), the representation of image information gives the impression of a real 3-dimensional angiographic or urographic views.[26] The resultant MIP images with subtraction techniques allow the adequate visualization of the renal vessels - renal arteries, renal veins and inferior vena cava. This form of imaging allows a simpler spatial orientation and is especially suitable for the presentation of suspicious findings.

MPR images allow the three-dimensional view of partial volumes within the abdomen. These are also based on postprocessed subtraction images. In special cases, these clarify the topographic relationship between a suspicious lesion and defined anatomical structures.

3D imaging of tumours using VRT and 3D data sets allow the ascertainment of the size (T1 and T2 staging) and the precise location of the tumour within the kidney as well of relation to the major vessels and the renal collecting system. This influences the decision as to whether nephron-sparing surgery can be performed. In case of tumour resection, the depth of incision can be calculated, the conservation of normal renal parenchyma is ensured and complications are minimized.[27,28]

In case of tumoural lesion, the time-resolved perfusion of the cortex of the lesion could be compared in a curve to the perfusion of the normal cortical parenchyma of the same kidney.

Conclusions

The concept of a comprehensive imaging evaluation has been an evolving theme during the past decade, with the vision of a complete examination that could be performed in a relatively short time. Advances in the rapid MRI technology and its application to oncology imaging have shown that MRI has a tremendous potential for the evaluation of renal tumours and renal disease in general. A comprehensive MR examination including CE 3D MRA, MRU and MR nephrogram offers several potential advantages compared with conventional X-ray studies. By combining all three techniques into an all in one protocol the same information can be obtained as with conventional studies; however, the patient convenience will be improved, the potential morbidity is lower and the substantial costs decrease. The use of contrast-enhanced dynamically collected multiplanar acquisitions permits local, lymph node, and hepatic staging, all within the same examination. At the same time the use of Gadolinium chelates are considered to be safe and can be performed in patients with the impaired renal function.

The combination of different MR techniques in one examination with the simultaneous morphologic and functional analysis appears to be the »Holly Grail« of Magnetic Resonance Imaging. Such kind of technique has several advantages:

1. The duration of the combined MR examination is approximately 30-40min.
2. The all-in one approach examination based on MR imaging provides the good visualization of the renal parenchyma, the renal vascular supply and the collecting system, irrespective of the renal function.
3. The combination of nonenhanced and enhanced MRU gives the possibility of the evaluation of both dilated and nondilated collecting systems.
4. The combination of standard MRI, MRA

and MRU expands the MR evaluation of patients with the oncologic disease of the urinary tract, which is probably the major current indication for the complex examination

References

1. Reznek RH. Imaging in the staging of renal cell carcinoma. *Eur Radiol* 1996; **6:** 120-8.
2. McClennan BL, Deyoe LA. The imaging evaluation of renal cell carcinoma; diagnosis and staging. *Radiol Clin North Am* 1994; **32:** 55-69.
3. Frank JA, Choyke PL, Austin HA 3rd, Girton ME, Weiss G. Gadopentetate Dimeglumine as a marker of renal function. Magnetic resonance imaging to glomerular filtration rates. *Invest Radiol* 1991; **26(Suppl 1):** S134-6.
4. Verswijvel GA, Oyen RH, Van Poppel HP, Goethuys H, Maes B, Vaninbrouckx J, et al. Magnetic resonance imaging in the assessment of urologic disease: an all-in one approach. *Eur Radiol* 2000; **10:** 1614-9.
5. Dong Q, Schoenberg SO, Carlos RC, Neimatallah M, Cho KJ, Williams DM, et al. Diagnosis of renal vascular disease with MR angiography. *Radiographics* 1999; **19:** 1535-54.
6. Jeong JY, Kim SH, Lee HJ, Sim JS. Atypical low-signal-intensity renal parenchyma: causes and patterns. *Radiographics* 2002; **22:** 833-46.
7. Levine E. Acquired cystic kidney disease. *Radiol Clin North Am* 1996; **34:** 947-64.
8. Helenon O, Merran S, Paraf F, Melki P, Correas JM, Chretien Y, et al. Unusual fat-containing tumors of the kidney: a diagnostic dilemma. *Radiographics* 1997; **17:** 129-44.
9. Hood MN, Ho VB, Smirniotopoulos JG, Szumowski J. Chemical shift: the artifact and clinical tool revisited. *Radiographics* 1999; **19:** 357-71.
10. Leroy-Willig A, Bittoun J, Luton JP, Louvel A, Lefevre JE, Bonnin A, et al. In vivo MR spectroscopic imaging of the adrenal glands: distinction between adenomas and carcinomas larger than 15mm based on lipid content. *AJR Am J Roentgenol* 1989; **153:** 771-3.
11. Reinig JW, Stutley JE, Leonhardt CM, Spicer KM, Margolis M, Caldwell CB. Differentiation of adrenal masses with MRI: comparison of techniques. *Radiology* 1994; **192:** 41-6.
12. Halpern EJ, Mitchell DG, Wechsler RJ, Outwater EK, Moritz MJ, Wilson GA. Preoperative evaluation of living renal donors: comparison of CT angiography and MR angiography. *Radiology* 2000; **216:** 434-9.
13. Glockner JF. 3D Gadolinium enhanced MR angiography: applications for abdominal imaging. *Radiographics* 2001; **21:** 357-70.
14. Vosshenrich R, Fischer U. Contrast-enhanced MRA of abdominal vessels: is there still a role for angiography? *Eur Radiol* 2002; **12:** 218-30.
15. Laissy JP, Menegazzo D, Debray MP, Toublanc M, Ravery V, Dumont E, et al. Renal carcinoma: diagnosis of venous invasion with Gd-enhanced MR venography. *Eur Radiol* 2000; **10:** 1138-43.
16. Schoenberg SO, Bock M, Aumann S, Just A, Essig M, Floemer F, et al. [Quantitative recording of renal function with MR tomography]. [German]. *Radiologe* 2000; **40:** 925-37.
17. Baumann D, Rudin M. Quantitative assessment of rat kidney function by measuring the clearance of the contrast agent Gd(DOTA) using dynamic MRI. *Magn Reson Imaging* 2000; **18:** 587-95.
18. Prasad PV, Priatna A. Functional imaging of the kidneys with fast MRI techniques. *Eur J Radiol* 1999; **29:** 133-48.
19. Katzberg RW, Buonocore MH, Ivanovic M, Pellot-Barakat C, Ryan JM, Whang K, et al. Functional, dynamic, and anatomic MRU: feasibility and preliminary findings. *Acad Radiol* 2001; **8:** 1083-99.
20. Dalla-Palma L, Panzetta G, Pozzi-Mucelli RS, Galli G, Cova M, Meduri S. Dynamic magnetic resonance imaging in the assessment of chronic nephropathies with impaired renal function. *Eur Radiol* 2000; **10:** 280-6.
21. Birnbaum BA, Jacobs JE, Ramchandani P. Mutiphasic renal CT: comparison of renal mass enhancement during the corticomedullary and nephrograohic phases. *Radiology* 1996; **200:** 753-8.
22. Knesplova L, Krestin GP. Magnetic resonance in the assessment of renal function. *Eur Radiol* 1998; **8:** 201-11.
23. Nolte-Ernstin CCA, Adam GB, Gunter RW. MRU: examination techniques and clinical applications. *Eur Radiol* 2000; **11:** 355-72.
24. O'Malley ME, Soto JA, Yucel EK, Hussain S. MR Urography: evaluation of a three-dimensional Fast

Spin-Echo technique in patients with hydronephrosis. *AJR Am J Roentgenol* 1997; **168:** 387-92.

25. Nolte-Ernsting CC, Tacke J, Adam GB, Haage P, Jung P, Jakse G, et al. Diuretic-enhanced Gd excretory MRU: comparison of conventional gradient-echo sequences and echo-planar imaging. *Eur Radiol* 2001; **11:** 18-27.

26. Stringer WA. MRA image production and display. *Clin Neurosci* 1997: **4:** 110-6.

27. Coll DM, Herts BR, Davros WJ, Uzzo RG, Novick AC. Preoperative use of 3D volume rendering to demonstrate renal tumors and renal anatomy. *Radiograpics* 2000; **20:** 431-8.

28. Winterer JT, Strey C, Wolffram C, Paul G, Einert A, Altehoefer C, et al. [Preoperative examination of potential kidney transplantation donors: value of gadolinium-enhanced 3D MR angiography in comparison with DSA and urography]. [German]. *Rofo* 2000; **172:** 449-57.

Radiol Oncol 2005; 39(1): 37-47.

Is quadrant biopsy adequate as first-line sampling scheme in men likely to have non-organ-confined prostate cancer: comparison to extended biopsy protocol

Zoran Brnić [1], Petar Anić [1], Slavko Gašparov [2], Nikola Radović [3], Damir Kučan [3], Željko Vidas [3], Žarko Zeljko [3], Petar Lozo [5], Vesna Ramljak [6]

[1]Department of Diagnostic and Interventional Radiology, [2]Department of Pathology, [3]Department of Urology; University Hospital Merkur, Zagreb, Croatia; [4]Poliklinika Lozo, Department of Ultrasound, Zadar, Croatia; [5]University Hospital for Tumors, Zagreb, Croatia

Background. *While extensive prostate biopsy (PB) in the patients with early prostate cancer (PC) provides better sensitivity and more precise tumour staging, in the patients with advanced PC, it is virtually only a confirmation of malignancy. The purpose of our study was to find out whether the quadrant prostate biopsy (QPB) provides a sufficient first-line pathological evaluation in the patients likely to have advanced PC, and whether the reduction of core number impairs the competence of PB through missing quantitative histology information.*

Methods. *We studied 84 men who underwent PB and classified into groups »H« (highly-) and »L« (low likely to have advanced PC). Pathological results of 5-12 cores PB and simulated QPB were retrospectively compared, particularly for the presence of PC, tumour volume, Gleason score (GS), and the presence of high-grade prostatic intraepithelial neoplasia (HGPIN).*

Results. *The PC detection rate was not impaired in group H, but dropped significantly in group L, while the percentage of positive cores was insignificantly changed in group H (p=0.39), but significantly decreased in group L (p=0.04) due to the sampling scheme reduction. No HGPIN was missed with QBP in group H, while 2 HGPIN were missed in group L. Insignificant GS changes resulted in both groups as a consequence of the limitation to QPB.*

Conclusions. *QPB is an appropriate first-line scheme in the patients with advanced PC as the information lost due to the core number reduction is mainly not critical for patient management.*

Key words: prostatic neoplasms - pathology; biopsy, needle; prostate-specific antigen

Received 26 July 2004
Accepted 9 August 2004

Correspondence to: Zoran Brnić, MD, PhD, University Hospital "Merkur", Department of Diagnostic and Interventional Radiology, Zajčeva 19, 10000 Zagreb, Croatia. Phone: +385 98 199 12 26; Fax: +385 1 243 14 14; E-mail: zoran.brnic@zg.htnet.hr

Introduction

Standard sextant prostate biopsy (PB) is proved to be of limited sensitivity in prostate cancer (PC) detection. An increase of the number of tissue cores per PB session improves the PC detection rate,[1-5] and contributes to a

better preoperative staging accuracy.[6-8] Recently, many urologists abandoned biopsying hypoechoic focal lesions, and focused on systematic sampling of the gland with as much cores as possible. Although even he extensive PB was proved to be relatively safe, discomfort and minor complications occur in many patients;[9-11] it is therefore sensible to avoid them if possible. In the *patients with presumed high tumour burden*, with regard to PSA level, suspicious digital rectal examination (DRE) or transrectal ultrasound (TRUS), and suspicion of metastases,[12-15] it does not seem reasonable to take large number of cores in initial PB because PC has very probably spread all over the gland volume, and exact assessment of intraprostatic tumour distribution is of minor importance. As these men are at high risk to have a non-organ-confined (NOC) PC, they are rarely candidates for radical prostatectomy (RP); hence only histological confirmation of the diagnosis of prostatic malignancy is virtually needed. There is scant literature[16] dealing with the possibility to reduce the PB protocols when an extensive sampling is not strictly necessary in order to spare the invasiveness of the procedure and its costs.

We hypothesized that the extensive first-line PB is redundant in the *patients with presumed high tumour burden*, and that the quadrant PB (QPB) can fulfil the task of preoperative pathological evaluation in the patients likely to have NOC PC. The purpose of the present study was to investigate whether the reduction of core number from 5-12 to 4 in the patients in whom PSA and/or clinical evaluation indicate high likelihood to have NOC PC, would impair the diagnostic competence of PB through missing clinically relevant information usually obtained by this procedure.

Patients and methods

Patients

We retrospectively studied 84 consecutive patients (mean age 71.8 years, range 50-89) in whom systematic PB was performed during one-year period. The men were previously untreated for PC and biopsied for the first time. The patients were classified into two study groups according to serum PSA, DRE and TRUS findings, the factors which can

Table 1. Selection criteria for stratifying the patients into two categories according to probability of the presence of advanced (non-organ confined) PC. Number of patients in each sub-category is given.

Likelihood for the presence of advanced PC	PSA[a] level	TRUS[b] and DRE[c] finding	Number of patients
Low	<4 ng/mL	TRUS suspect or DRE suspect	5
Low	4-10 ng/mL	TRUSP non-suspect and DRE non-suspect	24
High	<4 ng/mL	TRUSP suspect and DRE suspect	4
High	4-10 ng/mL	TRUSP suspect and/or DRE suspect	12
High	>10 ng/mL	Irrespective of TRUS and DRE-finding	39
Total			84

[a] PSA test (Elecsys 1010, Roche Diagnostics GmbH, Manheim, Germany) was done prior to any prostate manipulation, to avoid false positive findings; no patients in our series had acute prostatitis (possible cause of elevated PSA); mean prostate size was similar in groups H and L.

[b] TRUS was considered suspicious of malignancy if hypoechogenic sector or nodule in peripheral zone was detectable, if the prostate was inhomogeneous without zonal discrimination, or if unsharp prostate margins or infiltration of extraprostatic tissues was seen.

[c] DRE was considered suspicious of malignancy if considerable irregularity of the prostate surface, »rocky hard« induration/nodule or considerable asymmetry is detected on palpation.

Abbreviations: PC = prostate cancer, PSA = prostate-specific antigen, TRUS = transrectal ultrasound, DRE = digital rectal examination

predict the PC burden in a patient.[12-15] The group more likely to have NOC PC (*high* tumour burden) is assigned »H«, while other patients (with presumed *low* tumour burden) are classified in »group L«. The selection criteria for the groups are listed in Table 1.

Prostate biopsy protocol

We perform US-guided PB by transrectal approach, routinely taking 6-8 tissue cores from <50 cm^3 of prostate glands, and 8-12 cores from >50 cm^3 of glands at the first-line PB. Six cores are taken from the very lateral parts of peripheral zone at the base, mid-gland and apex bilaterally, followed by additional cores from the posterolateral parts of peripheral zone, similarly to protocols used in the studies.[17,18] The number of cores intended to be taken in a particular patient is dependent exclusively upon the prostatic size, irrespective of the parameters of suspicion for PC. However, we occasionally reduce the number of cores *ad hoc* if bleeding from haemorrhoids occurs, or on the patient's demand due to pain. We usually obviate more medial cores, as also those less expected to be positive.[1,2] As a consequence of such approach, the material in the present study consists of 5-12 cores per biopsy session.

Equipment and technique

HP ImagePoint ultrasound system (Hewlett-Packard Company, Andover, MA, USA) with 5.0-7.5 MHz sector endorectal probe and plastic biopsy needle guide was used to assist PB, performed with spring-loaded Bard Magnum device (Bard Urological Division, Covington, GA, USA) coupled with 18-G-needles. A new needle was taken for every 3 - 4 tissue cores. Biopsy cores from different sites of the prostate were submitted for analysis in individually labelled separate containers,[19] and core sites were charted on a dedicated form. Pathologist (G.S.) who analysed the specimens was unaware of the aims of this study.

Methods

Pathological report for the entire set of PB samples (5-12 cores) was available for each patient. We verified each individual tissue core whether it was positive for PC, and whether high-grade prostatic intraepithelial neoplasia (HGPIN) was present. Gleason score (GS) was determined on the basis of the complete 5-12 PB set. With the evidence of pathohistology of the complete set of biopsies (5-12 cores) for each patient, we simulated the situation as if only 4 biopsy cores would have been taken (quadrant PB, QPB). In the hypothetical biopsy scheme the apical and medial cores were eliminated. For each patient, we retrospectively compared the pathological results of the actual complete 5-12 PB with the presumed results of QBP. The two compared sampling schemes are shown in Figure 1. The following relevant pathologic parameters were considered in comparison of the two PB schemes: presence of PC in the prostate, presence of HGPIN and percentage of positive cores. Additionally, for the purpose of the study only, the same pathologist (G.S.), unaware of previously reported GS,

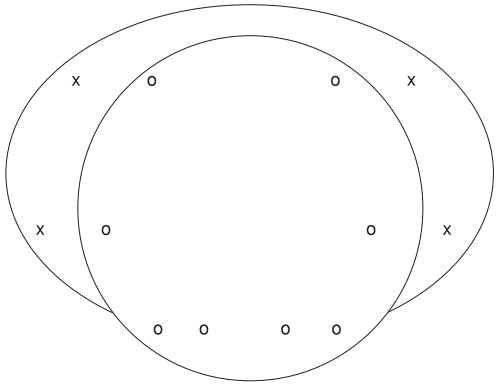

Figure 1. The distribution of biopsy sites in the two compared sampling schemes: o + x = 5-12 PB scheme, x = QPB scheme.

determined GS for each patient on the basis of the set of 4 cores, which matched the sites of QBP. GS was then compared with that determined from 5-12 PB. T-test was used in statistical analysis.

Oral and written *informed consent* was obtained from each patient before PB, and information on possible complications of systematic PB was given. Our study did not influence the patient management in any way, as QPB was only an imaginatively rather than really applied procedure. Local Medical Ethics Committee approved this investigation.

Results

The mean age of patients was 71.8 years (range, 50-89), and did not differ significantly between the groups H and L (71.2 vs. 72.9 years, p=0.86). The mean *PSA* for the whole series was 36.3 ng/mL (range, 0.03-346); significant difference (p=0.0002) was observed between group H (52.9 ng/mL, range 1-346) and group L (5.8 ng/mL, range 0.03-9). *Prostate volume* ranged 16-192 cm3, and did not differ significantly between the groups H and L (63.2 vs. 63.7 cm^3, p=0.19). *GS* determined from the 5-12 BP and QPB material are given in Table 2. Positive correlation between GS and PSA (c=0.39), and between GS and the percentage of positive cores (c=0.53) was shown in the 5-12 PB material. GS determined from the QPB material did not differ significantly from GS determined from the material of 5-12 PB, either for the whole series, or for each particular study groups H (p=0.13) and L (p=0.12), with a maximum individual difference of 2 points. In one L-patient, GS=4 was overgraded as GS=6 from the QPB material, while in one H-patient GS=8 was undergraded as GS=6 also from the QPB material. In 22/46 (47.8%) patients, GS defined by both PB sets was identical, while in 20/46 (43.5%), it was undergraded, and in 2/46 (4.4%) overgraded by 1 point by QPB. Overall results of 5-12 PB and QBP for groups H and L are shown in Tables 3 and 4. Total number of cores taken from 84 patients was 605. Median number of cores per PB was 8 (range 5-12). Of all cores, 54.5% were positive for PC: 69.3% in group H, and 14.1% in group L. The percentage of positive cores in the 5-12 PB and QPB material in both compared study groups are shown in Tables 5 and 6. In 19/84 (22.6%) patients, all cores in the 5-12 PB material were positive for malignancy (1 patient in group L, 18 patients in group H). The number of patients with PC detected in only one tissue core in both PB materials is shown in Tables 3 and 4. Pathological results allowing for the following parameters, presence of PC, presence of HGPIN, and percentage of positive cores for two different PB schemes are shown in Tables 5 and 6. The data, which

Table 2. Gleason scores determined from 5-12 PB and QPB material.

Gleason score	5-12 PB	QPB	Difference observed
Overall series	median 6	median 6	0
	mean 6.59	mean 6.32	p=0.13 (NS)
	range 3-9	range 3-9	
Group H	median 7	median 6	-1 point
	mean 6.79	mean 6.36	p=0.13 (NS)
	range 4-9	range 3-9	
Group L	median 4	median 5	+1 point
	mean 4.50	mean 5.50	p=0.12 (NS)
	range 3-5	range 4-6	

Abbreaviations: PB=prostate biopsy, QPB=quadrant prostate biopsy, NS=non-significant

would have been missed if only QPB were done, are given in the last column.

Discussion

The two fundamental shortages of systematic PB - its sampling error and invasiveness, lie in reciprocity: sampling extensiveness decreases sampling error at the cost of higher patient discomfort and postbiopsy morbidity. The recent tendency to increase the number of cores per one PB session is based on the evidence that an extensive sampling yields a higher PC detection rate and staging accuracy.[2-4,6-8,17,19,20] To balance the diagnostic yield and risk, the PB protocol needs to be individualized for each patient according to his PSA level, TRUS and DRE findings, prostate volume, age and life expectancy. In the present

Table 3. Overall results of 5-12 PB outcome: the number of patients in each study group with respect to the presence of PC and PIN

Patient group	5-12 PB positive for PC		5-12 PB negative for PC		Total
	>1 core positive	1 core positive	no PIN	HGPIN+LGPIN	
L	3	5	10	4+7	29
H	43	1	3	5+3	55
Total	46	6	13	9+10	84

Abbreviations: PB=prostate biopsy, PC=prostate cancer, LGPIN = low-grade prostatic intraepithelial neoplasia, HGPIN = high-grade prostatic intraepithelial neoplasia

Table 4. Overall results of QPB outcome: the number of patients in each study group with respect to the presence of PC and PIN

Patient group	QPB positive for PC		QPB negative for PC		Total
	>1 core positive	1 core positive	no PIN	HGPIN+LGPIN	
L	1	4	15	2+5	27
H	42	2	6	5+2	57
Total	43	6	21	7+7	84

Abbreviations: PB=prostate biopsy, PC=prostate cancer, LGPIN = low-grade prostatic intraepithelial neoplasia, HGPIN = high-grade prostatic intraepithelial neoplasia

Table 5. Comparative results of different PB schemes in group H

Parameter analysed	5-12 PB	QPB	Missed with QPB
Presence of PC	44	44	0
Presence of PIN	5 HGPIN	5 HGPIN	0
	3 LGPIN	2 LGPIN	1 LGPIN
Percentage of positive cores	69.3%	63.1%	6.2%, p=0.39 (NS)

Abbreviations: PB=prostate biopsy, QPB=quadrant prostate biopsy, HGPIN=high-grade prostatic intraepithelial neoplasia, LGPIN=low-grade prostatic intraepithelial neoplasia, NS=non-significant

Table 6. Comparative results of different PB schemes in group L

Parameter analysed	5-12 PB	QPB	Missed with QBP
presence of PC	8	5	3
presence of PIN	4 HGPIN	2 HGPIN	2 HGPIN
	7 LGPIN	5 LGPIN	2 LGPIN
percentage of positive cores	14.1%	9.8%	4.3%, p=0.04

Abbreviations: PB=prostate biopsy, QPB=quadrant prostate biopsy, HGPIN=high-grade prostatic intraepithelial neoplasia, LGPIN=low-grade prostatic intraepithelial neoplasia, NS=non-significant

study, we focused our attention to the patients with high laboratory and clinical suspicion of advanced PC. Despite the presumptive diagnosis of PC, most of these men have to undergo PB to obtain the tissue diagnosis before treatment with androgen ablation. A very accurate staging is mostly not critical for the therapy, which is rarely radical. Extensive sampling protocols do not seem to be reasonable in the first-line BP in such patients, because the confirmation of prostate malignancy and orientation on tumour biology could be reached even with few biopsy cores, and unnecessary discomfort, risks and costs may be avoided by such an approach.

Cancer detection rate (sensitivity) can decrease due to PB scheme reduction for two reasons: overall sampling density reduction and eliminating the gland areas, in which PC is frequently located, from sampling. The impact of sampling density on the sensitivity of PB is well known.[2-5,17,20] It is particularly expressed in the patients with negative DRE and TRUS, and PSA<10 ng/mL,[3,4] corresponding to patient population similar to our group L. Thus, the strategy of reducing PB protocol does not seem convenient *for* the *men with presumed low tumour burden* because only the extensive sampling provides a proper sensitivity for the early detection of a potentially curable malignancy.[4] This is concordant to our results: using QBP in group L, 3 of 8 PC would have remained undetected, which is a considerable drop of sensitivity. However, in the *men with presumed high tumour burden*, the risk that PC will remain undetected with limited number of cores is little because their tumour is probably not small, and cancer-free areas in prostate are less likely to exist. Moreover, as many PC are predominantly infiltrating rather than only expansive, even the finding of cancer-free cores does not warrant that this part of the prostate is not involved. Our results reassured these assumptions: QPB would detect malignancy in all 44 men with PC detected with 5-12 PB protocol in group H, with neither significant nor insignificant PC missed due to sampling scheme reduction. Other authors similarly showed that PC detection rate is less affected by the core number increase in the patients with PSA>10 ng/mL, while significantly improved in those with PSA<10 ng/mL.[1,3,20] Aus *et al.* showed that the reduction of sextant PB protocol to QPB resulted in the decrease of sensitivity for PC by only 4% in the patients with elevated PSA and positive DRE and/or TRUS.1 Damiano *et al* have recently demonstrated that the reduction of 14- to 8-cores regimen resulted in only 3.1% lower PC detection rate, and concluded that 8-cores PB may be appropriate as initial PB for general male population.[16]

A question arises whether, in the series larger than our, some H-patients positive for PC on 5-12 PB would have appeared negative on QPB. As a rule, any patient with *high suspicion of PC* and negative initial PB have to be rebiopsied, and rebiopsy need to be more extensive than the first-line PB.[2] In such a way, a part of false-negative H-patients on QPB will be correctly detected as positive. Thus, adhering to QPB as the first-line BP in H-patients, we spare discomfort and costs in at least 98% of positives on initial QBP, paying the price of rebiopsy in <2.2% (theoretically 1 of ≥45) false negatives on QPB. This »price« is considerably lower than unnecessary extensive sampling in every H-patient, which yields no clinically relevant information for these patients.

Excluding different prostate areas from sampling will yield in the same sensitivity decrease because the likelihood to be an origin of PC varies. We eliminated medial biopsies in our reduced PB because the medial cores are less frequently positive for PC than the lateral ones,[1,2,4,17] and the lateral parts of peripheral zone can be sampled by transrectal approach more efficiently than the medial parts. As the biopsy needle passes more orthogonally across the posteromedial periph-

eral zone and more longitudinally through the lateral parts of peripheral zone, the lateral tissue cores almost completely include peripheral zone, while the medial cores usually include also a considerable part of transitional zone. Finally, it is our impression that medial passes cause bleeding more frequently than lateral ones and that they are more painful. It seems harder to argument apical biopsies elimination from the first-line PB protocol. Quite a lot of PC are localized near the midline at the prostate apex,[2,17] which may remain undetected after the exclusion of apical biopsies from the first-line PB. Two apical biopsies added to 2 middle lobar lateral biopsies increase the sensitivity by 13%,[1] and most tumours missed on the initial BP were located just in apico-dorsal region.[2] Nevertheless, the apex-directed PB have superior sensitivity compared with the sextant PB in the patients with PSA<10 (comparable to our group L), but the sensitivity was lower than in the sextant PB in the patients with PSA>10 (comparable to our group H).[21] This may indicate that the sampling of the apex is unavoidable only for the detection of early stage PC, while less critical when an advanced PC is more probable. Therefore, when searching for PC in general population or population similar to our group L, it would not be advisable to obviate apical cores. In H-patients, however, even if originated in the apex, PC would probably have infiltrated into the majority of the gland, with positive basal and mid-gland cores, and would possibly be NOC. Obviating the apical cores in such patients would consequently not be critical for PC detection rate, as we have confirmed in our results.

»One-core« prostate tumours. In men with limited life expectancy, it is important to determine whether T1c PC is clinically significant and needs treatment at all. As tumour significance is related to its volume (>0.5 mL), hence to the number of cores that contain neoplastic tissue,[22] PC detected as only one positive core may be insignificant. A dilemma arises of how many biopsies should be performed to increase the overall PC detection rate without over-diagnosing clinically insignificant neoplasms,[5,22] and whether a less extensive sampling decreases that risk.

In our group L, 5 of 8 tumours were detected as »one-core tumours« on 5-12 PB. On QPB, 1 of 5 »one core CP« would have been missed. In low range PSA patients, many PCs are detected by chance, being not responsible for patient's clinical presentation, and missing such an insignificant PC is not detrimental, particularly if PC tumour is of low aggressiveness. However, in group L, 2 of 3 significant CP would have also been missed on QPB - a considerable drop of overall PC detection rate.

In group H, the number of »one-core PC« increased from 1 to 2. One PC with GS=8, which was detected in 2 adjacent cores on 5-12 PB, would have become »one-core PC« on QPB. This patient would have been managed similarly, irrespective of the number of positive cores, due to its high GS. Even if some insignificant PC would remain undetected on QPB in group H (if our series were larger), this would not be a serious shortcoming as such small PC is not likely to be responsible for clinical and laboratory presentation, which, indeed, prompted PB in group H. Such a small PC could be detected in many H-patients on an extensive rebiopsy, and its significance would be estimated from the complete set of cores.

Organ confinement of the tumour. The ability of pre-treatment variables to identify the patients with organ-confined PC (OCPC) is a challenging issue. The presence of extraprostatic extension (EPE) is a feature of T3-stage, unfavouring radical treatment. The tumour volume is an important independent predicting parameter of the margin status and disease progression after RP, and underestimation of tumour volume may result in overindication of RP. Number, percentage and bilaterality of positive cores in PB are valuable

predictors of tumour volume, EPE and prognosis.[5-8,19] Ipsilateral EPE is more likely, as the number of positive biopsies on that side increases, while the patients with >3 and bilaterally positive cores had greater likelihood of EPE.[8] It was demonstrated that such quantitative histology data are especially valuable in the *men with presumed low tumour burden* (similar to our group L), thus better predicting the final pathological stage.[19] Therefore, the information on the percentage of positive cores in PB must not be sacrificed in any reduced sampling scheme, particularly in group L in which RP is often considered as a treatment option.

In only one patient in group H, PC was detected with one instead of ≥2 positive cores, and in only one patient with 2 instead of 3 positive cores, as a consequence of scheme reduction to QPB. This does not preclude the use of QPB as the first-line PB scheme in H-patients.

Grossklaus et al. compared <6 vs. >6 cores PB and concluded that the reduction of core number could impair the PC detection rate, but not other information, particularly the percentage of positive cores and bilaterality of PC.[5] In our study, the percentage of positive cores decreased significantly (14.1% to 9.8%, p=0,04) in group L, but insignificantly in the whole series (54.5% to 45.1%, p=0.17), and in group H (69.3% to 63.1%, p=0.39), due to the limitation to QPB. Maximum individual differences in the percentage were 20% and 25% in two H-patients, respectively. Therefore, considering the parameter »percentage of positive cores«, the use of QPB as the first-line PB scheme is not appropriate in group L, while acceptable in group H. Although the conclusions by Grossklaus *et al*[5] and ours are similar for the overall series, the patient populations are not quite comparable as Grossklaus *et al* studied two different groups of men with different sampling schemes, while we compared two PB schemes on the same bioptic material.

The association of *high-grade prostatic intraepithelial neoplasia (HGPIN)* on PB specimen with concurrent invasive PC next to it or elsewhere in the gland is evident,[23] and a significant proportion of patients with HGPIN detected on initial PB will be found to have PC on repeat PB.[24,25] Thus, the identification of HGPIN on PB is an imperative as it may prompt further search for coexistent or subsequent invasive PC in the patient.[23] The number of cores with HGPIN was an independent predictor of the risk for PC.[25] It was shown that the extensive »five-region PB« detected significantly more HGPIN compared to the sextant BP.[24] Thus, the reduction of core number in PB can decrease the HGPIN detection sensitivity, which can in consequence decrease the CP detection rate. The detection of HGPIN on the first-line PB is an imperative, particularly in L-patients, in whom the finding of HGPIN may be decisive for rebiopsy; had this information been missed, a number of rebiopsies would not have been ordered and early PCs could have remained undetected. QPB would miss 2 HGPIN lesions in 21 PC negative L-patients (9.5%); thus, QPB is not appropriate as the first-line PB regimen in L-patients. On the contrary, none HGPIN was missed with QPB in group H. In larger H-population, some HGPIN theoretically could have been missed, but this lack would not have been critical, as every PC-negative H-patient has to be rebiopsied also for reasons other than HGPIN, mainly for persistent clinical and biochemical suspicion.

Proper estimation of *Gleason score (GS)* from PB specimens is essential in making treatment decision as high GS precludes radical treatment even when CP seems to be organ-confined.[26] GS determined from a PB specimen may be discordant to that determined from a surgical specimen.[27-30] GS assigned to PB material were identical to RP specimen in 51-67% of cases, greater in 4-15%, and lower in 22-54%. The magnitude of

discrepancy was directly related to the quantity of tissue in PB specimen, being greater among specimens with GS<7 than among those with higher GS.[27,28] GS defined by 18-cores BP speciment exactly matched that of surgical specimen in 37-57% of cases,[27,29] being within the interval of +1 point in 93% of cases.[29] Undergrading is particularly precarious as it may lead the clinician to underestimate falsely the true biological potential of PC and to proceed to RP in the patient with great likelihood to have NOC PC; of most concern are the patients with GS>6 detected as GS<6 on QPB. As predisposing factors for errors in histological grading by needle PB were limited core length and *limited number of biopsy cores*.[30] PB is to be repeated when low-grade PC was initially diagnosed on only limited quantities of neoplastic tissue to reduce the risk of underestimation the GS. In our study, GS of group H was not significantly influenced by the core number limitation to 4, but the accuracy was decreased in group L (more low grade PC-higher grading error according to).[28] In group H, in which less patients may be <T2 (RP candidates), GS inaccuracy is not critical. In our series, undergrading was ranging predominantly from GS=7 to GS=6 (10 patients in group H), and less often from 8 to 7. As these scores are classified as »high-risk«, their influence on the treatment choice is similar. When QPB indicated low GS in an L-patient, more extensive repeat PB should be done. If GS were higher on a more extensive PB material, this finding may influence the management decision.

Multiple-core PB is an *invasive and uncomfortable procedure*. Minor complications were reported in up to 78% patients.[9,10] Although the rate of macrohaematuria, pyrexia, and need for hospitalisation after 10-core PB did not excess significantly in comparison to these rate after sextant-PB,[11] the rate of haematospermia and rectal bleeding was higher after extensive sampling.[11] PB is associated with certain pain and discomfort, which is present in up to a half of patients.[9,10] We were often faced with the dilemma whether the risk of complications, and increasing anxiety and pain experienced by patients can be justified by real diagnostic needs, and whether an extensive PB must be routinely and non-selectively applied to all patients suspicious of PC. We think that, in some patients, we do not need to take all 12 or more cores in one PB session, if it does not significantly improve the quality of their preoperative diagnostic work-up.

In our experience, some patients do have low pain tolerance. In that case, we interrupted the procedure or, in some instances, reduce the number of samples on the patient's demand. The reduction of extensive PB protocols may be favourable also in elderly patients on chronic anticoagulation therapy and those with severe comorbidities. Moreover, some authors think that PB is completely unnecessary in the patients in whom PSA>50 ng/mL indicates PC with a positive prediction value of 98.5%.[12] Another advantages of reduced PB are higher safety for performance on an out-patient basis, less patients' anxiety for future PB, lower time consumption and workload to pathologists, lower costs (one needle per patient), and lower risk of seeding tumour cells.

Our study may have limitations. Although PSA level and DRE finding may, to some extent, indicate statistical risk of PC in a defined population,2-14 our study groups H and L were defined arbitrarily, with the aim of sorting out patients with significantly different likelihood to have PC. We can estimate that the likelihood of L- and H-patients to have PC is <30% and >60%, respectively.[13] These rates are, however, only for orientation, as our classification does not match strictly the criteria.[13,14] Thus, H- vs. L- classification is a provisional tool for rapid estimation of the likelihood for the presence of PC and tumour burden, but not an attempt to

stage the tumour or give a prognosis. It is aimed only to serve for identifying the patients who might benefit from PB reduction.

We conclude that in the patients with high likelihood to have NOC PC, the reduction of the number of cores does not impair the overall sensitivity, and minimally changes the staging accuracy. In the patients likely to have an early PC, the reduction of the number of cores significantly impairs the overall sensitivity. QPB can be an appropriate first-line sampling scheme in H-patients, as the information lost due to the core number reduction is mainly not critical for the patient management; a more extensive PB is necessary for other patients, for proper sensitivity and staging accuracy.

References

1. Aus G, Bergdahl S, Hugosson J, Lodding P, Pihl CG, Pileblad E. Outcome of laterally directed sextant biopsies of the prostate in screened males aged 50-66 years. Implications for sampling order. *Eur Urol* 2001; **39:**655-61.

2. Chon CH, Lai FC, McNeal JE, Presti JC Jr. Use of extended systematic sampling in patients with a prior negative prostate needle biopsy. *J Urol* 2002; **167:**2457-60.

3. Nava L, Montorsi F, Consonni P, Scattoni V, Guazzoni G, Rigatti P. Results of a prospective randomised study comparing 6, 12, 18 transrectal ultrasound guided sextant biopsies in patients with elevated PSA, normal DRE and normal prostatic ultrasound. *J Urol* 1997; **157(Suppl):** 59A.

4. Babaian RJ, Toi A, Kamoi K, Troncoso P, Sweet J, Ewans R, et al. A comparative analysis of sextant and an extended 11-core directed biopsy strategy. *J Urol* 2000; **163:** 152-7.

5. Grossklaus DJ, Coffey CS, Shappell SB, Jack GS, Cookson MS. Prediction of tumour volume and pathological stage in radical prostatectomy specimens is not improved by taking more prostate needle-biopsy cores. *BJU Int* 2001; **88:** 722-6.

6. Grossklaus DJ, Coffey CS, Shappell SB, Jack GS, Chang SS, Cookson MS. Percent of cancer in the biopsy set predicts pathological finding after prostatectomy. *J Urol* 2002; **67:** 2032-5.

7. Borboroglu PG, Amling CL. Correlation of positive sextant biopsy locations to site of positive surgical margins in radical prostatectomy specimens. *Eur Urol* 2001; **39:** 648-53.

8. Tigrani VS, Bhargava V, Shinohara K, Presti JC Jr. Number of positive systematic sextant biopsies predicts surgical margin status at radical prostatectomy. *Urology* 1999; **54:**689-93.

9. Djavan B, Waldert M, Zlotta AR, Dobronski P, Seitz C, Remzi M, et al. Safety and morbidity of first and repeat transrectal ultrasound-guided prostate needle biopsies: results of the prospective European Prostate Cancer Detection Study. *J Urol* 2001; **166:** 856-60.

10. Peyromaure M, Ravery V, Messas A, Toublanc M, Boccon-Gibod L. Pain and morbidity of an extensive prostate 10-biopsy protocol: a prospective study of 289 patients. *J Urol* 2002; **167:** 218-21.

11. Naughton CK, Ornstein DK, Smith DS, Catalona WJ. Pain and morbidity of transrectal ultrasound guided prostate biopsy: a prospective randomized trial of 6 versus 12 cores. *J Urol* 2000; **163:** 168-71.

12. Gerstenbluth RE, Seftel AD, Hampel N, Oefelein MG, Resnick MI. The accuracy of the increased prostate specific antigen level (greater than or equal to 20 ng./ml.) in predicting prostate cancer: is biopsy always required? *J Urol* 2002; **168:** 1990-93.

13. Potter SR, Horniger W, Tinzl M, Bartsch G, Partin AW. Age, prostate-specific antigen, and digital rectal examination as determinants of the probability of having prostate cancer. *Urology* 2001; **57:** 1100-4.

14. Eastham JA, May R, Robertson JL, Sartor O, Kattan MW. Development of a nomogram that predicts the probability of positive prostate biopsy in men with an abnormal digital rectal examination and a prostate-specific antigen between 0 and 4 ng/mL. *Urology* 1999; **54:** 709-13.

15. Yamamoto T, Ito K, Ohi M, Kubota Y, Suzuki K, Fukabori Y, et al. Diagnostic significance of digital rectal examination and transrectal ultrasonography in men with prostate-specific antigen levels of 4 ng/mL or less. *Urology* 2001; **58:** 994-8.

16. Damiano R, Autorino R, Perdona S, De Sio M, Oliva A, Esposito C et al. Are extended biopsies really necessary to improve prostate cancer detection? *Prostate Cancer Prostatic Dis* 2003; **6:** 250-5.

17. Gore JL, Shariat SF, Miles BJ, Kadmon D, Jiang N, Wheeler TM, et al. Optimal combinations of systematic sextant and laterally directed biopsies for the detection of prostate cancer. *J Urol* 2001; **165:** 1554-9.

18. Ravery V, Goldblatt L, Royer B, Blanc E, Toublanc M, Boccon-Gibod L. Extensive biopsy protocol improves the detection rates of prostate cancer. *J Urol* 2000; **164:** 393-6.

19. Tombal B, Tajeddine N, Cosins JP, Feyaerts A, Opsomer R, Wese FX, et al. Does site-specific labelling and individual processing of sextant biopsies improve the accuracy of prostate biopsy in predicting pathological stage in patients with T1c prostate cancer? *BJU Int* 2002; **89:** 543-8.

20. Aus G, Ahlgren G, Hugosson J, Pedersen KV, Rensfeldt K, Soderberg R. Diagnosis of prostate cancer: optimal number of prostate biopsies related to serum prostate-specific antigen and findings on digital rectal examination. *Scand J Urol Nephrol* 1997; **31:** 541-4.

21. Brossner C, Madersbacher S, Bayer G, Pycha A, Klingler HC, Maier U. Comparative study of two different TRUS-guided sextant biopsy techniques in detecting prostate cancer in one biopsy session. *Eur Urol* 2000; **37:** 65-71.

22. Furuya Y, Fuse H, Nagakawa O, Masai M. Preoperative parameters to predict tumor volume in Japanese patients with nonpalpable prostate cancer. *Int J Clin Oncol* 2002; **7:** 109-13.

23. Ellis WJ, Brawer MK. Repeat prostate needle biopsy: who needs it? *J Urol* 1995; **153:** 1496-8.

24. Rosser CJ, Broberg J, Case D, Eskew LA, McCullough D. Detection of high-grade prostatic intraepithelial neoplasia with the five-region biopsy technique. *Urology* 1999; **54:** 853-6.

25. Kronz JD, Allan CH, Shaikh AA, Epstein JI. Predicting cancer following a diagnosis of high-grade prostate intraepithelial neoplasia on needle biopsy: data on men with more than one follow-up biopsy. *Am J Surg Pathol* 2001; **25:** 1079-85.

26. Manoharan M, Bird VG, Kim SS, Civantos F, Soloway MS. Outcome after radical prostatectomy with a pretreatment prostate biopsy Gleason score of >/=8. *BJU Int* 2003; **92:** 539-44.

27. Djavan B, Kadesky K, Klopukh B, Marberger M, Roehrborn CG. Gleason scores from prostate biopsies obtained with 18-gauge biopsy needles poorly predict Gleason scores of radical prostatectomy specimens. *Eur Radiol* 1998; **33:** 261-70.

28. San Francisco IF, DeWolf WC, Rosen S, Upton M, Olumi AF. Extended prostate needle biopsy improves concordance of Gleason grading between prostate needle biopsy and radical prostatectomy. *J Urol* 2003; **169:** 136-40.

29. King CR, Long JP. Prostate biopsy grading errors: a sampling problem? *Int J Cancer* 2000; **90:** 326-30.

30. Ruijter E, van Leenders G, Miller G, Debruyne F, van de Kaa C. Errors in histologic grading by prostatic needle biopsy specimens: frequency and predisposing factors. *J Pathol* 2000; **192:** 229-33.

Radiol Oncol 2005; 39(1): 49-53.

Multiple primary malignancies in patients with lung cancer

Koichi Kurishima[1], Hiroaki Satoh[1], Shinsuke Homma[1], Katsunori Kagohashi[1], Hiroichi Ishikawa[2], Morio Ohtsuka[1], Kiyohisa Sekizawa[1]

[1]Division of Respiratory Medicine, Institute of Clinical Medicine, University of Tsukuba; [2]Department of Internal Medicine, Tsukuba Medical Center Hospital, Japan

Background. *To evaluate the incidence of multiple primary malignancies in lung cancer patients, we summarized our experience in lung cancer patients with multiple primary malignancies.*

Methods. *A total of 1194 consecutive lung cancer patients, who were admitted to our division over a 29-year period up to August 2004, were retrospectively analyzed.*

Results. *Ninety-eight (8.2%) of 1194 lung cancer patients had multiple primary malignancies. Metachronous malignant disease comprised 77.6% and synchronous 21.4%. Multiple primary tumours in our patients were detected more frequent in the advanced stage of lung cancer (IIIA-IV 67.3%) than in the early stage (IA-IIB 32.7%). The histological examination of lung cancer revealed a preponderance of squamous cell carcinoma (40 patients, 40.8%). First primary tumours developed most commonly in gastrointestinal tract, followed by lung and uterus. Fifty-seven (85.1%) of 67 patients with aerogastrointestinal and head and neck cancers had a smoking habit. In 98 patients with multiple primary cancers, forty (40.8%) patients had stage IA-IIIA lung cancer, however, 26 (26.5%) had a surgical resection.*

Conclusions. *Existing metachronous primary tumours proved to be a worse prognostic factor in non-small cell lung cancer patients (p=0.0480), while synchronous primary tumours were not, as well as there was not proven that multiple primary tumours were worse prognostic factors in patients with small cell lung cancer.*

Key words: lung neoplasms; neoplasms, multiple primary

Introduction

Nearly one hundred years ago, Billroth[1] first reported on synchronous cancers in various organs. About 40 years later, Warren and Gated established the criteria for the diagnosis of multiple primary tumours.[2] According to the criteria, such tumours occurring at different locations must be histologically malignant and separated by normal mucosa, and one tumour must not be a metastasis of another. Thereafter, a greater awareness, improved diagnostic techniques and facilities account for the observed increase in the incidence of metachronous and synchronous malignancies. Of patients with lung cancer, 3.2 -

Received 23 September 2004
Accepted 20 October 2004

Correspondence to: Hiroaki Satoh, M.D., Division of Respiratory Medicine, Institute of Clinical Medicine, University of Tsukuba, Tsukuba-City, Ibaraki, 305-8575, Japan; Fax: +81-29-853-3320; E-mail: hirosato@md.tsukuba.ac.jp

9.7% are considered to have a metachronous or synchronous malignancy in various sites at presentation.[3-5] This article summarizes our experience in lung cancer patients with metachronous or synchronous malignancies at various sites.

Methods

A total of 1194 consecutive lung cancer patients, who were admitted to our division over a 29-year period up to August 2004, were retrospectively analyzed. In all patients, the diagnosis of lung cancer was confirmed pathologically. Patients were classified using the International System for Staging Lung Cancer.[6] The following criteria have been used for the designation of synchronous cancers: (1) the tumours were anatomically separate; (2) the tumours were histologically different. If the tumours were histologically the same ones, the gross appearance of each tumour was strongly suggestive of the primary cancer.[7]

The criteria that we have used to determine metachronous cancers were related: (1) the tumours were anatomically separated; (2) tumour-free interval was at least 2 years.

At the time of admission, the past medical history including malignancies was taken from all patients. Staging procedures including physical examination, brain magnetic resonance imaging (MRI), chest computed tomographic (CT) scan, abdominal CT scan or ultrasonography, and bone scintigraphy were performed in all patients.

A Cox's proportional hazard model[8] was used for the multivariate regression analysis to clarify the independent prognostic importance of the following variables: gender, age, stage, performance status (PS), resectability at surgery, and existing multiple primary tumours.

Table 1. Characteristics of lung cancer patients with multiple primary malignancies (n=98)

	Number of patients
Gender	
Male	78
Female	20
Age in years	
Range; median	45-85; 70
Histology	
Adenocarcinoma	35
Squamous cell carcinoma	40
Small cell carcinoma	19
Large cell carcinoma	3
Others	1
Performance status (ECOG)	
0-1 / 2-3 / 4	76/20/1
Clinical stage	
IA-B/IIA-B/IIIA/IIIB/IV	20/12/8/24/34
Malignant diseases	
Synchronous/matachronous/both	21/76/1
Gastrointestinal	49
Urogenital	15
Lung	9
Head and neck	9
Others	19
Treatment	
Chemotherapy	37
Surgery	26
Radiation	20
Best supportive care	15

Results

Among the 1194 patients with lung cancer, 98 (8.2%) patients were diagnosed as having metachronous and synchronous malignancies. All relevant data relating to the patients who had metachronous and synchronous malignancies are shown in Table 1. The mean age at presentation of lung cancer was 70 years (range 45-85). Eighty-six (87.8%) of patients were 60 years of age or more. There were 78 men and 20 women. Among 98 patients, 76 had metachronous malignancies, 21 had synchronous malignancies, and 1 had both. As metachronous or synchronous ma-

lignancy, gastric cancer found in 32 patients, colon and rectal cancers in 10, lung cancer in 9, uterus cancer in 6, and prostate cancer in 5, respectively.

A histological examination of lung cancer revealed a preponderance of squamous cell carcinoma (40 patients, 40.8%). There were 35 patients (35.7%) with adenocarcinoma, 19 patients (19.4%) with small cell carcinoma and 3 patients (3.1%) with large cell carcinoma. This distribution of pathologic types is in striking contrast to that found in patients without multiple primary tumours, in whom there was a lower frequency of squamous cell carcinomas (29.5%) and a higher frequency of adenocarcinomas (47.1%).

With regard to tobacco smoking, 77.6% of patients with multiple primary tumours were habitual smokers including 68 patients (69.4%) with 30 pack year or more history of smoking. Fifty-seven (85.1%) of 67 patients with aerogastrointestinal and head and neck cancers were smokers. On the other hand, 76.3% of patients without multiple primary tumours were smokers including 65.1% of patients with 30-pack year or more history of smoking. There was no significant difference in smoking habit between the two groups (p = 0.3510). However, there was a significant difference in 30 pack year or more history of smoking in the two groups (p=0.0005).

In 98 patients with multiple primary cancers, forty (40.8%) patients had stage IA-IIIA lung cancer, however, 26 (26.5%) had a surgical resection. Twenty (20.4%) received chest irradiation, and 15 (15.3%) had only the best supportive care.

A Cox's proportional hazard model was used for the multivariate regression analysis to clarify the independent prognostic importance of the following variables: gender, age, stage, PS, resectability at surgery, and existing multiple primary tumours. For each variable, the proportional hazard assumption was examined graphically. In 1194 patients with lung cancer, gender ($p<0.0001$), stage ($p<0.0001$), PS ($p<0.0001$), and resectability at surgery ($p<0.0001$) were significantly related to the survival. In these patients, the existing multiple primary tumours were not proved to be a worse prognostic factor for the survival ($p=0.1919$). However, in 1018 patients with non-small cell lung cancer, the existing metachronous primary tumours were a significant prognostic factor for survival ($p=0.0480$) (Table 2).

Discussion

The criteria of double primary cancers enunciated by Warren and Gates[2] are now generally accepted. Of patients with lung cancer, an incidence for multiple primary tumours of 3.2 - 9.7% has been reported in the literature.[3-5] Cahan reported the incidence of second malignancies was 3.2% of patients with lung cancer.[3] Antakli *et al*[4] demonstrated 4.1% incidence of the second primary lung cancer in 1572 cases of cancer patients, the metachronous cancer comprised 60% and the synchronous are 40%. Reynolds *et al*[5] found an unusually high association of another primary cancer (9.7%) in cases of lung cancer,

Table 2. Prognostic factors in 1018 patients with non-small cell lung cancer determined by the Cox proportional hazard model

Variables	Coefficient	Standard error	p-value
Age	- 0.095	0.236	0.6884
Performance status	0. 752	0.100	<0.0001
Stage	- 0.633	0.122	<0.0001
Existing metachronous primary tumours	- 0.381	0.193	0.0480
Resectability at surgery	1.019	0.122	<0.0001

and the analysis by the stage of lung cancer as the second primary cancer showed a higher incidence of associated malignancies in the early stage lung cancer than in the advanced stage. In our 1194 lung cancer patients, 98 (8.2%) of them had multiple primary malignancies; the metachronous malignant disease comprised 77.6% and the synchronous one 21.4%. Inconsistent with the report by Reynolds *et al*,[5] more multiple primary tumours in our patients were detected in the advanced stage of lung cancer (in stage IIIA-IV 67.3%) than in the early stage(in IA-IIB 32.7%). We cannot explain the reason why the difference in incidence with regard to the stage was derived from. The precise incidence varies from series to series and might also be related to the length of the follow-up. Moreover, greater awareness and improved diagnostic techniques account for the apparent increase in incidence.

All retrospective studies published so far have revealed that multiple primary tumours occur more frequently than it would be expected by chance in patients who have primary lung cancer. Several environmental factors are thought to play a role in the development of primary and second malignancies. The role of tobacco and/or alcohol use in susceptible tissues of the upper aerodigestive tract is of major importance in multiple primary tumours including lung cancer. In our patients, 85.1% of patients with aerogastrointestinal and head and neck cancers had a smoking habit. The possible roles of immunity, heredity, nutrition are not completely known. The development of the second primary cancer has been well known following the chemotherapy,[9-11] but in this series no patients received chemotherapy for the first primary cancers.

There have been reported that a grater percentage of multiple primary cancers occur in the same organ or in the organs of the same system than in the unrelated organs.[12] The association between unrelated organs, such as lung, stomach and kidney may indicate the circulation of carcinogenic metabolites.[13] Our study showed that the first primary tumours occurred most commonly in gastrointestinal tract, followed by lung and uterus. Our results also revealed that the existing multiple primary tumours were not proved to be a worse prognostic factor for the survival in 1194 patients with lung cancer. However, in 1018 patients with non-small cell lung cancer, the existing metachronous primary tumours were a significant prognostic factor for the survival.

The second primary cancers may develop as much as 30 years later, and therefore, the possibility of a second cancer should be kept in mind in all cancer cases although the concept of a 5-year cure may be valid for the first cancer in most cases.[14] Recognizing that the incidence of the development of the second malignant tumour depends on the exactitude of evaluation, length of follow-up, curability of the first primary tumour, and patterns of tobacco and alcohol use, we should approach the problem of the second malignancies in lung cancer from several angles in the future. When a second primary cancer appears, a careful search for the metastatic disease should be made and a consideration for the curative intervention should be given. An aggressive curative approach conserving as much organ function as possible still offers the greatest chance for the long-term survival.

References

1. Billroth T. Die allgemeine chirurgische pathologie und therapie in 51 vorlesungen. In: Reimer G, editor. *Handbuch für studierende und ärzte*. Berlin; 1882. p. 908.

2. Warren S, Gates O. Multiple primary malignant tumors. *Am J Cancer* 1932; **16:** 1358-414.

3. Cahan WG. Lung cancer associated with cancer primary to other sites. *Am J Surg* 1955; **89:** 494-514.

4. Antakli T, Schaefer RF, Rutherford JE, Reed RC. Second primary lung cancer. *Ann Thorac Surg* 1995; **59:** 863-6.

5. Reynolds RD, Pajak TF, Greenberg BR, Shirley JH, Lucus RN, Hill RP, et al. Lung cancer as a second primary. *Cancer* 1978; **42:** 2887-93.

6. Mountain CF. Revisions in the International System for Staging Lung Cancer. *Chest* 1997; **111:** 1710-7.

7. Carter D, Eggleston JC. Tumours of the lower respiratory tract. Washington, DC: Armed Forces Institute of Pathology; 1974. p. 70-94; p 113-27.

8. Cox DR. Regression models and life tables. *J Royal Stat Soc B* 1972; **34:** 187-220.

9. Johnson BE, Linnoila RI, Williams JP, Venzon DJ, Okunieff P, Anderson GB, et al. Risk of second aerodigestive cancers increases in patients who survive free of small-cell lung cancer for more than 2 years. *J Clin Oncol* 1995; **13:** 101-11.

10. Johnson BE. Second lung cancers in patients after treatment for an initial lung cancer. *J Natl Cancer Inst* 1998; **90:** 1335-45.

11. Waller CF, Fetscher S, Lange W. Secondary chronic myelogenous leukemia after chemotherapy followed by adjuvant radiotherapy for small cell lung cancer. *Leuk Res* 1999; **23:** 961-4.

12. Watanabe S, Kodama T, Shimosato Y, Arimoto H, Sugimura T, Suemasu K, et al. Multiple primary cancers in 5456 autopsy cases in the National Cancer Center of Japan. *J Natl Cancer Inst* 1984; **72:** 1021-7.

13. Barbin A. Role of etheno DNA adducts in carcinogenesis induced by vinyl chloride in rats. *IARC Sci Publ* 1999; **150:** 303-13.

14. Kogelnik HD, Fletcher GH, Jesse RH. Clinical course of patients with squamous cell carcinoma of the upper respiratory and digestive tracts with no evidence of disease 5 years after initial treatment. *Radiology* 1975; **115:** 432-27.

Radiol Oncol 2005; 39(1): 55-9.

Cranium eroding sweat gland carcinoma: a case report

Mehmet Arslan, Ahmet N. Karadeniz, Görkem Aksu, Murat Güveli

Istanbul University, Institute of Oncology, Istanbul, Turkey

Background. *Sweat gland carcinomas are rare tumors. Eccrine sweat gland carcinomas are also very rare, with only about 200 cases reported in the world literature and only one of them was eroding the cranium. Treatment modalities of these carcinomas are not well known.*

Case report. *Our patient was 47 years old female. Since 1989, she was operated on six times because of the tumour relapses. After each operation, the pathological results were: sweat gland adenoma, sweat gland tumour, cylindroma, turban tumour, malign cylindiroma. That was her seventh relapse. On examination, a lesion of the size 10 x 6 cm was observed in the left parietal region. Computed tomography showed the lesion had the size of 11 x 5 cm, and was destroying the tabula externa, diploic region and tabula. The tumour was invading the dura and causing periost reaction. Surgery and postoperative radiotherapy treatment was planned because of malign transformation and risk of recurrence.*

Conclusions. *Only one case with cranium erosion was reported in literature. In our case, also intracranial extension of the tumor was observed.*

Key words: sweat gland neoplasms; parietal bone; neoplasms invasiveness

Introduction

Little is known about these rare sweat gland carcinomas and their treatment modalities. We reviewed the literature on sweat gland carcinomas to elucidate the nature of these tumours and best treatment course. The mean patients' age is 57 years with equal male-to-female distribution. Tumour distribution is: lower extremities, 32.9%; upper extremities, 27.6%; trunk, 11.9%; head, 26.3%; neck, 1.3%. Metastasis sites are: lymph nodes, 30.2%; viscera, 22%. Malignant sweat gland carcinomas have a propensity for local and regional lymph node recurrence.[1] The roles of lymph node dissection, radiation, and chemotherapy were reviewed.

Apocrine gland carcinoma is a rare sweat gland neoplasm with distinctive cytological appearance. Although the region of the axilla remains the most common site for these tumours, apocrine gland carcinoma of the anogenital region, eyelid, ear, chest, wrist, lip, foot, toe, and finger have been reported. Classically, these slow-growing lesions present as painless, colourless or reddish, firm or

Received 24 March 2004
Accepted 14 May 2004

Correspondence to: Prof. Mehmet Arslan, MD, Institute of Oncology, Istanbul University, Çapa, 34390, Istanbul, Turkey; Phone: +90 532 686 4659; E-mail: marslan19@yahoo.com

cystic nodules. More than half of the reported patients with apocrine carcinoma had lymph node metastases at the time of diagnosis. Wide local excision is standard therapy for these lesions. A therapeutic lymph node dissection is indicated if lymph node metastases are confirmed. It may be effective in the setting of a large or highly aggressive tumour with narrow surgical margins. As apocrine gland carcinoma responds poorly to chemotherapy, adjuvant radiotherapy may be applied in advanced, local, or regional diseases.[2]

Malignant eccrine sweat gland tumours are rare and usually develop from pre-existing eccrine appendage tumour of lesser maturity.[3-6] Clinical features of these tumours are non-specific, and final diagnosis is always based on histology. The tumours are usually located on the head, neck, or extremities and manifest as slow-growing nodules or infiltrated plaques. These tumours are rare, with only about 200 cases reported in the world literature.[7] A review of the literature reveals only 25 published reports of malignancies arising from eccrine spiradenoma. These tumours have a metastasis rate of >50 per cent in reported cases with high mortality rates as a result.[3] The case that is reported by Ritter *et al* is the only porocarcinoma eroding the cranium. A review of the literature failed to reveal any other such case.[4]

Dermal eccrine cylindroma or turban tumour is a rare benign tumours of the eccrine sweat glands. Despite its histological benign behaviour, the disease process is distressing for the patients and cylindromas rarely progress to cylindrocarcinoma.[8]

Case report

Our case is 47 years old women patient. She first visited the health care centre in 1989 for a solitary, colourless and painless lesion that she had on the scalp for a long time. On examination, colourless and painless 2 cm solid scalp lesion was palpated. The lesion was excised and not examined pathologically at that time. For about two years later, the lesion relapsed. It was excised and diagnosed pathologically as sweat gland adenoma. Adjuvant therapy was not needed. For about two years later, the lesion relapsed again. It was excised thirdly and diagnosed pathologically as sweat gland tumour. For about two years later, the lesion relapsed thirdly; this time, it was reddish. It was excised fourthly and diagnosed pathologically as sweat gland cylindroma. For about one year later, the lesion relapsed multifocally. The largest lesion was 4 cm long, reddish and painful. Other lesions were colourless, painless and solitary. The lesion was excised again and diagnosed as turban tumour. Adjuvant therapy was not needed.

Short time later, the lesion relapsed multifocally again. Dimensions of the lesions were up to 5 x 6 cm (Figure 1). The excision of the lesions, increasing in number and diameter and changing physically each time, was performed again. Pathologically, it was diagnosed as cylindroma with malign features (Figure 2).

On physical examination of the patient with recurrence referred to our clinic, a mass of the size 10 x 6 cm was found on the left

Figure 1. General appearance of the lesion (5x6cm).

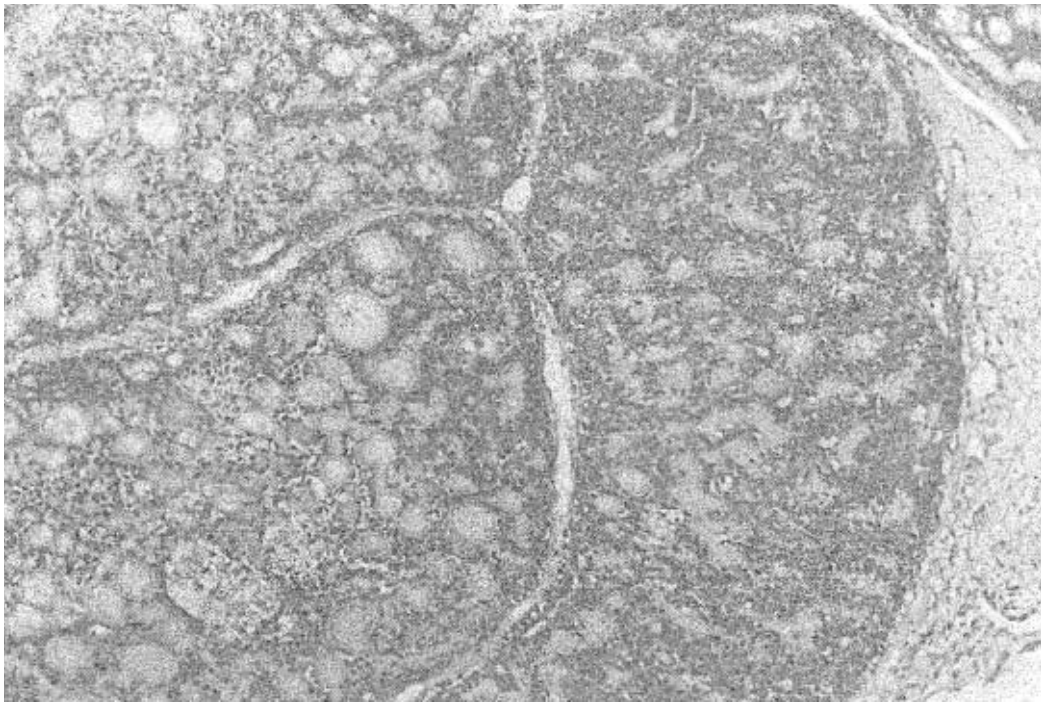

Figure 2. Pathological appearance of the lesion (H&E, X100).

parietal region of the scalp. With cranial direct roentgen and computed tomography, a mass, measuring 11 x 5 cm, was destructing tabula, tabula externa, and diploic region, invading the dura and causing periost reaction was identified (Figure 3). Surgery and postoperative radiotherapy with surgical consultation was planned because of malign transformation and risk of recurrence.

Discussion

Dermal eccrine cylindroma or turban tumour is a rare benign tumour of the eccrine sweat glands.[9,10] Women are affected 4 times more frequently than men. About 10% of all cylindromas are hereditary, transmitted autosomally dominantly and with variable penetrance. Papules, nodules, and tumours occur mainly on the scalp, but they may be found on the face and upper part of the trunk. If nodules of cylindromas cover the entire scalp and are heaped up, they resemble a turban. Despite its histological benign behaviour, the disease process is distressing for the patients.[8] Cylindromas rarely progress to cylindrocarcinoma.[11-13] Most of these cases of cylindrocarcinomas have developed from

Figure 3. Radiological appearance of the lesion invading the cranium (CT).

long persisting tumours of cylindroma. Histologically, the tumours are similar to cylindromas, but they are marked by large numbers of mitotic figures and atypical mitoses. Cylindrocarcinomas are aggressive, with metastases to lymph nodes, bone, and visceral organs.[6] In our case, despite its histological benign features, the disease relapsed seven times and increased in dimension and number. Thus, despite its benign pathology, it was distressing for the patient. Some of them become malignant. Last pathological report of our case was cylindroma with malign features; so, it changed to a malign form from a long persisting cylindroma. A review of the literature reveals only 25 published reports of malignancy arising from eccrine spiradenoma.

These tumours are rare tumours, with only about 200 cases reported in the world literature.[7] The case that was reported by Ritter *et al* is the only porocarcinoma eroding the cranium. A review of the literature failed to reveal any other such case.[4] Our case with cranial erosion, dural invasion, and intracranial extension is the first scalp eccrine sweat gland tumour, cylindroma. Multiple resections were required for local control and, finally, the lesion changed to a growth with malign histology.

Wide local excision is standard therapy for these lesions. A therapeutic lymph node dissection is indicated if lymph node metastases are confirmed, and it may be efficient in the setting of a large or highly aggressive tumour with narrow surgical margins. As sweat gland carcinoma responds poorly to chemotherapy, adjuvant radiotherapy may be used in advanced local or regional diseases.[2] The treatment plan for our patient comprised wide local excision and postoperative radiotherapy because of malign transformation and risk of recurrence. The tumour invaded the dura and extended intracranially. Adjuvant treatment such as chemotherapy and craniospinal irradiation may be applied. But these tumours respond poorly to chemotherapy and there is no experience of craniospinal irradiation.

Conclusions

The reported case with cranial erosion, dural invasion, and intracranial extension is the first scalp eccrine sweat gland tumour, cylindroma. Cylindromas rarely progress to cylindrocarcinoma. Most of these cases of cylindrocarcinomas have developed from long persisting tumours of cylindroma. In our case, it also changed to malign cylindroma. Wide local excision is standard therapy for these lesions. Multiple resections may be required in order to obtain local control even if the lesion is benign. Therapeutic lymph node dissection and adjuvant radiotherapy may be used in advanced local or regional diseases.

References

1. Asley I, Smith-Reed M; Chernys A. Sweat gland carcinoma. *Dermatol Surg* 1997; **23(2):** 129-33.

2. Chamberlain RS, Huber K, White JC, Travaglino-Parda R. Apocrine gland carcinoma of the axilla. *Am J Clin Oncol* 1999; **22(2):** 131-5.

3. Beekly AC, Brown TA, Porter C. Malignant eccrine spiradenoma. *Am Surg* 1999; **65(3):** 236-40.

4. Ritter AM, Graham RS, Amaker B, Broaddus WC, Young HF. Intracranial extension of an eccrine porocarcinoma. *J Neurosurg* 1999; **90(1):** 138-40.

5. Tay JS, Tapen EM, Solari PG. Malignant eccrine spiradenoma. *Am J Clin Oncol* 1997; **20(6):** 552-7.

6. Shafer WF, Hine MK, Levy BM, editors. *A textbook of oral pathology.* Philadelphia: WB Saunders; 1983. p. 20.

7. Safai B, Brash DE. Tumors of eccrine glands. In: Vincent T, DeVita, editors. *Cancer.* Philadelphia: Lippincott-Raven; 1997. p. 40.

8. Irwin LR, Bainbridge LC, Reid CA, Piggot TA, Brown HG. Dermal eccrine cylindroma (turban tumour). *Br J Plast Surg* 1990; **43(6):** 702-5.

9. Cotton DW, Braye SG. Dermal cylidromas originate from the eccrine sweat gland. *Br J Dermatol* 1984; **111:** 53-61.

10. Goette DK, McConnell MA, Fowler VR. Cylindroma and eccrine spiradenoma coexistent in the same lesion. *Arch Dermatol* 1982; **118:** 273-4.

11. Urbanski SJ, From L, Abramowicz A, Joaquin A, Luk SC. Metamorphosis of dermal cylindroma: possible relation to malignant transformation. Case report of cutaneous cylindroma with direct intracranial invasion. *J Am Acad Dermatol* 1985; **12:** 188-95.

12. Lyon JB, rouillard LM. Malignant degeneration of turban tumour of scalp. *Trans St Johns Hosp Dermatol Soc* 1961; **46:** 74-7.

13. Bondeson L. Malignant dermal eccrine cylindroma. *Acta Derm Venereol* 1979; **59:** 92-4.

Radiol Oncol 2005; 39(1): 61-70.

review

The dimethylhydrazine induced colorectal tumours in rat - experimental colorectal carcinogenesis

Martina Perše and Anton Cerar

Institute of Pathology, Medical Experimental Centre, Medical Faculty, University of Ljubljana, Slovenia

Animal models of colorectal carcinogenesis represent invaluable research tool for investigating colorectal cancer (CRC). Experimentally induced tumours in laboratory animals provide opportunity for studying certain aspects of tumours that cannot be effectively studied in humans. Significant information on human CRC aetiology or factors influencing it has derived from studies using dimethylhydrazine (DMH) model that is one of the experimental models appreciated for its morphological similarity to human CRC. Today, DMH model represents useful research tool for the studies of colon carcinogens and chemopreventive agents. The review offers insight into morphogenesis and genetic alterations of DMH induced colorectal epithelial tumours in rats.

Key words: colorectal neoplasms - chemically induced; azoxymethane; 1,2-dimethylhydrazine; disease models, animal; rats

Introduction

The beginnings of the first animal model appreciated for its macroscopic and histological similarity to human colorectal carcinoma (CRC) extend to 1963, when Laqueur discovered that rats fed cycasin, a plant product, developed intestinal cancer. The active substance was identified and soon a similar compound, methylazoxymethanol acetate (MAMA) was synthesized that was more effective than the natural product. In 1970 Druckrey found that two chemicals structurally related to MAMA, dimethylhydrazine (DMH) and azoxymethane (AOM), were even more potent intestinal carcinogens.[1]

Today, DMH and its metabolite AOM are the agents widely used in experimental models of colorectal carcinogenesis in rodents. They are highly specific indirect colorectal carcinogens that induce the initiation and promotion steps of colorectal carcinogenesis yielding colorectal tumour lesions in a dose-dependent manner in rats, mice and hamsters.[2-4] In rats they can produce colorectal tumour lesions in almost 100% of treated animals.[4-8] Nevertheless, various strains of rats differ in susceptibility to these carcinogens.[8-10]

Received 29 October 2004
Accepted 20 November 2004

Correspondence to: Martina Perše, DVM, Institute of Pathology, Medical Experimental Centre, Medical Faculty, Korytkova 2, 1105 Ljubljana, Slovenia. Phone: +386 1 543-71-91; Fax: +386 1 543-71-81; E-mail: martina.perse@mf.uni-lj.si

Decreased susceptibility was reported also in female rats.[11,12] In chemically induced colorectal studies mostly 6-10 weeks old male rats are used and most often-applied rat strains are Fisher, Sprague-Dawely and Wistar (Table 1).

DMH metabolism

DMH is highly specific colorectal carcinogen that is metabolically activated in liver by series of reactions through intermediates azomethane, AOM and methylazoxymethanol (MAM) to the ultimate carcinogenic metabolite, highly reactive methyldiazonium ion.[13] MAM is excreted into the bile and transported to the colon or enter directly into epithelial cells of the colon from the blood circulation.[2,13,14] Some studies have demonstrated that rat colon epithelial cells are capable of metabolising DMH into carcinogenic metabolite without previous metabolism by other tis-

Table 1. Protocols used for chemical induction of colorectal lesions

References	C	Strain, sex and initial age or weight	Dose	R	N	D
Rubio *et al.* 1986	DMH	Sprague-Dawley *(male, 200g)*	21 mg/kg	s.c.	1	32
McGarrity *et al.* 1988	DMH	Sprague-Dawley *(male, 220-260g)*	20 mg/kg	s.c.	20	30
Park *et al.* 1997	DMH	Wistar *(male, 8-10 weeks)*	15 mg/kg	s.c.	19	24
Onoue *et al.* 1997	DMH	Fischer *(male, 10 weeks)*	20mg/kg	i.p.	2	11 34
Ghirardi *et al.* 1999	AOM	Fischer *(male, 6 weeks)*	15 mg/kg	s.c.	2	6 36
Rubio *et al.* 1999	DMH	Sprague-Dawley *(male, female, 200g)*	21 mg/kg	s.c.	27	32
De Jong *et al.* 2000	DMH	Sprague-Dawley *(male, 6 weeks)*	30 mg/kg	p.o.	5	24
Bissonnette *et al.* 2000	AOM	Fischer *(male, 80-100g)*	15 mg/kg	i.p.	2	37
Narahara *et al.* 2000	AOM	Wistar *(male, 6 weeks)*	7,4 mg/kg	s.c.	5	45
Ravnik-Glavac *et al.* 2000	DMH	Wistar *(male, 9 weeks)*	20 mg/kg	s.c.	15	25
Yamada *et al.* 2000	AOM	Fischer *(male, 6 weeks)*	15 mg/kg	s.c.	3	10
Takahashi *et al.* 2000	AOM	Fischer *(male, 6 weeks)*	15 mg/kg	s.c.	2	36
Kishimoto *et al.* 2002	AOM	Fischer *(male, 6 weeks)*	15 mg/kg	s.c.	3	4 4
Rodrigues *et al.* 2002	DMH	Wistar *(male, 6 weeks)*	40 mg/kg	s.c.	2	30
Veceric *et al.* 2004	DMH	Wistar, Fischer *(male, 8-10 weeks)*	25 mg/kg	s.c.	20	25

Legend: C, carcinogen; R, route of application (s.c., subcutaneous; i.p., intra peritoneal; p.o., per oral); N, number of applications; D, duration of experiment (weeks)

sues or colon bacteria.[15,16] Although intestinal flora[17,18] and bile acids[19] have influence on the incidence of tumours, the latter were induced also in germ-free rats[17] and function-isolated segments of rat colon.[14]

The ultimate carcinogenic metabolite of DMH is responsible for methylation of DNA of various rat organs including epithelial cells in the proliferative compartment of the intestinal crypts.[20] Metabolically activated DMH modifies not only nucleic acids but also histones and other DNA-binding proteins in the target cells.[21]

Tumour lesions induced by DMH

DMH is highly specific for colonic epithelium and induces tumours mostly in large bowel.[14,20,22] Colon specific susceptibility for this carcinogen is a result of a delayed or incomplete repair of damaged DNA in the colon compared to other organs,[20] leading to accumulation of mutations, and in a small proportion of cells giving rise to CRC. Higher susceptibility to colon versus small intestine has been shown in experiment where segments of colon that were transposed to the middle part of small intestine developed tumours but segments of small intestine that were transposed to the colon did not.[22] Tumours are distributed in all parts of the colon, but in a majority are observed in the distal part of colon.[4,8,23,24] Gross tumours are initially detected in the distal colon at 16 weeks but in proximal colon after 22 weeks.[23] The tumour incidence can be modulated by the amount of carcinogen administered and the number of applications. With increasing doses of the carcinogen, the latency period decreases and the tumour incidence increases.[3,4] Usually carcinogen at a dosage of 15-25 mg/kg body weight per week is administered subcutaneously (Table 1). In our studies DMH at a dosage of 15-25 mg/kg-body weight was injected subcutaneously once a week, for 15-20 weeks consecutively.[8,11,25,26]

Besides the colorectal tumours, the small bowel tumours are also induced but in much lower incidence.[5,8,11] However, small bowel tumorigenesis is characteristic of high-dose regimens of DMH.[27] Small intestinal tumours are mostly well or poorly differentiated adenocarcinomas.[5,8,11] Well-differentiated adenocarcinomas only occasionally demonstrate invasion through the intestinal wall and into the adjacent tissues.[5] On the other hand the poorly differentiated type is more aggressive and mostly metastasises to the mesenteric lymph nodes and in advanced stages frequently develops carcinosis of peritoneum or conglomerate tumours in the area between the duodenum, stomach, hilus of the liver and affected small intestine.[5,6]

Extraintestinal tumours may also be induced by DMH. Some rats develop tumours of Zymbal's gland (auditory sebaceous glands), usually squamous cell carcinoma.[5,11,28]

Colorectal tumour lesions

Aberrant crypt foci

The first specific morphologically identifiable lesions for colonic carcinogenesis are aberrant crypt foci (ACF). They were first identified in the colon of carcinogen treated mice by the light microscopic examination of the mucosal surface of colons that had been stained with methylene blue.[29] ACF are stereoscopically distinguished from normal crypts by their darker staining and larger size, elliptical shape, thicker epithelial lining, and larger perycriptal zone.[30-34] They appear within two weeks after carcinogen injection as single crypts that expand by crypt branching or multiplication. Sequential histologic analysis of ACF revealed that with time the number of ACF with increasing crypt multiplicity increases and a higher number of ACF

exhibit dysplasia.[30,32] It was observed that ACF with increasing crypt multiplicity are more resistant to apoptotic cell death.[31]

Hyperplastic ACF (Figure 1A) are composed of mixture of goblet and absorptive cells with enlarged or sometimes crowded nuclei without stratification. The luminal opening of ACF is slightly elevated from the surrounding normal mucosa and the crypts are elongated and occasionally branching with partial mucin depletion. Mitotic figures are limited to the lower two-thirds of the crypts and are never observed on the surface of ACF.[33,34]

Dysplastic ACF (Figure 1B) are mostly composed of absorptive cells that display an unceasing proliferative activity.[33] Histologically these cells manifest cytoplasmic basophilia, a high nuclear-cytoplasmic ratio, prominent nucleoli and loss of cell polarity to variable degrees. The number of goblet cells is decreased and mucin depleted. The dysplastic crypt so formed tends to have an increased diameter, relatively smooth contour and dilated cryptal lumen in the lower half, and some irregularity and tortuosity with occasional evagination of the lining epithelium in the upper half.[33,34]

Adenomas and carcinomas

Two types of tumours can be distinguished grossly: polypoid (pedunculated or with a broad base) and non-polypoid (slightly elevated, flat or depressed).[5,35] Histologically, colorectal epithelial tumours are divided into adenomas and carcinomas.[36]

Adenomas are characterized by hypercellularity with enlarged, hyperchromatic nuclei, varying degrees of nuclear stratification, loss of polarity and decreased mucine excretion. Depending on the degree of glandular or villous complexity, extent of nuclear stratification and severity of abnormal nuclear morphology, dysplasia in adenomas can be divided into mild, moderate and severe (Figure 2A).

Tumours that penetrate through the muscularis mucosa into the submucosa are classified as carcinomas.[36] When no clear evidence

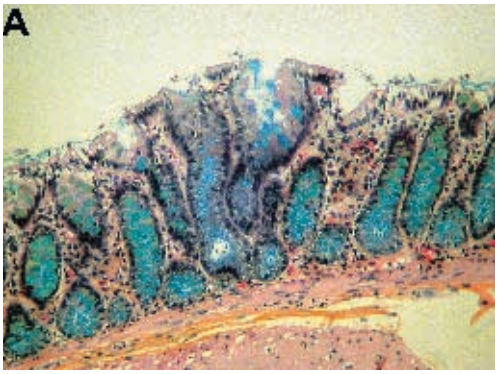

Figure 1. A. Hyperplastic aberrant crypt focus of colorectal mucosa. The focus is composed of three elongated crypts covered by slightly higher epithelium with nuclei at the base of cells. The luminal openings are elevated. **B.** Dysplastic aberrant crypt focus of colorectal mucosa. The focus is composed of epithelial cells with stratified, hyperchromatic nuclei, and with a loss of cell polarity and mucin secretion Ė the signs of dysplasia. Displacement of the surrounding normal crypts is evident.

of tumour growth through the muscularis mucosa is found additional criteria like sharp transition from unaltered epithelium to severe dysplasia, the presence of necrosis on the surface and desmoplastic stromal reaction are used.[37]

Carcinomas are divided into well, moderately and poorly differentiated adenocarcinomas (Figure 2B), mucinous adenocarcinomas (Figure 3A) if more than 50% of the lesion is composed of mucin and signet-ring cell carcinomas (Figure 3B) if more than 50% of tumour cells with prominent intracytoplasmic mucin are present.[36] Most frequently observed carcinomas in rat colorectal model are well-differentiated adenocarcinomas.[8,25,26] Some investigators[8,11,25] classify the stage of carcinomas according to Dukes staging system: stage A if tumour is limited to the intestinal wall, stage B if tumour grows through the lamina muscularis propria, stage C if tumour grows through the lamina muscularis propria and disseminates into the lymph nodes and stage D when carcinoma disseminates into distant organs.

Metastases

Metastases to the liver and lung are very uncommon in rats. The tumours that are capable of metastasis are almost exclusively the mucinous and signet ring cells carcinomas of the proximal colon. The adenocarcinomas of the distal colon have not been shown to metastasise. The metastases are generally

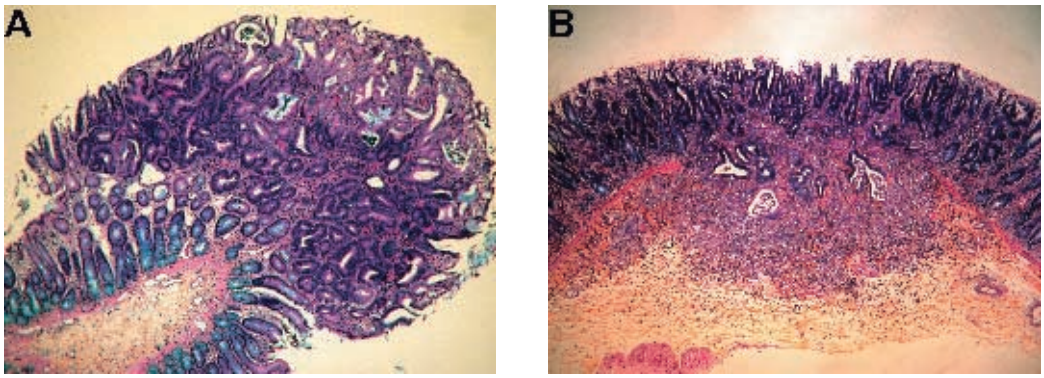

Figure 2. A. Polypoid tubular adenoma of colorectal mucosa with moderate grade of dysplasia. Muscularis mucosa is intact. **B.** A well-differentiated adenocarcinoma of colorectal mucosa. Submucosal invasion and accompanying fibroplastic stromal reaction is evident. Stage Dukes A.

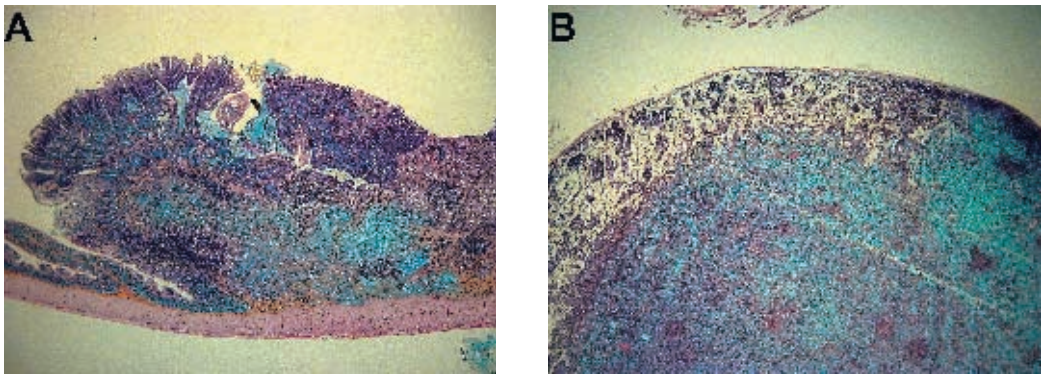

Figure 3. A. A mucinous carcinoma with a wide infiltration of submucosa. Note abundant extracellular mucin secretion. **B.** Signet-ring cell carcinoma metastasis in regional lymph node. Stage Dukes C.

found in regional lymph nodes (Figure 3B) or on the peritoneal surface.[5,11]

Tumour association with gut lymphoid tissue

Often, the earliest dysplastic mucosa is found over a mucosal lymphoid aggregate.[8,35,38,39] Significant association between tumour development, particularly non-polipoid adenomas[35] and mucinous adenocarcinomas,[38] and the presence of lymphoid aggregate have been observed. Hardman *et al*[39] have demonstrated that the association is due to higher proliferative activity in colonic crypts over the lymphoid aggregates.

Adenoma-carcinoma sequence and de novo formation of colorectal carcinoma

Several investigators[3,7,24,32,40,41] have observed differences in the histopathological findings of the carcinomas between the distal and the proximal colon in rats. The studies suggest that chemically induced carcinogenesis in the rat colon follows two distinct pathways: adenoma-carcinoma sequence, where histogenesis follows the ACF-adenoma-carcinoma sequences and *de novo* sequence where adenocarcinomas develop without passing through ACF stage.[3,7,24,40] The former is characteristic for middle and distal colon whereas the latter leads to the development of poorly differentiated, mucin-secreting carcinomas in the proximal colon.[3,7,24]

Molecular alterations

Mutations in the adenomatous polyposis coli gene (Apc), the gene coding for β-catenin (Ctnnb1) and K-ras gene were detected in colorectal tumours of rats administered DMH or AOM.[42] Alterations of specific oncogenes and tumour suppressor genes play role at different stages of carcinogenesis process. In rat carcinogenesis an extensive genomic instability was found, that is the necessary step for the generation of multiple mutations underlying the occurrence of cancer.[25,43]

Mutations in Apc gene were detected exclusively in the mutation cluster region of Apc[44] and were found only in 18% of tumours and not in ACF, suggesting that mutations of the Apc gene are associated with the transition from ACF to adenoma and adenocarcinoma and not from normal mucosa to ACF.[45] In rat tumorigenesis β-catenin mutations are more frequent event than Apc mutations,[44] suggesting that consequent alterations in the stability and localisation of the protein may play an important role in this colorectal carcinogenesis model.[46] Mutation causes activation of the β-catenin-Tcf pathway resulting in the accumulation of β-catenin in the cytosol and nucleus. Most of the mutations occur as single nucleotide substitution within functionally significant phosphorylation sites on exon 3. The most common mutation in the early lesions is G:C to A:T transitions that is recognised as the representative mutation in rat colorectal tumours.[46,47] β-catenin gene mutations were detected in tumours and dysplastic ACF, none in hyperplastic ACF. Also alteration in expression and cellular localization of β-catenin and inducible nitric oxide synthase were observed in all dysplastic ACF, adenomas and adenocarcinomas, but not in any hyperplastic ACF.[48]

K-ras mutations are important early event in the progression of chemically induced colorectal carcinogenesis in rodents,[49,50] frequently detected in tumours, dysplastic ACF[51] and even in hyperplastic ACF.[48] The majority of K-ras mutations are identified in codon 12 and 13.[49,50] Constitutive activation of K-ras by point mutation occurs with a frequency of 40-60%. K-ras point mutations occur mostly as G to A transitions.[49]

In carcinogen induced tumours elevated expression of c-myc,[52] c-jun[44] and c-fos[30] were detected and increased expression of cyclin D1 were observed, particularly by muta-

tions in either K-ras or β-catenin.[42]

In a subset of carcinogen induced rat colorectal tumours without detectable K-ras mutations constitutively activated wild-type p21ras have been observed, presumably due to increased expression of c-erbB1 receptor and decreased expression of GTPase activating protein. Mitogen-activated protein kinase (MAPK) activation and cyclooxygenase-2 expression were increased in tumours with mutated or activated wild-type p21ras. Colonic tumours with activated wild type p21ras, like those with mutated p21ras, have increased activation of extracellular signal regulated kinase-1 and extracellular signal regulated kinase-2, presumably via the activation of Raf-1 and MAPK kinase.[42]

Long-term and short-term assays

Repeated injections of DMH are needed to induce irreversible molecular and histological alterations in rat colons leading to development of ACF, adenomas and carcinomas. Based on duration of experiment assays can be divided into short-term and long-term.

Short-term assays require 4-11 weeks to complete (Table 1). In that time only ACF are induced, which are identified by light microscopic examination of large bowel.[29,30] They are precancerous lesions that are used as intermediate biomarkers to predict the ability of a test agent to affect tumour outcome.[29-34,53] Based on ability to retard or induce the appearance of ACF, compounds are classified as tumour inhibitors or tumour promoters.[29,30,53] However, it is important to take into consideration that ACF are a heterogeneous group of lesions[33,34,53] not equally distributed in colon. Ghirardi *et al*[41] observed the majority of ACF in the middle colon. Also Rodrigues *et al*[32] reported that majority of ACF were observed in the middle and distal colon and that induction of ACF by DMH in the short-term assay was correlated with development of well-differentiated adenocarcinomas. Park *et al*[24] demonstrated, that ACF are marker lesions for colorectal tumours, but only in distal colon where tumours follow the adenoma-carcinoma sequence. Therefore, compounds, which appear to be effective in the short-term, are usually examined in long-term experiments.

In contrast to short-term assays, the long-term usually take 20-40 weeks to complete (Table 1). In that time ACF, adenomas and adenocarcinomas are induced, which are further examined to assess the effect of testing substances on colorectal tumorigenesis.

Conclusions

Studies on DMH model allow monitoring the step-wise development of CRC by examining the dissected colons of randomly selected animals from a group, at different time intervals, as the disease progresses and under defined experimental conditions. They have already produced much important information on histology and biochemistry of tumour development as well as on factors that retard or enhance tumorigenesis. Even today, DMH model represents invaluable research tool for studying the molecular events of CRC and for developing and evaluating of a variety of novel cancer chemopreventive agents.

References

1. Nigro ND, Bull AW. Experimental intestinal carcinogenesis. *Br J Surg* 1985; S36-S41.

2. Shinchi N, Isamu K. Morphogenesis of experimental colonic neoplasms induced by dimethylhydrazine. In: Pfeiffer CJ, editor. Animal models for intestinal disease. Boca Raton, Florida: CRC Press Inc.; 1985. p. 99-121.

3. Maskens AP, Dujardin-Loits RM. Experimental adenomas and carcinomas of the large intestine behave as distinct entities: most carcinomas arise de novo in flat mucosa. *Cancer* 1981; **47:** 81-9.

4. Shirai T, Nakanowatari J, Kurata Y, Fukushima S, Ito N. Different dose-response relationships in the induction of different types of colonic tumors in Wistar rats by 1,2-dimethylhydrazine. *Gann* 1983; **74:** 21-7.

5. Tatematsu M, Imaida K. Tumours of the small intestine. In: Stinson SF, Schuller HM, Reznik GK, editors. Atlas of tumorpathology of the Fischer rat, Boca Raton, Florida: CRC Press Inc., 2000. p.117-32.

6. Elsayed AM, Shamsuddin AM. Neoplasms of the colon. In: Stinson SF, Schuller HM, Reznik GK, editors. Atlas of tumorpathology of the Fischer rat, Boca Raton, Florida: CRC Press Inc., 2000. p.133-91.

7. Sunter JP, Appleton DR, Wright NA, Watson AJ. Pathological feature of the colonic tumours induced in rats by the administration of 1,2-dimethylhydrazine. *Virchows Arch B Cell Pathol* 1978; **29:** 211-23.

8. Veceric Z, Cerar A. Comparison of wistar vs. fischer rat in the incidence of 1,2-dimethylhydrazine induced intestinal tumours. *Radiol Oncol* 2004; **38:** 227-34.

9. Pollard M, Zedeck MS. Induction of colon tumors in 1,2-dimethylhydrazine-resistant Lobund Wistar rats by methylazoxymethanol acetate. *J Natl Cancer Inst* 1978; **61:** 493-4.

10. Kobaek-Larsen M, Fenger C, Hansen K, Nissen I, Diederichsen A, Thorup I, et al. Comparative study of histopathologic characterization of azoxymethane-induced colon tumors in three inbred rat strains. *Comp Med* 2002; **52:** 50-7.

11. Breskvar L, Cerar A. A role of gender in the occurrence of dimethylhydrazine induced colorectal tumors in Wistar rats. *Radiol Oncol* 1997; **31:** 374-9.

12. Izbicki JR, Wambach G, Hamilton SR, Harnisch E, Hogenschurz R, Izbicki W, et al. Androgen receptors in experimentally induced colon carcinogenesis. *J Cancer Res Clin Oncol* 1986; **112:** 39-46.

13. Fiala ES, Sohn OS, Puz C, Czerniak R. Differential effects of 4-iodopyrazole and 3-methylpyrazole on the metabolic activation of methylazoxymethanol to a DNA-methylating species by rat liver and rat colon mucosa in vivo. *J Cancer Res Clin Oncol* 1987; **118:** 145-50.

14. Rubio CA, Nylander G, Santos M. Experimental colon cancer in the absence of intestinal contents in Sprague-Dawley rats. *J Natl Cancer Inst* 1980; **64:** 569-72.

15. Glauert HP, Bennink MR. Metabolism of 1,2-dimethylhydrazine by cultured rat colon epithelial cells. *Nutr Cancer* 1983; **5:** 78-86.

16. Oravec CT, Jones CA, Huberman E. Activation of the colon carcinogen 1,2-dimethylhydrazine in a rat colon cell-mediated mutagenesis assay. *Cancer Res* 1986; **46:** 5068-71.

17. Onoue M, Kado S, Sakaitani Y, Uchida K, Morotomi M. Specific species of intestinal bacteria influence the induction of aberrant crypt foci by 1,2-dimethylhydrazine in rats. *Cancer Lett* 1997; **113:** 179-86.

18. Goldin BR, Gorbach SL. Effect of antibiotics on incidence of rat intestinal tumors induced by 1,2-dimethylhydrazine dihydrochloride. *J Natl Cancer Inst* 1981; **67:** 877-80.

19. Narahara H, Tatsuta M, Lishi H, Baba M, Uedo N, Sakai N, et al. K-ras point mutation is associated with enhancement by deoxycholic acid of colon carcinogenesis induced by azoxymethane, but not with its attenuation by all-trans-retinoic acid. *Int J Cancer* 2000; **15:** 157-61.

20. Swenberg JA, Cooper HK, Bucheler J, Kleihues P. 1,2 Dimethylhydrazine induced methylation of DNA bases in various rat organs and the effects of pre-treatment with disulfiram. *Cancer Res* 1979; **39:** 465-7.

21. Boffa LC, Gruss RJ, Allfrey VG. Aberrant and nonrandom methylation of chromosomal DNA-binding proteins of colonic epithelial cells by 1,2-dimethylhydrazine. *Cancer Res* 1982; **42:** 382-8.

22. Gennaro AR, Villanueva R, Sukonthaman Y, Vathanophas V, Rosemond GP. Chemical carcinogenesis in transported intestinal segments. *Cancer Res* 1973; **33:** 536-41.

23. McGarrity TJ, Peiffer LP, Colony PC. Cellular proliferation in proximal and distal rat colon during 1,2-dimethylhydrazine-induced carcinogenesis. *Gastroenterology* 1988; **95:** 343-8.

24. Park HS, Goodlad RA, Wright NA. The incidence of aberrant crypt foci and colonic carcinoma in dimethylhydrazine-treated rats varies in a site-specific manner and depends on tumor histology. *Cancer Res* 1997; **57:** 4507-10.

25. Ravnik-Glavac M, Cerar A, Glavac D. Animal model in the study of colorectal carcinogenesis. *Pflugers Arch* 2000; 440 **(Suppl5):** R55-7.

26. Perse M, Zebic A, Cerar A. Rofecoxib does not inhibit aberrant crypt foci formation but inhibits later steps in the development of experimental colorectal cancer. Rofecoxib in experimental colon cancer. *Scan J Gastroenterol* 2005; **40:** 61-7.

27. Ward JM, Yamamoto RS, Brown CA. Pathology of intestinal neoplasms and other lesions in rats exposed to azoxymethane. *J Natl Cancer Inst* 1973; **51:** 1029-39.

28. Shetye J, Mathiesen T, Fagerberg J, Rubio C. Ear tumours induced by experimental carcinogenesis in the rat: excision prevents early death. *Int J Colorectal Dis* 1994; **9:** 125-7.

29. Bird RP. Observation and quantification of aberrant crypts in the murine colon treated with a colon carcinogen: preliminary findings. *Cancer Lett* 1987; **37:** 147-51.

30. Bird RP, Good CK. The significance of aberrant crypt foci in understanding the pathogenesis of colon cancer. *Toxicology Letters* 2000; **112:** 395-402.

31. Bird RP. Role of aberrant crypt foci in understanding the pathogenesis of colon cancer. *Cancer Letters* 1995; **93:** 55-71.

32. Rodrigues MA, Silva LA, Salvadori DM, De Camargo JL, Montenegro MR. Aberrant crypt foci and colon cancer: comparison between a short- and medium-term bioassay for colon carcinogenesis using dimethylhydrazine in Wistar rats. *Braz J Med Biol Res* 2002; **35:** 351-5.

33. Shipitz B, Bomstein Y, Mekori Y, Cohen R, Kaufman Z, Neufeld D, et al. Aberrant crypt foci in human colons: distribution and histomorphologic characteristics. *Hum Pathol* 1998; **29:** 469-75.

34. Cheng L, Lai MD. Aberrant crypt foci as microscopic precursors of colorectal cancer. *World J Gastroenterol* 2003; **9:** 2642-9.

35. Rubio CA, Shetye J, Jaramillo E. Non-polypoid adenomas of the colon are associated with subjacent lymphoid nodules. *Scand J Gastroenterol* 1999; **34:** 504-8.

36. Hamilton SR, Vogelstein B, Kudo S, Riboli E, Nakamura S, Hainaut P, et al. Carcinoma of the colon and rectum. In: Hamilton SR, Aaltonen LA, editors. WHO Classification of Tumours. Pathology and Genetics of Tumours of the Digestive System. Lyon: IARC Press; 2000. p. 103-113.

37. Cerar A, Zidar N, Vodopivec B. Colorectal carcinoma in endoscopic biopsies; additional histologic criteria for the diagnosis. *Path Res Pract* 2004; **200:** 657-62.

38. Nauss KM, Locniskar M, Pavlina T, Newberne PM. Morphology and distribution of 1,2-dimethylhydrazine dihydrochloride- induced colon tumors and their relationship to gut-associated lymphoid tissue in the rat. *J Natl Cancer Inst* 1984; **73:** 915-24.

39. Hardman WE, Cameron IL. Colonic crypts located over lymphoid nodules of 1,2-dimethylhydrazine-treated rats are hyperplastic and at high risk of forming adenocarcinomas. *Carcinogenesis* 1994; **15:** 2353-61.

40. Rubio CA, Nylander G, Sveander M, Duvander A, Alun ML. Minimal invasive carcinoma of the colon in rats. *An J Pathol* 1986; **123:** 161-5.

41. Ghirardi M, Nascimbeni R, Villanacci V, Fontana MG, Di Betta E, Salerni B. Azoxymethane-induced aberrant crypt foci and colorectal tumours in F344 rats: sequential analysis of growth. *Eur Surg Res* 1999; **31:** 272-80.

42. Bissonnette M, Khare S, von Lintig FC, Wail RK, Nguyen L, Zhang Y, et al. Mutational and nonmutational activation of p21ras in rat colonic azoyxmethane-induced tumors: effects on mitogen-activated protein kinase, cyclooxygenase-2, and cyclin D1. *Cancer Res* 2000; **60:** 4602-9.

43. Luceri C, De Filippo C, Caderni G, Gambacciani L, Salvadori M, Giannini A, et al. Detection of somatic DNA alterations in azoxymethane-induced F344 rat colon tumors by random amplified polymorphic DNA analysis. *Carcinogenesis* 2000; **21:** 1753-6.

44. Blum CA, Tanaka T, Zhong X, Li Q, Dashwood WM, Pereira C, et al. Mutational analysis of Ctnnb1 and Apc in tumors from rats given 1,2-dimethylhydrazine or 2-amino-3-methylimidazo[4,5-f]quinoline: mutational »hotspots« and the relative expression of beta-catenin and c-jun. *Mol Carcinog* 2003; **36:** 195-203.

45. De Filippo C, Caderni G, Bazzicalupo M, Briani C, Giannini A, Fazi M, et al. Mutations of the Apc gene in experimental colorectal carcinogenesis induced by azoxymethane in F344 rats. *Br J Cancer* 1998; **77:** 2148-51.

46. Takahashi M, Fukuda K, Sugimura T, Wakabayashi K. Beta-catenin is frequently mutated and demonstrates altered cellular location in azoxymethane-induced rat colon tumors. *Cancer Res* 1998; **58:** 42-6.

47. Yamada Y, Yoshimi N, Hirose Y, Kawabata K, Matsunaga K, Shimizu M, et al. Frequent ?-catenin gene mutations and accumulations of the protein in the putative preneoplastic lesions lacking macroscopic aberrant crypt foci appearance in rat colon carcinogenesis. *Cancer Res* 2000; **60:** 3323-7.

48. Takahashi M, Mutoh M, Kawamori T, Sugimura T, Wakabayashi K. Altered expression of beta-catenin, inducible nitric oxide synthase and cyclooxygenase-2 in azoxymethane-induced rat colon carcinogenesis. *Carcinogenesis* 2000; **21:** 1319-27.

49. De Jong TA, Skinner SA, Malcontenti-Wilson C, Vogiagis D, Bailey, van Driel IR, et al. Inhibition of rat colon tumors by sulindac and sulindac sulfone is independent of K-ras (codon 12) mutation. Am J Physiol *Gastrointest Liver Physiol* 2000; **278:** G266-72.

50. Vivona AA, Shpitz B, Medline A, Bruce WR, Hay K, Ward MA, et al. K-ras mutations in aberrant crypt foci, adenomas and adenocarcinomas during azoxymethane-induced colon carcinogenesis. *Carcinogenesis* 1993; **14:** 1777-81.

51. Caderni G, Dolara P, Fazi M, Luceri C, Geido E, Rapallo A, et al. Cell cycle variantions in azoxymethane-induced rat colorectal carcinogenesis studied by flow cytometry. *Oncol Rep* 1999; **6:** 1417-20.

52. Kishimoto Y, Morisawa T, Hosoda A, Shiota G, Kawasaki H, Hasegawa J. Molecular changes in the early stage of colon carcinogenesis in rats treated with azoxymethane. *J Exp Clin Cancer Res* 2002; **21:** 203-11.

53. Ehrlich VA, Huber W, Grasl-Kraupp B, Nersesyan A, Knasmuller S. Use of preneoplastic lesions in colon and liver in experimental oncology. *Radiol Oncol* 2004; **38:** 205-16.

Radiol Oncol 2005; 39(1): 71-8.

IMRT point dose measurements with a diamond detector

Erin Barnett, Marc MacKenzie, B. Gino Fallone

Department of Physics, University of Alberta, and Department of Medical Physics, Cross Cancer Institute, Edmonton, Alberta, USA

Background. *Radiation dose distribution calculations used in treatment planning systems (TPS) describe dose deposition well for large fields. For small fields encountered in Intensity Modulated Radiation Therapy (IMRT) these models may be less accurate. Dose verification of IMRT fields is therefore essential in IMRT implementation and quality assurance. For these smaller fields, lateral electronic equilibrium may not exist and volume averaging effects in ion chambers become increasingly problematic. For this reason, detectors with sensitive volumes smaller than that of conventional ion chambers are preferable in both small fields and high dose gradient region. Diamond detectors are capable of making such accurate dosimetric measurements.*

Methods. *This study compares dosimetry measurements made with a PTW-Freiburg type 60003 diamond detector, an Exradin A12 ion chamber, a PTW-Freiburg PinPoint ion chamber and a Varian aS500 EPID. Dose measurements were made in a clinical prostate intensity modulated beam. Due to difficulties encountered when dosimetric measurements are made in high dose gradient regions, probe positioning within IMRT fields was investigated and a method to establish better probe positions is proposed. Measured doses were compared with HELAX-TMS calculated doses to verify performance of the TPS used in this center.*

Results. *The diamond detector dosimetry is extremely sensitive to positioning particularly in high dose gradient regions. The results indicate that improved agreement between doses measured with various dosimeters can be obtained by appropriate selection of the probe position. Avoidance of high dose gradient regions improves agreement between measured doses particularly for the PinPoint chamber, the diamond detector and the EPID.*

Conclusions. *The use of diamond detectors and EPIDs in dosimetry is an attractive option particularly for verification of IMRT treatments. Although 2D dose verification of IMRT treatments is a more desirable option than point dose verification, an independent check of EPID or film verification is beneficial. Use of a diamond detector is an excellent option for dose measurements in cases where portal imaging devices are not available such as the case of helical tomotherapy.*

Key words: radiotherapy dosage; radiotherapy; diamond detector, intensity modulated radiotherapy

Correspondence to: Prof. B. Gino Fallone, PhD, FCCPM, ABMP, Department of Physics and Oncology, University of Alberta, and Department of Medical Physics, Cross Cancer Institute, Edmonton, Alberta; Phone: +1 780 432-8750; Fax: +1 780 432-8615; E-mail: gfallone@phys.ualberta.ca

Received 4 August 2004
Accepted 14 August 2004

Introduction

The present day movement in radiation therapy is towards intensity modulated radiation therapy (IMRT). The aim of these conformal radiation treatments is to achieve a higher dose within the target volume(s) while minimizing the damage to the organs at risk. IMRT improves upon the technique of 3D conformal radiation therapy by not only improving the conformation of the treated volume to the target volume, but by allowing for more homogeneous doses to be delivered to target volumes.[1] IMRT is a particularly valuable technique when target volumes are concavely shaped and closely neighbored by sensitive volumes that can tolerate very little radiation damage.[2] The fields required to deliver intensity modulated treatments in step and shoot IMRT consist of a number of beam segments that can be more complex in shape than fields previously encountered in radiation therapy. Not only are the segments making up individual IMRT fields smaller than conventional radiotherapy beams, but higher dose gradients are also present in intensity modulated beams (IMB). Within high dose gradients volume averaging effects become more pronounced particularly for large volume point dosimeters. Volume averaging of a signal is not a significant problem if the signal is constant or changes in a linear manner within the sensitive volume of the detector.[3] In high dose gradients the response of a detector may differ substantially from the absorbed dose.[4] A reduction in the size of the sensitive volume yields a reduction in the magnitude of volume averaging effects and therefore leads to more accurate measurements in high dose gradient regions. Also within these dose gradients electronic equilibrium may not exist. The effect of electronic disequilibrium on dosimetric measurements in narrow beams has been investigated by various groups, particularly in the field of stereotactic radiosurgery.[6-8] According to Heydarian *et al.*, ion chamber based dosimetry in steep dose gradients in the absence of lateral electronic equilibrium is not appropriate.[8] The presence of ion chambers in a radiation field enhances the lateral electronic disequilibrium.[9] Bjärngard *et al.* examined the effect of incomplete lateral electronic equilibrium on central axis dose measurements and made comparisons with Monte Carlo simulation. This group concluded that the detectorís sensitive volume must be significantly smaller than the radius of the stereotactic beam in which dosimetric measurements are to be made. Their simulations indicated that at a beam radius of 1.5 cm, lateral electronic equilibrium was reached for a 6 MV simulated beam.[5] For higher beam qualities, a larger field size is required to ensure the existence of lateral electronic equilibrium.

Diamond detectors are an attractive option for making dosimetric measurements in small fields due to the inherently small sensitive volume of these devices as well as energy and directional independence as documented by a number of groups.[10-12] In a study conducted by Heydarian *et al.* it was found that lateral electronic disequilibrium can cause dose measurement errors particularly for large volume non-tissue equivalent detectors.[8] Since diamond detectors are small volume essentially tissue equivalent dosimeters, the presence of lateral electronic equilibrium is not a strict requirement for diamond detector dosimetry.

The objective of this investigation was to determine the feasibility of making point dose measurements in IMBs that may contain small segments and high dose gradients. Dose measurements in solid water phantom were conducted for 15 MV linear accelerator generated beam generated by a Varian 2100 EX linear accelerator [Varian Medical Systems, Palo Alto, CA]. Dose measurements were made using a PTW-Freiburg type 60003 diamond detector, Exradin A12 ion chamber, PTW-Freiburg PinPoint ion chamber and a Varian aS500 EPID.

Materials and methods

The diamond detector employed in this study is a type 60003 (S/N 9-032) [PTW-Freiburg, Germany]. The sensitive volume consists of a natural diamond crystal with a sensitive area of 6.8 mm^2, a thickness of 0.25 mm giving a sensitive volume of 1.7 mm^3. This volume is oriented in the probe housing such that the sensitive volume is positioned 1 mm from the front face of the cylindrical probe. Prior to all dosimetric measurements, the diamond detector was irradiated to a dose of at least 5 Gy to ensure the stability of the response.

Diamond detectors are known to exhibit a dose rate dependence that is described by

$$i = R \cdot (\dot{D})^{\Delta} + i_{dark} \qquad [1]$$

where i is the diamond current, R is a constant of proportionality, $\dot{D}$ is the dose rate, Δ is the sublinear response parameter of the diamond detector and i_{dark} is the dark current of the detector.[13,14] The magnitude of the dark current of diamond detectors is sufficiently small that this additive term in this equation can be neglected. The Δ and R value of this detector are 0.995 ± 0.002 and 0.0254 ± 0.0003 nA/cGy/min, respectively. Corrections for the dose rate dependence were made according to equation 1.

The PinPoint ion chamber used in this study is a PTW-Freiburg type 31006 (S/N 0290) [PTW-Freiburg, Germany]. This detector has a 0.015 cm^3 air filled sensitive volume. The wall material is 0.56 mm of PMMA and 0.15 mm of graphite. The sensitive volume is cylindrical in shape with a length of 5 mm and a radius of 1 mm. The pre-irradiation dose of 2 Gy as recommended in the instruction manual was delivered prior to all dosimetric measurements.

The primary substandard ion chamber used by this centre is an Exradin A12 ion chamber (S/N 396) [Standard Imaging, Middleton, WI]. This dosimeter is a Farmer type chamber with a collecting volume of 0.651 cm^3. The diameters of the sensitive volume and the collector are 6.1 mm and 1.0 mm respectively. The wall, collector and guard material of this device are made with Shonka air-equivalent plastic C552 with a wall thickness of 0.5 mm.

The Varian Portalvision aS500 EPID [Varian Medical Systems, Palo Alto, CA] consists of an amorphous silicon solid state flat-panel imaging device. Dosimetry measurements using a PortalVision aS500 EPID [Varian Medical Systems, Palo Alto, CA] were made with a technique involving convolution-type calculations described by B. Warkentin *et al.* and S. Steciw *et al.*[15,16]

Dosimetry of clinical prostate intensity modulated beam

The probes were positioned at isocenter of a Varian 2100 EX linear accelerator [Varian Medical Systems, Palo Alto, CA] at a depth of 10 cm in a solid water phantom [Gammex, Middleton, WI] with their axes of symmetry perpendicular to the beam central axis (CAX). The responses of the dosimeters to a step and shoot clinical prostate plan were monitored as a function of time using a Wellhöfer Dosimetrie System [Scanditronix-Wellhofer, Schwarzenbruck, Germany]. The Wellhöfer system outputs a signal in terms of percent dose. In order to relate this percent dose during the delivery of the irradiations at various field sizes, the percent dose response of the dosimeters in a 10 x 10 cm^2 field was also observed for all point dosimeters. At the time of experimentation the output of the linac was measured with a PR-06C Farmer type chamber [CNMC Company, Nashville, TN] in a 10 x 10 cm^2 field in a constancy device that ensures the uniform probe positioning that is used for routine quality assurance. The percent dose output of the Wellhöfer system was converted to a dose rate by making use of the relationship between the Wellhöfer electrometer response to the 10 x 10 cm^2 radiation

field at a depth of 10 cm and the dosimetry measurements under the same conditions. In addition to monitoring the diamond response using the Wellhöfer system, the diamond current response to a 10 x 10 cm^2 irradiation field at a depth of 10 cm was monitored using a Keithley 6514 electrometer [Keithley Instruments, Inc., Cleveland, OH]. This additional step is required when conducting dosimetry using a diamond detector as the diamond current is related to the dose rate by equation 1. The percent dose rate output of the Wellhöfer system was converted to a diamond current by means of this cross calibration. The resulting diamond current was subsequently converted to a dose rate. To arrive at the total dose during the IMB delivery, the dose rates were integrated with time. EPID dose distributions for each field segment were measured according to the method described by B. Warkentin *et al* and S. Steciw e*t al* The method described in these works results in the dose distribution at a depth of 10 cm for an source surface distance of 90 cm.[15,16] The central pixel values of the EPID dose distributions for each segment were extracted and compared with doses measured with the point dosimeters.

Dose calculations of this IMB delivered to a water phantom were made using HELAX-TMS [Nucletron, Veenendaal, The Netherlands]. In addition to the IMB, a 5 x 5 cm^2 field centered about a different isocenter was included in the calculation space to allow for the conversion of calculated percent doses to doses. This 5 x 5 cm^2 field was positioned sufficiently far from the IMBs so that the scatter contribution from this field to the IMB was negligible.[17] Comparison of the calculated point dose at isocenter was made to the dose measured with the various dosimeters.

Dosimetry of clinical prostate intensity modulated beam at improved detector positions

Due to the difficulties associated with conducting point dose measurements in high dose gradients, it is desirable to make point dose measurements in low dose gradient regions. In order to establish improved detector positions, Matlab code [Mathworks, Natick, MA] was written that excluded probe positions based on their vicinity to segment edges. For a given segment, possible probe positions were deemed acceptable if the beam edges were distanced 1 cm from the probe position thereby avoiding measurement positions within the penumbral regions of that segment. A probe position map for the IMB was then generated based on the acceptable probe positions for each of the segments comprising the beam according to the respective segment weightings in the IMB. Although probe positions outside the treatment field are considered to be improved detector positions according to segment edge exclusion criteria, these positions were not considered to be improved positions. The dose within the treatment field is the quantity of interest, not the dose delivered via scatter to the surrounding volume. Comparison between measured and calculated doses was made.

Results

Dosimetry of clinical prostate intensity modulated beam

The beam segments that comprise the prostate step and shoot IMB are shown in Figure 1. The coordinates (0,0) of each segment correspond to isocenter. The results of the dose measurements at isocenter of the clinical prostate IMRT treatment are summarized in Table 1.

By viewing the segment shapes shown in Figure 1 it is apparent that the poorest agreement between the measured doses occurs in cases where segment edges abut the point of measurement. This poor agreement is attributed to volume averaging effects within the

sensitive volumes and errors introduced by probe positioning. Although the extremely small sensitive volume of the diamond detector is desirable for many applications, it makes the positioning of the probe critical. Since the thickness of the sensitive volume of this diamond detector is 0.25 mm, an uncertainty of ± 0.5 mm in probe positioning can mean the difference between centering the sensitive volume in the open portion of the beam or in the penumbral region of segments that abut the point of measurement. Thus di-

Table 1. Doses measured at isocenter during delivery of 8 segment clinical prostate intensity modulated beam

	Dose (cGy)				
Segment	A12	PinPoint	Diamond detector	EPID	HELAX-TMS
1	25.5 ± 0.4	29.0 ± 0.2	10.9 ± 0.1	19 ± 4	23.6
2	25.9 ± 0.4	29.5 ± 0.2	11.2 ± 0.1	19 ± 4	23.8
3	26.1 ± 0.4	28.2 ± 0.2	15.2 ± 0.2	21 ± 4	21.7
4	40.3 ± 0.6	40.0 ± 0.3	40.2 ± 0.5	39.9 ± 0.1	39.5
5	36.0 ± 0.4	35.9 ± 0.2	36.1 ± 0.5	35.9 ± 0.1	35.6
6	34.9 ± 0.5	38.9 ± 0.3	40.2 ± 0.5	39.7 ± 0.1	40.5
7	9.3 ± 0.1	10.8 ± 0.1	7.5 ± 0.1	10 ± 2	2.7
8	2.18 ± 0.03	2.24 ± 0.01	2.26 ± 0.01	2.5 ± 0.1	0.0
Total	200 ± 1	214.5 ± 0.5	164 ± 1	186 ± 7	187

Table 2. Doses measured at improved detector position 1 (-1.3 cm 1.7 cm) during delivery of 8 segment intensity modulated field

	Dose (cGy)				
Segment	A12	PinPoint	Diamond detector	EPID	HELAX-TMS
1	2.58 Ī 0.04	1.61 Ī 0.02	1.40 Ī 0.02	1.7 Ī 0.1	1.1
2	2.63 Ī 0.04	1.65 Ī 0.02	1.47 Ī 0.02	1.7 Ī 0.1	1.1
3	10.1 Ī 0.2	3.23 Ī 0.05	2.61 Ī 0.04	3.0 Ī 0.3	2.6
4	40.6 Ī 0.7	41.0 Ī 0.6	40.9 Ī 0.6	40.2 Ī 0.1	39.5
5	36.4 Ī 0.7	36.9 Ī 0.6	36.5 Ī 0.6	36.2 Ī 0.1	35.6
6	39.4 Ī 0.6	40.6 Ī 0.5	40.2 Ī 0.5	40.0 Ī 0.2	39.9
7	5.0 Ī 0.1	4.69 Ī 0.05	4.61 Ī 0.05	4.5 Ī 0.5	1.3
8	3.17 Ī 0.04	2.75 Ī 0.03	2.72 Ī 0.03	2.8 Ī 0.2	0.0
Total	140 Ī 1	132 Ī 1	130 Ī 1	130.1 Ī 0.7	121.2

Table 3. Doses measured at improved detector position 2 (0.7 cm, 3.0 cm) during delivery of 8 segment intensity modulated field

	Dose (cGy)				
Segment	A12	PinPoint	Diamond detector	EPID	HELAX-TMS
1	1.23 Ī 0.02	1.15 Ī 0.01	1.00 Ī 0.01	1.36 Ī 0.05	0.2
2	1.26 Ī 0.02	1.22 Ī 0.01	1.04 Ī 0.01	1.35 Ī 0.04	1.1
3	1.26 Ī 0.02	1.18 Ī 0.01	1.00 Ī 0.01	1.26 Ī 0.04	0.9
4	37.3 Ī 0.6	39.7 Ī 0.3	39.2 Ī 0.5	38.4 Ī 0.3	39.2
5	33.8 Ī 0.5	36.3 Ī 0.2	35.6 Ī 0.5	35.0 Ī 0.2	35.5
6	38.2 Ī 0.6	41.2 Ī 0.3	40.4 Ī 0.5	39.7 Ī 0.3	36.6
7	45.6 Ī 0.7	49.9 Ī 0.3	49.8 Ī 0.7	48.7 Ī 0.2	49.6
8	36.9 Ī 0.6	44.9 Ī 0.3	45.6 Ī 0.4	44.9 Ī 0.1	46.1
Total	196 Ī 1	216 Ī 1	214 Ī 1	210.8 Ī 0.5	209.1

amond detector dosimetry is extremely sensitive to positioning particularly in high dose gradient regions.

The doses calculated by HELAX-TMS appearing in Table II are included for comparative purposes only. It is not assumed that these values represent the most accurate determination of dose.

Dosimetry of clinical prostate intensity modulated beam at improved detector positions

The map used to establish improved detector positions for the clinical IMB is shown in Figure 2. The positions within the treatment

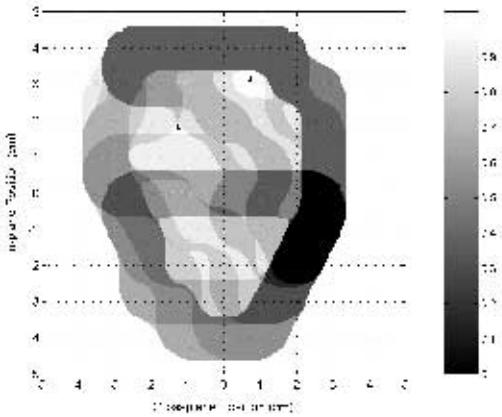

Figure 2. Map used to determine appropriate probe positions for a clinical prostate intensity modulated beam.

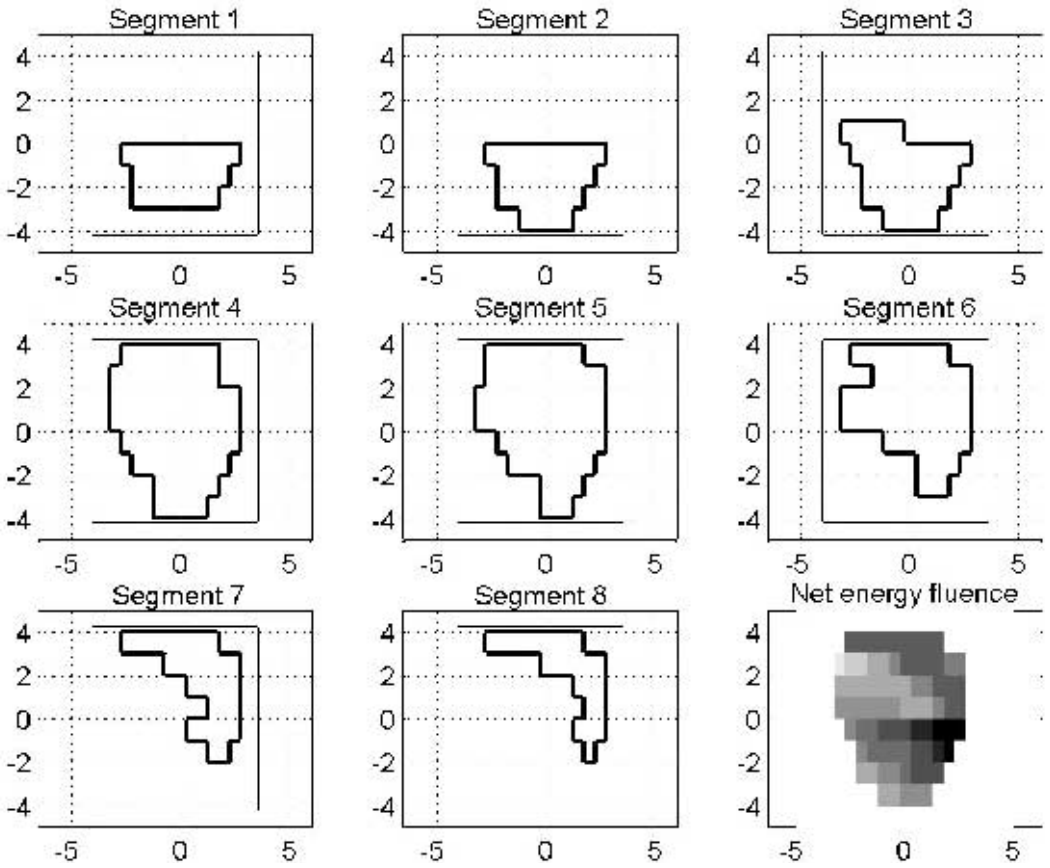

Figure 1. Shape of eight segments that comprise single intensity modulated beam and »fluence map« resulting from delivery of eight step and shoot segments - thick lines illustrate segment geometry, thin lines illustrate main collimator settings.

field with the highest value assigned to them are the most appropriate positions to make point measurements according to the criteria described in the preceding section. The arrows in Figure 2 indicate the positions that best avoid high dose gradients, (0.7 cm, 3.0 cm) and (-1.3 cm, 1.7 cm), the cross-plane and in-plane positions respectively relative to isocenter. The results of the dose measurements at the improved probe positions as established using the in house software of the clinical prostate IMRT treatment are summarized in Tables 2 and 3.

The results summarized in Tables 2 and 3 indicate that improved agreement between doses measured with various dosimeters can be obtained by appropriate selection of the probe position. Avoidance of high dose gradient regions improves agreement between measured doses particularly for the PinPoint chamber, the diamond detector and the EPID. By measuring the dose at the first improved detector position as determined by the technique previously described, excellent results are obtained. The total doses measured by the PinPoint chamber, diamond detector and EPID are very nearly in agreement within one standard error. Although the agreement between the doses measured at the second improved detector position is not as good as at the first improved detector position, the PinPoint and EPID values differ by less than 1.5 % from the diamond detector measured value. Comparison of the results summarized in Tables 1 through 3 indicates that improvement in the agreement between doses measured with various dosimeters can be obtained by choosing measurement points appropriately. Avoidance of high dose gradient regions is necessary to avoid volume averaging effects that greatly affect large volume chamber and to eliminate the high sensitivity of dosimeters to small errors in positioning.

Discussion

IMRT gives rise to smaller field sizes and higher dose gradients than were previously encountered in conventional radiation therapy with the exception of stereotactic radiosurgery. Point dose measurement of IMBs can be complicated by the presence of high dose gradients within these fields. Dose measurement in the absence of these gradients is necessary to avoid volume averaging effects. The technique employed in this investigation to select better probe positions for the clinical IMB that avoid these high dose gradients gave rise to improved agreement between the dosimeters used in this study. Sub-optimal agreement was obtained between measured and HELAX-TMS calculated doses. This result is attributed to the difficulties associated with penumbral modeling in the release of HELAX-TMS used in this center.

The use of diamond detectors and EPIDs in dosimetry is an attractive option particularly for verification of IMRT treatments. Although 2D dose verification of IMRT treatments is a more desirable option than point dose verification, an independent check of EPID or film verification is beneficial. Use of a diamond detector is an excellent option for dose measurements in cases where portal imaging devices are not available such as the case of helical tomotherapy. Also for accelerators that are equipped with multi-leaf collimators but lack a portal imager, diamond detector dosimetry is a viable technique. The EPID dosimetry technique employed in this study is applicable only to specific geometric conditions at the present time, while diamond detector dosimetry is not limited by these conditions allowing for point verification at different positions and depths within phantom.

Acknowledgments

E. Barnett would like to thank NSERC and AHFMR for their financial support as well as Dr. S. Steciw and B. Warkentin for use of software to convert EPID images to dose distributions and H. Warkentin for assistance with HELAX-TMS.

References

1. Martens C, Claeys I, De Wagter C, De Neve W. The value of radiographic film for the characterization of intensity-modulated beams. *Phys Med Biol* 2002; **47:** 2221-34.

2. Webb S. *Intensity-Modulated Radiation Therapy*. Bristol: Institute of Physics Publishing; 2001.

3. Mack A, Scheib SG, Major J, Gianolini S, Pazmandi G, Feist H, et al.. Precision dosimetry for narrow photon beams used in radiosurgery-determination of Gamma Knife output factors. *Med Phys* 2002; **29:** 2080-9.

4. Martens C, De Wagter C, De Neve W. The value of the PinPoint ion chamber for characterization of small field segments used in intensity-modulated radiotherapy. *Phys Med Biol* 2000; **45:** 2519-30.

5. Bjarngard BE, Tsai JS, Rice RK. Doses on the central axes of narrow 6-MV x-ray beams. *Med Phys* 1990; **17:** 794-9.

6. Houdek PV, VanBuren JM, Fayos JV. Dosimetry of small radiation fields for 10-MV x rays. *Med Phys* 1983; **10:** 333-6.

7. Arcovito G, Piermattei A, D'Abramo G, Bassi FA. Dose measurements and calculations of small radiation fields for 9-MV x rays. *Med Phys* 1985; **12:** 779-84.

8. Heydarian M, Hoban PW, Beddoe AH. A comparison of dosimetry techniques in stereotactic radiosurgery. *Phys Med Biol* 1996; **41:** 93-110.

9. Heydarian M, Hoban PW, Beddoe AH. Dose rate correction factors for diamond detectors for megavoltage photon beams. *Phys Med Biol* 1997; **13:** 55-60.

10. De Angelis C, Onori S, Pacilio M, Cirrone GA, Cuttone G, Raffaele L, et al. An investigation of the operating characteristics of two PTW diamond detectors in photon and electron beams. *Med Phys* 2002; **29:** 248-54.

11. Laub WU, Kaulich TW, Nusslin F. A diamond detector in the dosimetry of high-energy electron and photon beams. *Phys Med Biol* 1999; **44:** 2183-92.

12. Laub WU, Wong T. The volume effect of detectors in the dosimetry of small fields used in IMRT. *Med Phys* 2003; **30:** 341-7.

13. Laub WU, Kaulich TW, Nusslin F. Energy and dose rate dependence of a diamond detector in the dosimetry of 4-25 MV photon beams. *Med Phys* 1997; **24:** 535-6.

14. Fowler JF, Attix FH. Solid state electrical conductivity doseimeters. In: Attix FH, Roesch WC, editors. *Radiation dosimetry*. Vol. 1. New York: Academic; 1966.

15. Steciw S, Warkentin BM, Rathee S, Fallone BG. A Monte Carlo based method for accurate IMRT verification using the aS500 EPID. *Med Phys* 2003; **30:** 1331.

16. Warkentin B, Steciw S, Rathee S and Fallone B G. Dosimetric IMRT verification with a flat-panel EPID. *Med Phys* 2003; **30:** 3143-55.

17. MacKenzie MA, Lachaine M, Murray B, Fallone BG, Robinson D and Field G C. Dosimetric verification of inverse planned step and shoot multileaf collimator fields from a commercial treatment planning system. *J Appl Clin Med Phys* 2002; **3:** 97-109.

Radiol Oncol 2005; 39(1): 1-4.

Simptomatska neperforirana Cowperjeva siringokela pri 5-letnem dečku

Roić G, Borić I, Posarić V, Bastić M, Župančić B

Izhodišča. Cowperjeva siringokela je redka anomalija Cowperjeve žleze pri otrocih. Nastane zaradi obstrukcije žleznega izvodila. Simptomatske oblike zdravimo glede na velikost siringokele in starost bolnika. Odločamo se za endoskopsko ali odprto perinealno operacijo.
Prikaz primera. Poročamo o simptomatski neperforirani siringokeli pri 5-letnem dečku. Čeprav običajno siringokelo najlepše prikažemo z izpraznitveno cistouretrografijo, s to preiskavo nismo zaznali nobene utesnitve ali polnitvenega defekta v bulbarnem delu sečnice. Seringokelo smo dokazali z ultrazvočno vodeno perinealno punkcijo, med katero smo injicirali kontrast v cistično spremembo.
Zaključki. Pri neperforirani siringokeli je ultrazvočna preiskava koristna metoda, zlasti pri mladih bolnikih in nam pomaga pri odločitvi za perinealni operativni poseg.

Radiol Oncol 2005; 39(1): 5-8.

Ultrazvočni pregled plevralnega prostora pri zdravih nosečnicah - preliminarni rezultati

Kocijančič I

Izhodišča. Namen naše študije je bil ugotoviti pogostnost ultrazvočnega prikaza fiziološke plevralne tekočine pri zdravih nosečnicah.

Bolnice in metode. Pri 47 zdravih nosečnicah smo naredeli ultrazvočno preiskavo plevralnega prostora, najprej v položaju na komolcu in potem še sede, obakrat z 9-12 MHz linearno sondo. Če smo na ta način našli anehogen plašč plevralne tekočine širok vsaj 2 mm, smo preiskavo ponovili še z 3-6 MHz konveksno abdominalno sondo.

Rezultati. Anehogen plašč plevralne tekočine tipične klinaste oblike je bil viden pri 28/47 (59·5%) nosečih prostovoljkah, od tega na obeh straneh pri 18/47 (38·3%) in le na eni strani pri 10/47 (21·2%). Povprečna širina plašča tekočine (povprečje rezultatov v obeh položajih) je bila 2,79 mm (SD 0,91 mm, razpon od 1,8 mm do 6,4 mm). Število nosečnic z vidno plevralno tekočino, ki so nosile ženske in moške plodove je bilo enako, toda razlika v povprečni širini plašča tekočine enih in drugih je bila statistično pomembna (t-test: p=0,041). Več kot 3 mm plevralne tekočine smo z lahkoto prikazali s 3-6 MHz abdominalno konveksno sondo pri 7/47 (15%) vseh preiskovank.

Zaključki. Pri ultrazvočnem pregledu plevralnega prostora, pa tudi zgornjega dela trebušne votline lahko včasih najdemo manjšo količino plevralne tekočine pri sicer zdravih nosečnicah. Take izolirane slučajne najdbe ne smemo smatrati kot bolezenski znak.

Radiol Oncol 2005; 39(1): 9-13.

Poškodba aksilarne arterije. Diagnosticiranje pooperativne arterijske okluzije in kolateralnega pretoka z dvojnim ultrazvokom

Krnić A, Sučić Z, Vučić N, Bilić A

Izhodišča. Poškodba aksilarne arterije je življenjsko nevarna. Zahteva takojšnjo pomoč s kompresijo žile in pri mnogih bolnikih moramo narediti eksplorativno operacijo. Zaradi ugotavljanja prehodnosti žile je po posegu često potrebno narediti tudi angiografijo.

Prikaz primera. Poročamo o poškodbi aksilarne arterije pri 28-letni bolnici. Čeprav smo z dvojnim ultrazvokom natančno opredelili postoperativne prestenotične in poststenotične spremembe, smo jih potrdili še z angiografijo. Preiskava je pokazala obsežen kolateralen pretok v aksili in motnje perfuzije z aksilarno arterijo. Bolnico smo ponovno operirali, narejena je bila trombektomija v aksilarni arteriji in prišlo je do znatnega izboljšanja prekrvavitve zgornjega uda.

Zaključki. V opisanem primeru smo z dvojnim ultrazvokom natančno opredelili spremembe v aksili in bi lahko celo opustili preiskavo z angiografijo.

Radiol Oncol 2005; 39(1): 15-21.

Ultrazvočne značilnosti akutnega vnetja slepiča pri otrocih

Vegar-Zubović S, Lincender L, Dizdarević S, Sefić I, Dalagija F

Izhodišča. Najpogostejši vzrok bolečin v trebuhu pri otrocih, ki zahteva kirurško obravnavo, je akutno vnetje slepiča. Nobeden od kliničnih znakov nima absolutne diagnostične in napovedne vrednosti. Namen naše raziskave je bil opredeliti ultrazvočne značilnosti akutnega vnetja slepiča ter jih povezati s patomorfološkimi izvidi in intenzivnostjo vnetja.

Metode. V prospektivni raziskavi smo ultrazvočno pregledali 50 otrok z znaki akutnega abdomna. Pri vseh bolnikih smo ultrazvočno diagnozo potrdili kirurško in patohistološko.

Zanimalo nas je ali se trajanje simptomov do bolnišnične obravnave razlikuje glede na patohistološki izvid. Pri raziskavi smo uporabljali Toshiba Sonolayer ultrazvok s 3,75 MHz konveksno in 8 MHz linearno sondo.

Rezultati. Od 8 ultrazvočnih znakov akutnega vnetja slepiča so se zanesljivi pokazali le anteriorno-posteriorna debelina slepiča, debelina periapendikularnega maščobnega tkiva in odsotnost peristaltike. Najpogostejši patohistološki izvid je bilo flegmonozno vnetje slepiča (44%). Pri več kot polovici bolnikov smo odkrili perforirano gangrenozno vnetje slepiča (30%) ali samo gangrenozno vnetje (22%), kar kaže na dolg časovni interval trajanja simptomov pred bolnišnično obravnavo. Statistična analiza je pokazala možnost ocenjevanja stopnje vnetja z anteriorno-posteriorno debelino slepiča in debelino periapendikularnega maščobnega tkiva kot znakoma zadebelitve stene črevesa.

Zaključki. Ultrazvočna preiskava je metoda izbire, kadar ob klinični preiskavi dvomimo, ali ima otrok akutno vnetje slepiča. Z anteriorno-posteriorno debelino slepiča, debelino stene in debelino periapendikularnega maščobnega tkiva lahko zanesljivo ultrazvočno ocenimo stopnjo intenzivnosti vnetja slepiča.

Radiol Oncol 2005; 39(1): 23-35.

Odkrivanje ledvičnih tumorjev in določevanje razširjenosti bolezni z magnetnoresonačno preiskavo

Kirova K

Izhodišča. Magnetnoresonančna preiskava je ena najbolj ustreznih preiskovalnih metod, saj bolnik ni izpostavljen ionizirajočemu sevanju in ne zahteva injiciranja jodovih kontrastnih sredstev. Visoka zmogljivost, dobra računalniška podpora in tehnologija hitrih pulznih frekvenc so tiste lastnosti, ki omogočajo dobro celostno oceno ledvičnih bolezni.

Zaključki. Pri magnetnoresonačnih preiskavah predstavljajo posebno težavo različni protokoli preiskav, zato je pomembno, da tehnike preiskav čimbolj standardiziramo. Na ta način omogočimo ponovljivost in primerljivost rezultatov preiskav.

Radiol Oncol 2005; 39(1): 37-47.

Primerjava kvadrantne in razširjene biopsije prostate kot prvo vzorčenje pri bolnikih z napredovalo obliko raka prostate

Zoran Brnić Z, Anić P, Gašparov S, Radović N, Kučan D, Vidas Ž, Zeljko Ž, Lozo P, Ramljak V

Izhodišča. Pri bolnikih z zgodnjim rakom prostate omogoča razširjena biopsija prostate (BP) boljšo senzitivnost in natančnejšo zamejitev tumorja, pri bolnikih z razširjenim rakom prostate pa je potrebna samo potrditev raka z BP.
Z raziskavo smo želeli ugotoviti, ali je kvadrantna BP primerna za patološko oceno pri bolnikih, ki imajo verjetno napredovali rak prostate. Prav tako smo želeli ugotoviti, ali zmanjšanje števila vzorcev poslabša zanesljivost BP zaradi manjkajočih kvantitativnih histoloških podatkov.
Bolniki in metode. Pregledali smo podatke 84 moških, pri katerih je bila opravljena BP in so bili razdeljeni v skupini »H« (verjeten) in »L« (malo verjeten) napredovali rak prostate. Patohistološke izvide 5-12 vzorcev BP in simuliranih kvadrantnih BP smo retrospektivno primerjali med seboj, posebej glede na prisotnost raka prostate, volumen tumorja, Gleasonovo točkovanje in prisotnost prostatične intraepitelne neoplazme visokega gradusa (HGPIN).
Rezultati. V skupini H je bila stopnja detekcije raka prostate primerljiva, signifikantno pa je padla v skupini L pri simuliranih kvadrantnih BP. Tako se je število pozitivnih vzorcev v skupini H samo neznačilno spremenilo ($p = 0,39$) in se je značilno zmanjšalo v skupini L ($p = 0,04$) zaradi zmanjšanja vzorčenja. Prav tako v skupini H nismo spregledali nobene HGPIN, medtem ko smo v kupini L spregledali dve. Kot posledica zmanjšanja števila vzorcev se je Gleasonovo točkovanje v obeh skupinah neznačilno spremenilo.
Zaključki. Pri bolnikih z napredovalim rakom prostate je kvadrantna BP primeren prvi diagnostični postopek, saj z njo dobimo dovolj pomembnih podatkov. Zmanjšanje števila vzorcev praviloma ne vpliva na odločitev o vrsti zdravljenja napredovalega raka prostate.

Radiol Oncol 2005; 39(1): 49-53.

Multipli primarni malignomi pri bolnikih s pljučnim rakom

Kurishima K, Satoh H, Homma S, Kagohashi K, Ishikawa H, Ohtsuka M, Sekizawa K

Izhodišča. Da bi ugotovili incidenco in vrsto multiplih primarnih malignomov pri bolnikih s pljučnim rakom, smo naredili retrospektivno raziskavo.
Metode. Analizirali smo podatke o 1194 bolnikih s pljučnim rakom, ki smo jih na našem oddelku obravnavali v 29-letnem obdobju do avgusta 2004.
Rezultati. Ugotovili smo, da je 98 (8,2%) od 1194 bolnikov s pljučnim rakom imelo multipli primarni malignom. Metahrono so bili odkriti v 77,6% , sinhrono pa v 21,4%. Bolj pogosto so nastajali pri napredovalih oblikah pljučnega raka (v stadijih IIIA do IV 67,3%) kot pa v zgodnji oblikah (v stadijih IA do IIB 32,7%). Najpogostejši je bil skvamoznocelični karcinom (pri 40 bolnikih oz. pri 40,8%). Najpogostejši prvi primarni tumor smo našli v gastrointestinalnem traktu, nato v pljučih in maternici. 57 (85,1%) od 67 bolnikov, ki je imelo malignom v prebavilih, dihalih ter glavi in vratu, je bilo kadilcev. Od 98 bolnikov, ki so imeli multipli primarni malignom, jih je bilo kirurško zdravljenih le 26 (26,5%), čeprav jih je 40 (40,8%) imelo omejeno obliko pljučnega raka s stadijem IA-IIIA.
Zaključki. Ugotovili smo, da pri bolnikih z nedrobnoceličnim pljučnim rakom predstavlja metahroni multipli primarni malignom statistično značilen napovedni dejavnik (p=0,0480), kar pa nismo uspeli potrditi pri bolnikih z drobnoceličnim pljučnim rakom in pri sinhronih malignomih.

Radiol Oncol 2005; 39(1): 55-9.

Prikaz primera karcinoma znojnih žlez, ki je razjedal lobanjske kosti

Arslan M, Karadeniz AN, Aksu G, Güveli M

Izhodišča. Karcinomi znojnih žlez so redki tumorji. Prav tako so redki tisti karcinomi znojnih žlez, ki so žlezno aktivni. Do sedaj je v literaturi opisanih le okoli 200 primerov in samo eden je razjedal lobanjske kosti. Zaradi njihove redkosti tudi ne poznamo najprimernejšega in najučinkovitejšega zdravljenja.

Prikaz primera. Opisujemo 47-letno bolnico, ki so jo po začetni operaciji leta 1989 še šestkrat operirali zaradi ponavljajočega se tumorja v predelu kože kraniuma. Patomorfološki pregled je po vsaki operaciji pokazal benigni tumor (adenom znojne žleze, cilindrom), razen po zadnji, ko smo ugotovili maligni cilindrom.

Pred zadnjo operacijo smo ugotovili, da je recidivni tumor, ki je ležal v levi parietalni regiji velik 10 x 6 cm. Z računalniško tomografijo pa smo videli, da je 11 x 5 cm velik tumor poškodoval lobanjske kosti, vraščal v duro ter povzročal periostalno reakcijo.

Zaradi maligne transformacije in velike nevarnosti ponovitve bolezni smo se odločili za postoperativno radioterapijo.

Zaključki. Do sedaj je ob naši bolnici opisan samo še en primer, kjer je tumor znojnih žlez vraščal v lobanjske kosti.

Radiol Oncol 2005; 39(1): 61-70.

Z dimetilhidrazinom inducirani tumorji debelega črevesa in danke pri podgani

Perše M, Cerar A

Živalski modeli so pri raziskavah raka na debelem črevesju in danki nepogrešljivi, saj omogočajo raziskovanje in testiranje številnih dejavnikov, ki jih ni mogoče neposredno ugotavljati pri ljudeh.

Edinega izmed živalskih modelov raka na debelem črevesju in danki predstavljajo z dimetilhidrazinom (DMH) inducirane podgane, ki razvijejo tumorje debelega črevesa in danke zelo podobne humanim. S člankom želimo predstaviti morfološke in genetske spremembe tega modela, ki je veliko prispeval k današnjemu poznavanju etioloških in drugih dejavnikov, ki vplivajo na nastanek in razvoj raka. Danes pa je nepogrešljiv pri raziskavah črevesnih karcinogenov in kemopreventivnih substanc.

Radiol Oncol 2005; 39(1): 71-8.

Uporaba diamantnega detektorja pri meritvah absorbirane doze pri IMRT

Barnett E, MacKenzie M, Fallone BG

Izhodišča. Pri velikih obsevalnih poljih lahko s sistemi za načrtovanje obsevanja natančno izračunamo prostorsko porazdelitev absorbirane doze, pri manjših poljih, ki jih uporabljamo v intenzitetno modulirani radioterapiji (IMRT), pa utegnemo biti manj natančni. Za zagotovitev kvalitete obsevanja so tako nujno potrebne dodatne meritve absorbirane doze pri uporabi IMRT polj. V manjših poljih ni lateralnega elektronskega ravnovesja, zaradi česar ionizacijska celica, ki povpreči dozo po vsej svoji prostornini - pri meritvah doze v točki - ni zanesljiva. V majhnih poljih z visokimi gradienti doze so primernejši dozimetri z manjšimi občutljivimi prostorninami, kakršen je diamantni detektor.

Material in metode. V študiji primerjamo dozimetrične meritve, opravljene z diamantnim detektorjem PTW-Freiburg (tip 60003), z ionizacijsko celico Extradin A12, s točkovno ionizacijsko celico PTW-Freiburg PinPoint in z Varianovim elektronskim sistemom za verifikacijo obsevalnega polja (ESVOP) aS500 EPID. Meritve so bile opravljene v intenzitetno moduliranem žarku načrtovanem za obsevanje prostate. Zaradi težav z nameščanjem dozimetra, ki nastopijo pri meritvah v točki v območju visokih doznih gradientov, smo razvili metodo iskanja najprimernejše lege dozimetra. Izmerjene doze so primerjane z dozami, izračunanimi s sistemom za načrtovanje obsevanja HELAX-TMS.

Rezultati. Diamantni detektor je izredno občutljiv na premike znotraj območij z visokim gradientom doze. Skladnost rezultatov meritev z različnimi dozimetri se poveča s primerno izbiro lege dozimetrov. Z izogibanjem območjem z visokimi doznimi gradienti izboljšamo ujemanje rezultatov meritev predvsem med točkovno ionizacijsko celico PinPoint, diamantnim detektorjem in Varianovim sistemom ESVOP.

Zaključki. Diamantni detektorji predstavljajo uporabno rešitev za dozimetrično preverjanje obsevanj z IMRT, še posebej v primerih, kjer sistem ESVOP ni primeren (npr. pri vijačni tomoterapiji).

Notices

Notices submitted for publication should contain a mailing address, phone and/or fax number and/or e-mail of a ***Contact*** *person or department.*

Radiation oncology

March, 2005

The ISRO international teaching course on »Palliative Care in Cancer Treatment« will take place in Dar es Salaam, Tanzania.

See http://www.isro.be

Brachytherapy

May 5-7, 2005

The Annual Brachytherapy Meeting GEC-ESTRO and pre-meeting workshop on breast cancer will take place in Budapest, Hungary.

Contact ESTRO office, Avenue E. Mounier, 83/12, B-1200 Brussels, Belgium; or call +32 775 93 40; or fax +32 2 779 54 94; or e-mail info@estro.be; or see http://www.estro.be

Clinical oncology

May 13- 17, 2005

The ASCO Meeting will be offered in Orlando, USA.

E mail enews@asco.org; or see http://www/asco.org

Lung cancer

July 3-6, 2005

The »11th World Conference on Lung Cancer« will be offered in Barcelona, Spain.

Contact Heather Drew, Imedex, Inc., 70 Technology Drive, Alpharetta, GA 30005 USA; or call +1 770 751 7332, or fax +1 770 751 7334; or e-mail h.drew@imedex.com, or see www.imedex.com/calenders/oncology/htm

Radiation oncology

September - October, 2005

The ISRO international teaching course on »Rational Developments from developing to developed Countries« will take place in Lombok, Indonesia.

See http://www.isro.be

Lung cancer

October 17-19, 2005

The IASLC workshop »Biology and Prevention of Lung Cancer« will be offered in Woodstock, Vermont, USA.

Contact Taryn Klocke at Envision Communications; call +1 770 763 5690; or see www.lungcancerprevention.net

Oncology

October 30 - November 3, 2005

The ESTRO 24 / ECCO 13 Conference will take place in Paris, France.

Contact FECS office, Av. E. Mounier, 83/4, B-1200 Brussels, Belgium; or call +32 7759340; or fax +32 2 7795494; or e-mail info@estro.be; or see http://www.fecs.be

As a service to our readers, notices of meetings or courses will be inserted free of charge.
Please send information to the Editorial office, Radiology and Oncology, Zaloška 2, SI-1000 Ljubljana, Slovenia.

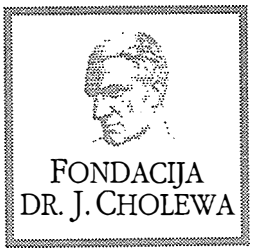

Fondacija "Docent dr. J. Cholewa"
je neprofitno, neinstitucionalno in nestrankarsko
združenje posameznikov, ustanov in organizacij, ki želijo
materialno spodbujati in poglabljati raziskovalno
dejavnost v onkologiji.

Mesesnelova 9
1000 Ljubljana
tel 01 519 12 77
faks 01 251 81 13

ŽR: 50100-620-133-05-1033115-214779

Activity of »Dr. J. Cholewa« Foundation for Cancer Research and Education - A Report for the First Quarter of 2005

The Dr. J. Cholewa Foundation for Cancer Research and Education continues to support activities associated with cancer research and education in Slovenia throughout the first quarter of 2005. Several initiatives are in the course of examination and evaluation by the members of the Foundation and any problems, associated with the public calls for Foundationís grant applications are being dealt with immediately and thoroughly. Several problems and successful endeavours of the Foundation were thoroughly discussed during the course of 2004 and already during the first quarter of 2005. It is worth mentioning that many study and research grants have been already bestowed to researchers from various scientific fields associated with oncology in Slovenia and that many of them were also given grants and means to attend scientific meetings, congresses, conferences and symposia dealing with oncology worldwide.

Needless to say, the Dr. J. Cholewa Foundation for Cancer Research and Education is also determined to continue to support the regular publication of »Radiology and Oncology« international scientific journal, which is edited, published and printed in Ljubljana, Slovenia, as it has done over the last couple of years.

As an ongoing concern of the Supervisory and Executive Boards of the Foundation, it has to be acknowledged that various public and privately owned enterprises find it ever more difficult to contribute financially to help running day to day operations of the Foundation and its numerous scopes of activity. Several new initiatives and suggestions were discussed and evaluated during the recent meetings of the Foundation to address this problem. It is important to note that many public companies and private individuals remain committed to support the Foundationís activities.

Andrej Plesničar, MD
Borut Štabuc, MD, PhD
Tomaž Benulič, MD

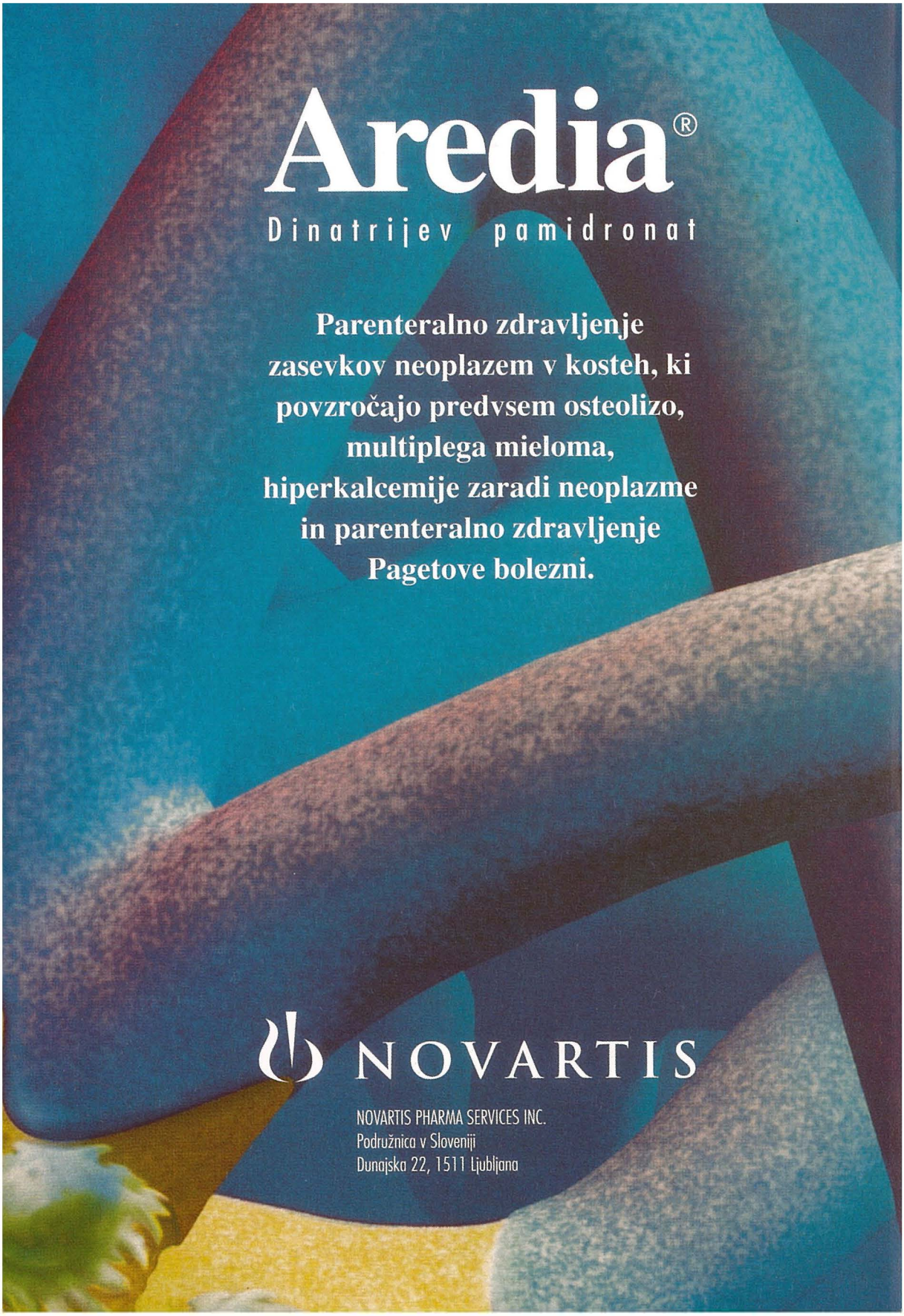
Aredia®
Dinatrijev pamidronat
Parenteralno zdravljenje zasevkov neoplazem v kosteh, ki povzročajo predvsem osteolizo, multiplega mieloma, hiperkalcemije zaradi neoplazme in parenteralno zdravljenje Pagetove bolezni.
NOVARTIS
NOVARTIS PHARMA SERVICES INC.
Podružnica v Sloveniji
Dunajska 22, 1511 Ljubljana

temodal®
temozolomid
kapsule

resnično upanje

Izboljša kvaliteto življenja bolnikov.
Zmanjšuje potrebe po kortikosteroidih.
Omogoča varno in enostavno zdravljenje.

Schering-Plough CE AG **[bolnišnična enota]** Dunajska 22, 1000 Ljubljana, t: 01 3001070, f: 01 3001080

Ime zdravila Temodal® 100 mg, 20 mg, 250 mg. Sestava zdravila Vsaka kapsula zdravila Temodal vsebuje 20 mg, 100 mg ali 250 mg temozolomida. Terapevtske indikac KapsuleTemodal so indicirane za zdravljenje bolnikov z malignimi gliomi, kakor sta npr. multiformni glioblastom ali anaplastični astrocitom, ki se po standardnem zdravlje ponovijo ali napredujejo. Odmerjanje in način uporabe Odrasli bolniki in pediatrični bolniki, stari 3 leta ali starejši: Posamezen ciklus zdravljenja traja 28 dni. Bolniki, ki še niso zdravljeni s kemoterapijo, naj jemljejo Temodal peroralno v odmerku 200 mg/m² enkrat na dan prvih 5 dni, potem pa naj sledi 23-dnevni premor (skupaj 28 dni). Pri bolnikih, so bili že prej zdravljeni s kemoterapijo, je začetni odmerek 150 mg/m² enkrat na dan, v drugem ciklusu pa se poveča na 200 mg/m² na dan, pod pogojem, da je na 1. d naslednjega ciklusa absolutno število nevtrofilcev (ANC) ≥1,5 x 109/l in število trombocitov ≥100 x 109/l. Uporaba pri bolnikih z motenim delovanjem jeter ali ledvic: Pri bolni z blago ali zmerno jetrno okvaro je farmakokinetika temozolomida podobna kot pri tistih z normalnim delovanjem jeter. Kljub temu svetujemo previdnost pri uporabi Temodala teh bolnikih. Uporaba pri starejših bolnikih: Analiza farmakokinetike je pokazala, da starost ne vpliva na očistek temozolomida. Kljub temu svetujemo posebno previdnost uporabi zdravila Temodal pri starejših bolnikih. Način uporabe Temodal mora bolnik jemati na tešče. Kapsule Temodal mora bolnik pogoltniti cele s kozarcem vode in jih ne s odpirati ali žvečiti. Predpisani odmerek mora vzeti v obliki najmanjšega možnega števila kapsul. Pred jemanjem zdravila Temodal ali po njem lahko bolnik vzame antiemetik. po zaužitju odmerka bruha, ne sme še isti dan vzeti drugega odmerka. Kontraindikacije Temodal je kontraindiciran pri bolnikih, ki imajo v anamnezi preobčutljivostne reakcije sestavine zdravila ali na dakarbazin (DTIC). Temodal je kontraindiciran tudi pri bolnikih s hudo mielosupresijo. Temodal je kontraindiciran pri ženskah, ki so noseče ali doj Posebna opozorila in previdnostni ukrepi Pri bolnikih, ki so močno bruhali (stopnja 3 ali 4) v prejšnjih ciklusih zdravljenja, bo lahko potreben antiemetik. Uporaba pri otro Kliničnih izkušenj z zdravilom Temodal pri otrocih, mlajših od 3 let, še ni. Uporaba pri starejših bolnikih: Zdi se, da je pri starejših bolnikih (starost >70 let) tveganje za nevtropen ali trombocitopenijo večje kot pri mlajših, zato svetujemo posebno previdnost pri uporabi zdravila Temodal pri starejših bolnikih. Moški bolniki: Temozolomid lahko del genotoksično. Interakcije Sočasna uporaba zdravila Temodal in ranitidina ni povzročila spremembe obsega absorpcije temozolomida. Jemanje zdravila Temodal s hrano povzročilo 33 % zmanjšanje Cmax in 9 % zmanjšanje AUC. Ker ne moremo izključiti možnosti, da bi bila sprememba Cmax lahko klinično pomembna, priporočamo jema zdravila Temodal brez hrane. Analiza populacijske farmakokinetike temozolomida v raziskavah druge faze je pokazala, da sočasna uporaba deksametazona, proklorperazin fenitoina, karbamazepina, ondansetrona, antagonistov receptorjev H2 ali fenobarbitala ne spremeni očistka temozolomida. Sočasno jemanje z valproinsko kislino je bilo poveza z majhnim, a statistično značilnim zmanjšanjem očistka temozolomida. Uporaba zdravila Temodal v kombinaciji z drugimi mielosupresivi lahko poveča verjetnost mielosupresi Neželeni učinki V kliničnih raziskavah so bili najpogostnejši neželeni učinki, povezani z zdravljenjem, prebavne motnje, natančneje slabost (43 %) in bruhanje (36 %). Pogostn hude slabosti in bruhanja je bila 4 %. Drugi pogostejši neželeni učinki so: utrujenost (22 %), zaprtje (17 %) in glavobol (14 %). Poročali so tudi o anoreksiji (11 %), driski (8 %) izpuščaju, zvišani telesni temperaturi in zaspanosti. Laboratorijski izvidi: trombocitopenija oz. nevtropenija 3. oz. 4. stopnje sta se pojavili pri 19 % oz. 17 % bolnikov, zdravlje zaradi glioma. Mielosupresija je bila predvidljiva (ponavadi se je pojavila v prvih nekaj ciklusih in je bila najizrazitejša med 21. in 28. dnem), okrevanje pa je bilo hitro, ponavad 1-2 tednih. Znakov kumulativne mielosupresije niso ugotavljali. Schering-Plough Central East AG, Luzern, Švica, Predstavništvo Sloveniji, Dunajska 22, 1000 Ljubljana Način in režimi izdaje Zdravilo se izdaja samo na recept, uporablja pa se pod posebnim nadzorom zdravnika specialista ali od nje pooblaščenega zdravnika. Datum priprave informacije: Januar 2005. Podrobnejše informacije o zdravilu so vam na voljo pri proizvajalcu

Diflazon®

flukonazol

kapsule
raztopina za intravensko infundiranje

Zaupanja vreden antimikotik za zdravljenje okužb s kandido

Sestava 1 kapsula vsebuje 50 mg, 100 mg ali 150 mg flukonazola. 1 viala vsebuje 200 mg flukonazola. **Indikacije** Sistemske kandidoze, mukozne kandidoze, preprečevanje kandidoze, kriptokokoze, vaginalna kandidoza in dermatomikoze. **Odmerjanje in način uporabe** Velikost odmerka je odvisna od indikacije. Odraslim dajemo običajno 50 do 800 mg flukonazola 1-krat na dan, otrokom pa 3 do 12 mg/kg telesne mase 1-krat na dan. Največji dnevni odmerek je 12 mg/kg telesne mase, za otroke, stare 5 do 13 let, pa 400 mg. Prvi dan zdravljenja priporočamo dvojni dnevni odmerek, ki je sicer predpisan za posamezno indikacijo. Trajanje zdravljena je odvisno od klinične slike in mikološkega odziva. *Bolniki z zmanjšanim delovanjem ledvic:* Pri zdravljenju z večkratnimi odmerki flukonazola dnevne odmerke prilagodimo vrednostim kreatininskega očistka. **Kontraindikacije** Preobčutljivost za zdravilo, pomožne sestavine zdravila in za druge azole. Sočasno jemanje flukonazola s terfenadinom ali cisapridom. **Posebna opozorila in previdnostni ukrepi** ~~Pri bolnikih~~ z motnjami v delovanju jeter je treba redno spremljati aktivnost jetrnih encimov in bolnikovo stanje. Ob povečani aktivnosti jetrnih encimov naj zdravnik presodi o koristnosti nadaljevanja zdravljenja in tveganju hujše jetrne okvare. Nosečnost in dojenje Nosečnica zdravilo lahko jemlje le, če je korist zdravljenja za mater večja od tveganja za plod. Ker so koncentracije flukonazola v materinem mleku podobne plazemskim koncentracijam, naj doječe matere med zdravljenjem s flukonazolom ne dojijo. **Medsebojno delovanje z drugimi zdravili** Pri enkratnem odmerku flukonazola za zdravljenje vaginalne kandidoze klinično pomembnih interakcij ni. Pri sočasnem zdravljenju z večkratnimi in večjimi odmerki flukonazola so možne interakcije s terfenadinom, cisapridom, astemizolom, varfarinom, derivati sulfonilureje, hidroklorotiazidom, fenitoinom, rifampicinom, ciklosporinom, teofilinom, indinavirom, midazolamom in zidovudinom. **Neželeni učinki** Lahko se pojavijo slabost, napenjanje, bruhanje, bolečine v trebuhu, driska. Možni so glavobol, krči in alopecija. Zelo redke so preobčutljivostne reakcije. Pri bolnikih s hudimi glivičnimi obolenji lahko pride do levkopenije, trombocitopenije, povečane aktivnosti jetrnih encimov ter hujše motnje v delovanju jeter. **Oprema in način izdajanja zdravila** 7 kapsul po 50 mg, 28 kapsul po 100 mg, 1 kapsula po 150 mg – na zdravniški recept; 1 viala s 100 ml raztopine za intravensko infundiranje (200 mg/100 ml) – uporaba **je dovoljena samo v bolnišnicah.**

Datum priprave besedila januar 2005

Že 50 let.

Podrobnejše informacije so na voljo pri proizvajalcu.

Krka, d. d., Novo mesto, Šmarješka cesta 6, 8501 Novo mesto, www.krka.si

KRKA

KEMOMED

PE: Stritarjeva 5, 4000 Kranj, Slovenija
tel.: (0)4/ 2015 050, fax: (0)4/ 2015 055
e-mail: kemomed@siol.net,
www.kemomed.si

Promega

SYNGENE

TPP

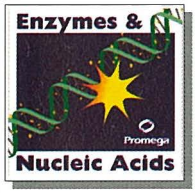

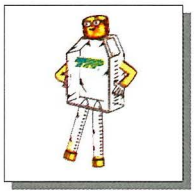

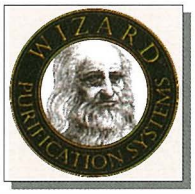

IZDELKI ZA MOLEKULARNO BIOLOGIJO

DOKUMENTACIJA IN ANALIZA GELOV

PLASTIKA ZA CELIČNE KULTURE

ELGA LABWATER

SANYO

Invitrogen life technologies

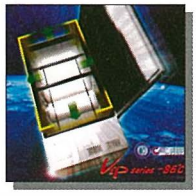

ČISTA VODA ZA LABORATORIJ

SKRINJE IN HLADILNIKI

CELIČNE KULTURE, GELI IN MOLEKULARNA BIOLOGIJA

BIOHIT

minerva biolabs

LI-COR Biosciences

ELEKTRONSKE IN MEHANSKE AVTOMATSKE PIPETE

DIAGNOSTIKA MIKOPLAZEM IN LEGIONEL

SEKVENATORJI

Instructions for authors

Editorial policy of the journal *Radiology and Oncology* is to publish original scientific papers, professional papers, review articles, case reports and varia (editorials, reviews, short communications, professional information, book reviews, letters, etc.) pertinent to diagnostic and interventional radiology, computerized tomography, magnetic resonance, ultrasound, nuclear medicine, radiotherapy, clinical and experimental oncology, radiobiology, radiophysics and radiation protection. The Editorial Board requires that the paper has not been published or submitted for publication elsewhere: the authors are responsible for all statements in their papers. Accepted articles become the property of the journal and therefore cannot be published elsewhere without written permission from the editorial board. Papers concerning the work on humans, must comply with the principles of the declaration of Helsinki (1964). The approval of the ethical committee must then be stated on the manuscript. Papers with questionable justification will be rejected.

Manuscript written in English should be submitted to the Editorial Office in triplicate (the original and two copies), including the illustrations: *Radiology and Oncology*, Institute of Oncology, Zaloška 2, SI-1000 Ljubljana, Slovenia; (Phone: +386 1 5879 369, Tel./Fax: +386 1 5879 434, E-mail: gsersa@onko-i.si). Authors are also asked to submit their manuscripts on a 3.5" 1.44 Mb formatted diskette. The type of computer and word-processing package should be specified (Word for Windows is preferred).

All articles are subjected to editorial review and review by independent referee selected by the editorial board. Manuscripts which do not comply with the technical requirements stated herein will be returned to the authors for correction before peer-review. Rejected manuscripts are generally returned to authors, however, the journal cannot be held responsible for their loss. The editorial board reserves the right to ask authors to make appropriate changes in the contents as well as grammatical and stylistic corrections when necessary. The expenses of additional editorial work and requests for reprints will be charged to the authors.

General instructions• Radiology and Oncology will consider manuscripts prepared according to the Vancouver Agreement (*N Engl J Med* 1991; **324:** 424-8, *BMJ* 1991; **302:** 6772; *JAMA* 1997; **277:** 927-34.). Type the manuscript double spaced on one side with a 4 cm margin at the top and left hand side of the sheet. Write the paper in grammatically and stylistically correct language. Avoid abbreviations unless previously explained. The technical data should conform to the SI system. The manuscript, including the references may not exceed 15 typewritten pages, and the number of figures and tables is limited to 4. If appropriate, organize the text so that it includes: Introduction, Material and methods, Results and Discussion. Exceptionally, the results and discussion can be combined in a single section. Start each section on a new page, and number each page consecutively with Arabic numerals.

Title page should include a concise and informative title, followed by the full name(s) of the author(s); the institutional affiliation of each author; the name and address of the corresponding author (including telephone, fax and e-mail), and an abbreviated title. This should be followed by the *abstract page*, summarising in less than 200 words the reasons

for the study, experimental approach, the major findings (with specific data if possible), and the principal conclusions, and providing 3-6 key words for indexing purposes. Structured abstracts are preferred. If possible, the authors are requested to submit also slovenian version of the title and abstract. The text of the report should then proceed as follows:

Introduction should state the purpose of the article and summarize the rationale for the study or observation, citing only the essential references and stating the aim of the study.

Material and methods should provide enough information to enable experiments to be repeated. New methods should be described in detail. Reports on human and animal subjects should include a statement that ethical approval of the study was obtained.

Results should be presented clearly and concisely without repeating the data in the tables and figures. Emphasis should be on clear and precise presentation of results and their significance in relation to the aim of the investigation.

Discussion should explain the results rather than simply repeating them and interpret their significance and draw conclusions. It should review the results of the study in the light of previously published work.

Illustrations and tables must be numbered and referred to in the text, with appropriate location indicated in the text margin. Illustrations must be labelled on the back with the author's name, figure number and orientation, and should be accompanied by a descriptive legend on a separate page. Line drawings should be supplied in a form suitable for high-quality reproduction. Photographs should be glossy prints of high quality with as much contrast as the subject allows. They should be cropped as close as possible to the area of interest. In photographs mask the identities of the patients. Tables should be typed double spaced, with descriptive title and, if appropriate, units of numerical measurements included in column heading.

References must be numbered in the order in which they appear in the text and their corresponding numbers quoted in the text. Authors are responsible for the accuracy of their references. References to the Abstracts and Letters to the Editor must be identified as such. Citation of papers in preparation, or submitted for publication, unpublished observations, and personal communications should not be included in the reference list. If essential, such material may be incorporated in the appropriate place in the text. References follow the style of Index Medicus. All authors should be listed when their number does not exceed six; when there are seven or more authors, the first six listed are followed by "et al.". The following are some examples of references from articles, books and book chapters:

Dent RAG, Cole P. *In vitro* maturation of monocytes in squamous carcinoma of the lung. *Br J Cancer* 1981; **43:** 486-95.

Chapman S, Nakielny R. *A guide to radiological procedures.* London: Bailliere Tindall; 1986.

Evans R, Alexander P. Mechanisms of extracellular killing of nucleated mammalian cells by macrophages. In: Nelson DS, editor. *Immunobiology of macrophage.* New York: Academic Press; 1976. p. 45-74.

Page proofs will be faxed to the corresponding author whenever possible. It is their responsibility to check the proofs carefully and fax a list of essential corrections to the editorial office within 48 hours of receipt. If corrections are not received by the stated deadline, proof-reading will be carried out by the editors.

Reprints: Fifty reprints are free of charge, for more contact editorial board.

For reprint information contact: International Reprint Corporation, 287 East "H" Street, Benicia, CA 94510, USA. Tel: (707) 746-8740; Fax: (707) 746-1643; E-mail: reprints@intlreprints.com

SIEMENS

SiemensMedical.com/oncology

SEEK-FIND-ACT-FOLLOW - the Continuum of Oncology Care™

Siemens oncology portfolio comprises comprehensive workflow solutions integrating the full spectrum of care from screening/early detection and diagnosis through therapy and follow-up. All from one provider — with over 100 years history of innovation in medical technology.

Siemens proven clinical methods can help you to achieve more successful outcomes. How? Through industry-leading technology, increased productivity measures for maximized utilization potential, and patient-friendly design and features.

Every day in the United States alone, 29,000 cancer patients receive radiation therapy delivered by Siemens linear accelerators. As clinical protocols transition to include IMRT and IGRT, Siemens seamlessly integrates the diagnostic and treatment modalities. That's what we call Best Practice Oncology Care.

Siemens medical
Solutions that help